



المسيلة في: 2025/02/11

شهادة موافقة علمية على مطبوعة بيداغوجية
للأستاذة بورزق يوسف اسلام - أستاذة محاضرة أ -

يشهد رئيس المجلس العلمي لكلية العلوم بجامعة محمد بوضياف بالمسيلة، أنه بعد الإطلاع على تقارير الخبرة الواردة من طرف الخبراء من صف الأستاذية:

- السيدة: هبة عزالدين ، أستاذة التعليم العالي بجامعة محمد بوضياف- المسيلة.
 - السيد : برادعي جمال، أستاذ التعليم العالي جامعة هواري بومدين للعلوم والتكنولوجيا باب الزوار
 - والمعينين من طرف المجلس العلمي لكلية العلوم في الاجتماع المنعقد في دورته العادية يوم 2024/11/25 لإجراء الخبرة للمطبوعة البيداغوجية الخاصة بالأستاذة بورزق يوسف اسلام - أستاذة محاضرة- أ- بقسم الفيزياء و المتعلقة بخبرة للمطبوعة البيداغوجية للمادة المعنونة بـ: Technology of Materials و المقررة في برنامج التكوين ليسانس، تخصص: « L3 PHYSIQUE DES MATERIAUX » و المفتوح بقسم الفيزياء.
- تمت الموافقة عليها شكلا ومضمونا.

رئيس المجلس العلمي لكلية العلوم



بعزير حليم

PEOPLE'S DEMOCRATIC REPUBLIC OF ALGERIA

**MINISTRY OF HIGHER EDUCATION
AND SCIENTIFIC RESEARCH**

UNIVERSITY OF MSILA

FACULTY OF SCIENCE



Course Material

Technology of Materials

Exercises and solutions

(February 2025)

Made by:

Dr. Yousf Islem BOUREZG

2024/2025

Contents

Aims and Concepts

Part I: Materials and their characteristics	1
Introduction	2
I.1 Materials classification	2
I.1.1 Metals and alloys	2
I.1.2 Ceramics	3
I.1.3 Polymers	4
I.1.4 Composites	5
I.2 Properties of Materials	6
I.2.1 Physical properties	6
I.2.1.1 Physical Change in state of matter	8
I.2.1.2 Density	8
I.2.1.3 Melting point	8
I.2.1.4 Specific heat	9
I.2.1.5 Thermal conductivity	9
I.2.1.6 Thermal expansion	9
I.2.1.7 Electrical conductivity	9
I.2.1.8 Magnetic properties	9
I.2.1.9 Temperature stability	10
I.2.2 Mechanical properties	10
I.2.2.1 Stress-Strain Diagrams	10
I.2.2.2 Strength	12
I.2.2.3 Ductility	13
I.2.2.4 Elasticity	13
I.2.2.5 Plasticity	13
I.2.2.6 Malleability	13
I.2.2.7 Brittleness	14
I.2.2.8 Hardness	14
I.2.2.9 Toughness	18
I.2.2.10 Creep and Creep testing	18
I.2.2.11 Basics of Stress Analysis	19
I.2.3 Chemical properties	21

Part II: Solid solutions	23
Introduction	24
II.1 Solid solutions	24
II.2 Types of Solid Solutions	24
II.2.1 Substitutional solid solution	25
II.2.1.1 Ordered and disordered substitutional solid solution	25
II.2.1.2 Conditions for extensive solid solubility	27
II.2.2 Interstitial solid solution	28
II.2.2.1 Octahedral and tetrahedral interstitial sites	28
II.3 Intermediate phases	32
Part III: Binary phase diagrams	34
Introduction	35
III.1 Phase diagram	35
III.2 Limitations of Phase Diagrams	36
III.3 Phase diagram applications	37
III.4 Intensive and extensive properties	37
III.5 Gibbs free energy	37
III.6 Gibbs phase rule	39
III.7 Some binary phase diagrams	39
III.7.1 Complete solid and liquid solution diagram	39
III.7.2 Binary diagram corresponding to domains of partial miscibility	40
III.7.3 Binary diagram showing intermediate phases	42
III.8 The Lever rule	43
III.9 Experimental determination of phase equilibriums diagrams	44
III.10 Phase diagram determination examples	44
III.11 Thermodynamics of phase diagrams	48
III.11.1 Thermodynamics' First and Second Law	48
III.11.1.1 Nomenclature	48
III.11.1.2 The First Law	48
III.11.1.3 The Second Law	49
III.11.1.4 The Fundamental Equation of Thermodynamics	50
III.11.2 Enthalpy	51
III.11.3 Gibbs Energy	54
III.11.4 Chemical Equilibrium	56

III.11.4.1 Gaseous Phase Equilibrium	57
III.11.4.2 Predominance Diagrams	58
III.11.5 Gibbs, Entropy, and Enthalpy energies Measurements	62
III.11.5.1 Gibbs Energy Change	62
III.11.5.2 Enthalpy Change	63
III.11.5.3 Entropy	64
III.11.5.4 Zero Enthalpy and Entropy	65
III.11.6 The Chemical Potential	65
Part IV: Diffusion	67
Introduction	68
IV.1 Diffusion	68
IV.2 Diffusion Mechanisms	68
IV.2.1 Interstitial Mechanism	68
IV.2.2 Direct exchange mechanism	69
IV.2.3 Ring mechanism	69
IV.2.4 Vacancy mechanism	69
IV.2.5 Interstitial-substitutional exchange mechanism	70
IV.3 Laws of Fick	71
IV.3.1 First law of Fick	71
IV.3.2 Second law of Fick	72
IV.4 Kirkendall Effect	72
IV.5 Darken Equations	73
Part V: Phase transformations	74
Introduction	75
V.1 Nucleation in pure metals	75
V.1.1 Homogeneous nucleation	75
V.1.2 Heterogeneous nucleation	77
V.2 Gibbs free energy of binary solutions	79
V.2.1 Ideal solutions	80
V.3 Time-Temperature-Transformation (TTT) Diagram	81
V.4 Austenite to Pearlite isothermal transformation	82
V.5 Illustration of the binary phase diagram with several reactions	84
V.6 Diffusion pairs or Multiples and Phase Formation and kinetics	89
References	92

Exercises	94
Exercise solutions	97
Exercises without solutions	102

Objectives and Concepts

This manuscript's objective is to provide preliminary information on the different families of materials and their properties, basic notions for solid solutions in order to have metallic alloys and improve the properties of materials, phase diagrams and their interests, thermodynamics of matter transport (diffusion) and finally the phase transformation in materials based on those of the Fe-C system.

Thus, the present manuscript targets the students of physics sector and precisely those in 3rd year degree in materials physics and condensed matter physics. It should also be of interest those studying related fields like mechanical engineering and material science, etc.

Readers should have some fundamental understanding of atomic physics and an introduction to general physics. It will be easier to read this manuscript if readers have a basic understanding of solid state physics, although the fundamental ideas will always be described.

Several exercises were provided with their solutions, at the end of this course.

Part I:
Materials and their
characteristics

Part I: Materials and their characteristics

Introduction

A material is the substance that makes up an object. The definition of this phrase is somewhat broad. According to their properties, they are classified. Materials have properties such as, strength, thermal conductivity, and permeability, etc. They are the fundamental substances that are processed and refined in industry to produce additional materials or useful items. Materials science is the branch of science that deals with the study of materials. Materials can be used for many different things. Therefore, they are also categorized according to the industries in which they are used. The process of choosing materials for a particular use is known as material selection

I.1 Materials classification

The list of materials utilized in contemporary production is infinite. Materials can be categorized into multiple groups according to their characteristics. Materials can be divided into:

- Metallic (Metals and alloys),
- Ceramic,
- Polymer,
- Composite.

I.1.1 Metals and alloys

Combinations of metallic elements (such as iron, aluminum, and gold) with trace amounts of non-metallic elements (such as carbon, and oxygen) make up an inorganic substance known as a metallic material (See Figure I.1).

A material that has a number of metals or non-metals added to it is called an alloy. It allows for better combinations of traits or improves a certain desirable property. In contrast to ceramics and polymers, the arrangement of atoms in the metals and their alloys is extremely ordered.

The metals and alloys may be categorized as:

- Ferrous metals and alloys: These are the ones that mostly consist of iron.
- Non-ferrous metals and alloys: These are those that are mostly composed of a metal other than iron, such copper, zinc, aluminum, etc.

Part I: Materials and their characteristics

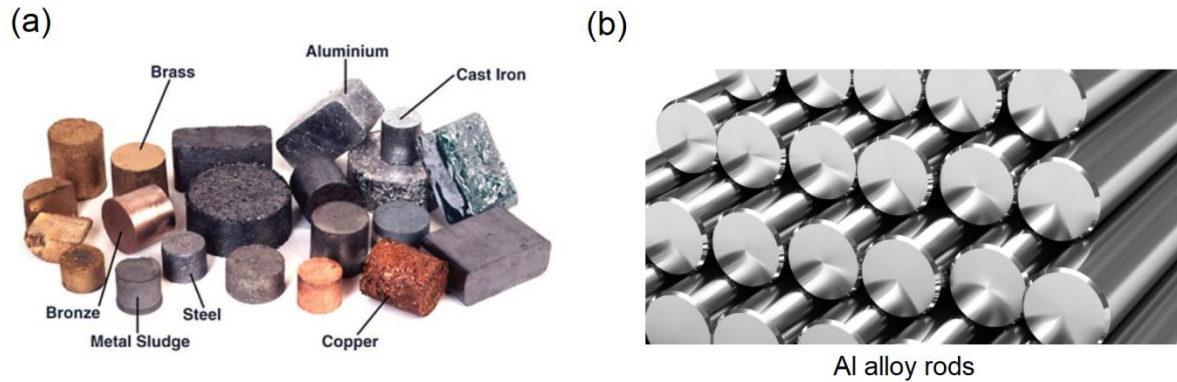


Figure I.1. Pictures for, (a) some metals, (b) Al-alloy rods.

Metals and alloys are comparatively strong, shock-resistant, and have excellent ductility or formability. Metals and alloys are not transparent to visible light, yet they are very good conductors of heat and electricity. Furthermore, a few of the metals Fe, Co, and Ni have advantageous magnetic qualities.

I.1.2 Ceramics

"Ceramic" is derived from the Greek word "keramikos," meaning "pottery." Compounds of metallic and nonmetallic elements, ceramics are made from powdered materials and formed into finished goods by heating them. They are most frequently oxides, nitrides, and carbides.

The most known ceramics include alumina- Al_2O_3 , calcia- CaO , silicon nitride (Si_3N_4), silicon dioxide (SiO_2), hydroxyapatite dental implantation. Additionally, what is known as classical ceramics, such as bricks, cement, porcelain and glass (See Figure I.2).



Figure I.2 Pictures for some ceramic products.

Ceramic materials have significant mechanical properties that are on par with those of metals. Ceramics are also usually extremely hard. However, they are exceedingly brittle (poor ductility) and prone to breaking too easily. Compared to metals and polymers, these materials are more resilient to extreme temperatures and harsh conditions and have lower electrical

Part I: Materials and their characteristics

conductivities. Ceramics can have either transparent or opaque optical properties, and some oxide ceramics (such Fe₃O₄) behave magnetically.

I.1.3 Polymers

They are typically organic materials. The polymeric substance is made up of complex polymer chains held together by secondary bonds and a lengthy chain of covalently bound atoms.

Rubber and plastic are examples of polymers (See Figure I.3), which are chemically composed of hydrogen, carbon, and other non-metallic substances (O, Si, and N).

- Plastics (for example, nylon). They can be classified into these classes:
 - Thermoplastic polymers, which include polyvinyl chloride, polyethylene, polypropylene, and polystyrene,
 - Thermosetting polymers include unsaturated polyesters, epoxies, polyurethanes, alkyds, and amino and phenolic resins.
- Elastomers or rubbers (for example, car tires).

Thermoplastics as well as thermosetting plastics are distinguished by their chemical and structural bonding. These materials are referred to as "thermoplastic" because they melt when heated and may be produced using a range of shaping and extrusion methods. On the other hand, "thermosetting" polymers are incapable of melting or remelting.

When a force is applied, rubbers or elastomers can undergo elastic deformation; when the load (.i.e. force) is released, they may revert to their original shape, or nearly so.

Part I: Materials and their characteristics



Figure I.3. Pictures for some polymer products.

Numerous characteristics of polymers make them desirable for usage under specific circumstances. Numerous polymers :

- Compared to metals or ceramics, they have lower densities and are more resistant to corrosion.
- They have a good affinity for human tissue,
- Have outstanding resistance to electrical current conduction,
- Very ductile.

Another drawback of polymers is that, because to their pliability, they might break down or soften in severe environments or at higher temperatures.

I.1.4 Composites

Usually made of two or more components, a composite has qualities that no single material can match. As examples, fiber-glass (glass fibers are embedded within a polymeric material), concrete, metal-matrix composite Al/Mg/Al proceeded with accumulative roll banding (ARB), etc (see Figure I.5).

Part I: Materials and their characteristics



Figure I.4. Macrostructure of AA7050/AA1050 components processed with ARB [1].

The variety of materials that fall under this wide category is reflected in the properties of composites. The composite's final characteristics under the optimum conditions are:

- Suitable mechanical properties.
- Impact resistant.
- Chemical/environmental stability.

I.2 Properties of Materials

What does "properties of materials" mean?

Whether by basic sense or the use of precise instruments and machinery to measure them, the properties of materials represent the qualities that set them apart from one another and provide the impression that they are unique.

We ought to be worried about three different kinds of properties:

- (a) Physical characteristics (such as electrical and magnetic qualities, colour, density, specific heat, melting and boiling points, thermal expansion, and conductivity),
- (b) Material mechanical attributes, such as ductility, elasticity, fatigue, creep, strength, toughness, and hardness.
- (c) Chemical characteristics (such toxicity, flammability, corrosion, and oxidation).

I.2.1 Physical properties

Any quantifiable attribute whose value characterizes the state of a physical system is considered a physical characteristic. A system's transitions or evolutions throughout its

Part I: Materials and their characteristics

transient states can be described by changes in its physical characteristics. Observables are a common term used to describe physical attributes. Modal properties are not what they are.

Physical attributes are frequently described as extensive and comprehensive. In contrast to an extensive property, which exhibits an additive relationship, an intensive property is independent of the system's size, extent, and matter. These divisions are generally only applicable when the sample's smaller subunits do not interact with one another in a physical or chemical process.

It is also possible to categorize properties according to the directional characteristics of how they are structured. Anisotropic qualities, for instance, exhibit spatial fluctuation, whereas isotropic traits remain constant independent of the direction of observation. It might be challenging to identify if a particular property qualifies as a material property. For instance, colour can be seen and measured, but ultimately, colour is an interpretation of a surface's reflecting qualities and the light that illuminates it. This is why many seemingly physical attributes are referred to as supervenient. Supervenient properties are genuine but subordinate to a more fundamental reality. The supervenience of items on atomic structure is comparable to this.

The mass, shape, color, temperature, and other physical characteristics of a cup may be supervening on the fundamental atomic arrangement, which may be supervening on the basic quantum structure. Chemical properties, which dictate a material's behavior in a chemical reaction, are contrasted with physical attributes. Physical characteristics are those that are observable without altering the substance's identity. Physical properties include things like color, density, and hardness, which are general characteristics of matter.

Chemical attributes are those that explain how a substance transforms into an entirely new substance. Chemical attributes include things like flammability and resistance to corrosion and oxidation. Until the material's phase is taken into account, the distinction between a chemical and physical attribute is simple. It appears as though a material transforms into a different substance when it goes from a solid state to a fluid to a vapor. But when a substance melts, solidifies, vaporizes, condenses, or sublimates, it just changes its condition. Think about ice, liquid water, and water vapor—all of which are just H₂O. There are four different states of matter: solid, liquid, gas, and plasma. Crystal structure is a physical characteristic of matter.

Part I: Materials and their characteristics

A physical property is a characteristic that is manifested without undergoing any compositional changes (Extensive or intensive).

- **Intensive:** A physical characteristic, such as density, color, etc., that remains constant with respect to the amount of material.
- **Extensive:** A physical attribute, such as mass or volume that will alter in response to changes in the amount of matter.

The following criteria will be used to determine which of these attributes is more significant:

I.2.1.1 Physical Change in state of matter

Alteration in which the content of the stuff stays the same but its physical appearance changes.

There are three primary states of matter: gas, liquid, and solid.

- A fixed structure is what sets a solid apart. Its volume and form remain constant. Atoms are firmly arranged in a definite configuration within a solid.
- Liquid is characterized by its continuous volume and pliable shape, which allows it to take on the shape of its container. Atoms in a liquid are near to one another but not in a set configuration.
- Atoms those are distinct from one another make up gas. However, a gas lacks a definite shape and volume, in contrast to a solid or liquid.

I.2.1.2 Density

A material's density is its mass per unit volume. The kg/m^3 (or g/m^3) is the derived unit that typically used.

$$\rho = \text{mass (m)} / \text{volume (V)} \quad \text{I.1}$$

I.2.1.3 Melting point

The substance transitions from a solid to a liquid phase at this temperature. The properties of the materials and alloys, and consequently their uses, are greatly influenced by the melting temperature.

Part I: Materials and their characteristics

I.2.1.4 Specific heat

The quantity of thermal energy required to increase a material's temperature by 1°C per unit mass.

A significant amount of heat is produced during machining and forming operations as a result of tool-workpiece deformation and friction. Poor surface finish will result from the work piece's temperature rising quickly if its specific heat is low. It may be necessary to use more effective coolants. Similarly, a low specific heat of the tool material will cause the tool to heat up quickly, reducing its lifespan.

I.2.1.5 Thermal conductivity

Thermal conductivity (k) is the material's capacity for conduction of heat energy. When a plate's opposite faces are exposed to a unit temperature gradient, the amount of heat that moves through the plate's area in a unit of time is known as its thermal conductivity (e.g. one degree difference in temperature through a thickness of one unit).

$$k = \text{Heat flow rate} / (\text{Area} \times \text{Temperature gradient}) \quad \text{I.2}$$

I.2.1.6 Thermal expansion

When a material's temperature increases by 1°C, the proportionate change in its length is known as a linear coefficient of heat expansion (α):

$$\alpha = \Delta L / (L \Delta T) \quad \text{I.3}$$

I.2.1.7 Electrical conductivity

The reciprocal of specific resistance is electrical conductivity. The majority of metals conduct well, although many rubbers, ceramics, plastics, and other materials conduct quite poorly.

I.2.1.8 Magnetic properties

Ferro-magnetic materials can be magnetized by induction because of their high magnetic permeability. Some materials can conduct magnetism well or poorly, just as those transmit electricity well or poorly. Reluctance is the term used to describe the resistance of a magnetic circuit. Low reluctance is a characteristic of good magnetic conductors, such as ferromagnetic materials, which derive their name from their composition of iron, steel, and related alloying metals like nickel and cobalt. Every other substance has a high resistivity to the magnetic field and is non-magnetic.

Part I: Materials and their characteristics

For instance, because grinding requires very little machining force, many grinding equipment use magnetic chucks. The steel work-piece is kept in place during the grinding process by magnetic force, which is generated by an electromagnet in the machine tool bed.

I.2.1.9 Temperature stability

The structure and characteristics of materials can be significantly impacted by any temperature fluctuations. However, temperature variations can have a number of impacts, including creep. The slow extension of a substance over an extended period of time while maintaining a constant applied load is known as creep. It must be taken into account when metals are constantly working at high temperatures, and it is also a significant consideration when thinking about plastic materials. Take gas turbine blades, for instance. Raising the temperature causes the creep rate to increase, while lowering it causes it to decrease.

I.2.2 Mechanical properties

Materials' mechanical qualities are those that are related to their capacity to withstand loads and mechanical forces. To predict how components will respond to mechanical stresses (forces, moments, etc.), mechanical characteristics are helpful.

The most significant and practical mechanical characteristics will be discussed after providing a general overview of the traction curves.

I.2.2.1 Diagrams of Stress-Strain

Stress is the material's internal resistance to the applied load, and strain is the deformation. Three categories of stress exist:

- Tensile stress: materials are pulled apart by force;
- Compressive stress: material is squeezed by the force;
- Shear stress: is when a force pushes one component against another.

Corresponding strains are classified into three categories. Using a Universal Testing Machine, the metals are examined. With stress (load) as the coordinate and strain (elongation, deflection, twist, etc.) as the abscissa, the stress-strain diagram is a diagram. Mechanical characteristics are determined by the crystal's structure, bonding forces, and internal flaws.

Figure I.6 displays the steel stress-strain diagram. The key points are:

Part I: Materials and their characteristics

Point a: Proportionality's limit. -a is a line that is straight, and strain and stress are proportionate. The Young's modulus of elasticity, or E, is indicated by the line's slope.

Point b: Also known as the elastic limit, it provides the material's yield point. After the load is removed, this is the maximum stress the material can withstand without permanently setting.

Point c: Corresponds to the lower yield point.

Point d: Provides the greatest amount of stress.

Point e: The material fails at this point, which is known as the breaking point.

The diagram above can be used to define or comprehend the different mechanical qualities. Data from a test on universal testing equipment is used to draw this.

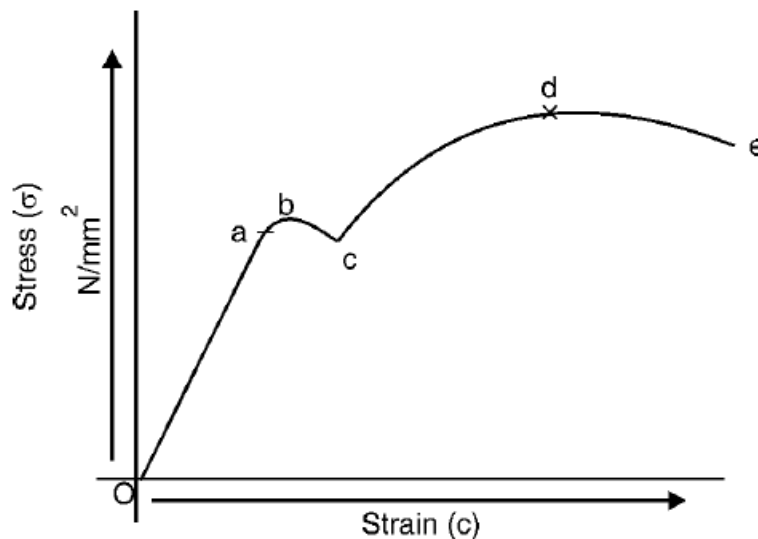


Figure I.5. Diagram of Stress-Strain.

Figure 1.7 displays the strain and stress curve for brittle materials such as cast iron and high carbon steel.

The breaking point is point b, while the limit of ratio is point a. There is no yield point on the curve.

Part I: Materials and their characteristics

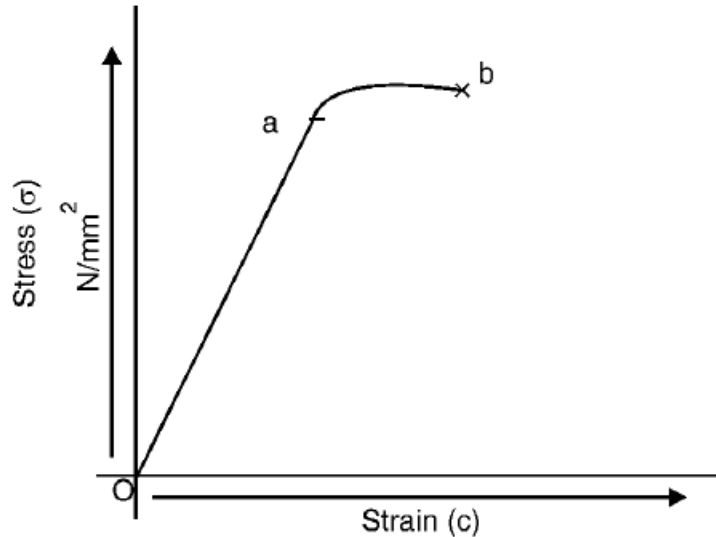


Figure I.6. Brittle Materials.

The important deformation features are:

Elastic deformation: Within this range, if the force is removed, the material will revert to its initial size, much like a spring. **Linear elastic range:** strain changes linearly with tension in the graph's first section.

Plastic region: Stretching a material past its elastic range causes its molecular structure to change and experience some permanent stretching; this is known as the "plastic region." The yield stress is the tension at which the deformation initially turns plastic.

UTS: The material abruptly loses strength when we increase the stress in the plastic range, and some cross sections become extremely narrow and extend freely (necking).

The UTS is the highest amount of stress it could tolerate.

I.2.2.2 Strength

It is a material's capacity to withstand forces from the outside without cracking or giving way. Therefore, a material's strength determines how much load it can support. Strength may include tensile, shear, compressive, or torsional, depending on the kind of load applied. According to Point d above, a material's ultimate strength is the highest stress it can sustain before breaking.

Part I: Materials and their characteristics

I.2.2.3 Ductility

It measures the amount of deformation or elongation a material can withstand under stress before breaking or fracture. When a load is applied, a material's ductility allows it to pull out into thin wire. The substance mild steel is ductile. Because of their ductility, wires made of metals (like, copper, silver, aluminium, gold), are pulled through a die hole or extruded. As the temperature rises, the ductility falls. As empirical indicators of ductility, the percentage elongation and the area under tension are frequently employed.

I.2.2.4 Elasticity

A material's ability to return to its initial form after deformation when external forces are eliminated is one of its properties. Elastic limit is the maximum stress a material can withstand without absorbing a permanent set (see Point an above).

I.2.2.5 Plasticity

It is a material's ability to permanently hold onto the deformation caused by load. Conversely, a material's plasticity refers to its capacity to experience a certain amount of continual deformation with no failing. Only when the elastic range is surpassed, beyond point b, can plastic deformation occur.

In many mechanical operations, including forming, shaping, extrusion, and numerous other both cold and hot working procedures, plasticity is a crucial characteristic that is frequently employed. Generally speaking, a material's flexibility rises with temperature and is advantageous for secondary forming operations. These characteristics allow different metals to be shaped into products of the desired size and shape. Stress, heat, or both can be applied to achieve this transformation into the required size and shape.

I.2.2.6 Malleability

The capacity of a material to be worked hot or cold to small pieces without breaking is known as malleability. Steel, lead, copper, tin, aluminum, and other metals are pliable. Although it cannot be twisted into wire, lead can be easily rolled and pounded into thin sheets. If malleability refers to a compressive quality, ductility represents a tensile characteristic. With rising temperatures, malleability rises.

Part I: Materials and their characteristics

I.2.2.7 Brittleness

The ability of a material to break without causing significant long-term distortion is known as brittleness. Many materials fail or break before significant deformation occurs. These materials, like cast iron and glass, are fragile. Consequently, a material that is not ductile is said to as brittle. Brittle materials typically have tensile strengths that are only a small portion of their compressive strengths. One should not assume that a fragile substance is weak. It merely demonstrates the absence of flexibility. These materials have a modest value of E on the stress-strain curve and no yield point.

I.2.2.8 Hardness

The ability of a material to tolerate (resist) localized persistent deformation, usually caused by indentation, is known as its hardness. All of mechanical characteristics of the material affect hardness.

Strength and hardness are strongly connected. It is a material's resistance to abrasion, penetration, indentation, and scratches. It is determined on specialized hardness measurement machines by measuring the material's resistance to the penetration of a specific indenter with a specific shape and substance under a specified load. It is proportional to tensile strength. There is no clear correlation between a metal's hardness and its ability to be hardened. How hard a metal can become through the hardening process—heating or quenching—is indicated by its hardenability. Tests such as the Vickers, Brinell, and Rockwell hardness tests can be used to assess the hardness of metallic materials. These tests are schematically described in the Figure I.7.



Metallurgy Fundamentals



General characteristics of hardness-testing methods and formulas for calculating hardness.

Test	Indenter	Shape of indentation		Load, P	Hardness number
		Side view	Top view		
Brinell	10-mm steel or tungsten-carbide ball			500 kg 1500 kg 3000 kg	$HB = \frac{2P}{(\pi D)(D - \sqrt{D^2 - d^2})}$
Vickers	Diamond pyramid			1-120 kg	$HV = \frac{1.854P}{L^2}$
Knoop	Diamond pyramid			25 g-5 kg	$HK = \frac{14.2P}{L^2}$
Rockwell					
A } C } D }	Diamond cone			60 kg	HRA
				150 kg	HRC
				100 kg	HRD
} = 100 - 500t					
B } F } G }	1.6-mm diameter steel ball			100 kg	HRB
				60 kg	HRF
				150 kg	HRG
} = 130 - 500t					
E	3.2-mm diameter steel ball			100 kg	HRE

IAMetallurgist

Figure I.7. Different Hardness tests [2].

A couple of the most popular ones are detailed in the following lines:

- **Mohs Hardness Test**

Everybody should know that one of the oldest ways of measuring the hardness of material has been devised by the German mineralogist called Friedrich Mohs back in 1812. The test was named after him, and it involves observing if the surface of the material can be scratched by a known substance or certain defined hardness. The goal was to give numerical values to the physical property, so the minerals were ranked along the Mohs scale. This scale contains ten minerals that received arbitrary hardness values. If you want to accurately gauge the hardness of industrial materials, including steel or ceramics, this is not the perfect fit for you. Mohs hardness test greatly facilitates the identification of several minerals in the field, but it's not suitable for steel or ceramics. When it comes to engineering materials, one can use a variety of instruments that, over the years, were developed to provide a precise measure of hardness level. Many usually apply a load and then measure the depth or even the size of the resulting

Part I: Materials and their characteristics

indentation. In conclusion, hardness can be measured in three ways: on the macro, micro, nano-scale.

- **Brinell Hardness Test**

It should be noted that the hardness of Brinell, which is applicable to engineering materials, is the most traditional way of testing for hardness. Dr. J. A. Brinell created this test in Sweden around 1900. It does employ a desktop computer to apply a particular load to a protected sphere with a given diameter. A figure known as the hardness of the Brinell number, or Brinell number, is calculated by division the weight (in kilogrammes) by the indentation's measured surface area (in square millimetres).

The hardness of metal forgings and castings with a significant grain structure are typically determined using this kind of test. This test can give a measurement across a sizable region that is less impacted by the materials' whole course grain structure than both the Vickers and Rockwell tests.

With the Brinell test, a wide range of materials can be tested by simply changing the test load and the size of the indenter ball. In the USA, a 10 mm diameter ball and a 3000 kg test force are often used to perform this test on iron and steel castings. Aluminium castings can be loaded with 1500 kg, copper, thin stock and brass can be loaded with 500 kg, and a ball with a diameter of 5 or 10 mm can be used. The identical test is carried out in Europe, but with a far wider range of ball sizes and forces. Generally speaking, tiny items are tested with a 1 kg load and a 1 mm carbide ball. Baby Brinell tests are a common term used to describe these stress testing. Reporting the test conditions and the Brinell hardness number is necessary. Given a 10mm diameter ball and a 1500 kg weight applied for 30 seconds, a number such as "60 HB 10/1500/30" indicates that the Brinell hardness is 60.

- **Rockwell Hardness Test**

This kind of test is often carried out by a machine that measures the size of the impression that is made on a surface after applying a particular stress. A steel ball with a specific diameter or a spherical diamond-tipped cone with a 120° angle and a 0.2 mm tip radius—known as a brale—can be used as the indenter. To insert the indenter and eliminate the impact of any surface defects, the tester will first apply a 10 kg load, which will limit the initial penetration. Following this, the tester applies the initial load and sets the dial to zero. The depth reading is taken while maintaining the small load after the substantial weight has been removed. At this point, the hardness number can be obtained straight from the scale. It is

Part I: Materials and their characteristics

important to remember that the hardness scale chosen—A, B, C, etc.—can be determined by the indenter and the measurement of load.

Soft materials, such as copper alloys, aluminum alloys, or soft steel, can be tested using a steel ball with a diameter of 1/16" and a load of 100 kg. The "B" scale can be used to determine the hardness value. Many steel alloys are tougher materials that must be tested using a 120 degree diamond cone with a maximum load of 150 kg. The hardness of these materials can be measured using the "C" scale. The "C" scale is the most commonly used scale. The "HR" letters on the scale letter and hardness number will be present in the right Rockwell value. For instance, 100 HRC indicates that the material's hardness value on the C scale is 100.

- **Rockwell Superficial Hardness Test**

This kind of test is frequently used to evaluate thin materials, surfaces of mildly carburized steel, or even pieces that keep bending or crush under standard test settings. Although the loads are far lower, the same components are required for this test as for the Rockwell tester. The examiner often employs a load of 3 kg, however the meaningful weight is typically around 15 and 45 kg. This test adds a "T" to the surface hardness classification and calls for a steel ball indenter with a 1/16" diameter. For instance, a hardness measurement of 23 HR15T indicates a steel ball, 15 kg of load, and so on.

- **Vickers and Knoop Microhardness Tests**

The Brinell test, which is used to determine the hardness of the top surface of case-hardened parts or the hardness of thin film coatings, is modified in this type of test. One tiny diamond pyramid is driven into the sample during these tests, which employ lower stresses than the Brinell test. Only the diamond pyramid indenter's form distinguishes the Vickers from the Knoop Tests. For this test, a square pyramidal indenter that may break fragile materials is needed. In addition, the test calls for a pyramidal indenter with a rhombic base. The indenter was designed to create indentations that were shallower and longer. Compared to the Vickers indentations, the Knoop indentations are 2.9 times longer for the same load.

This tiny amount can produce a tiny indent that will be examined under a microscope. The load ranges from 10 g to 1000 g. Because of the low indents, tests for hard coatings like TiN must be taken at a very high magnification. As a result, polishing is frequently necessary.

Part I: Materials and their characteristics

The hardness number, or VHN, will be determined by carefully measuring the impression's diagonals and using the results, which are often taken through a lookup table or chart. Some robust materials can be characterised by this test, although the hardness will only be assessed over a smaller area. In the case of a 26-gram force load, the hardness will be 2600 Knoop, as indicated by the expressions 2600 HK25 or HK25. It's also important to be aware that the Vickers and Knoop hardness ratings will vary somewhat. For hard coatings, these numbers can be used interchangeably because they are near enough to fall within the measurement error.

I.2.2.9 Toughness

The amount of energy required before a material fractures is a measure of its toughness. The relationship between stress and strain is readily apparent: energy expended = force x distance. Thus:

$$\text{Toughness} = \text{area under the stress-strain curve} \quad \text{I.4}$$

A material's strength is estimated by the height of the (σ - ϵ) curve, whereas toughness takes into consideration both the curve's width and height.

I.2.2.10 Creep and Creep testing

Creep is the gradual, permanent extension of a material over time at high temperatures and steady tension below the elastic limit. Even stresses below the elastic limit can result in some irreversible deformation on the stress-strain diagram at high temperatures. Creep occurs in three stages. The material elongates quickly but less quickly in the initial stage. The degree of elongation remains constant during the second stage. The third stage sees a sharp rise in the rate of elongation till the material breaks. Creep strength is the stress for a given amount of strain at a fixed temperature.

The creep test is conducted at elevated temperatures. A representation of a tensile specimen's elongation against time, at a specific temperature and under continuous load, is called a creep curve (Figure I.9). The duration of tests ranges from a few days to many years. With the right accessories, the exam can be administered on a universal testing machine. The creep curve displays four elongation stages:

- (a) Elongation that occurs instantly when a load is applied.
- (b) Primary creep: Recovery is sluggish and work hardening declines.

Part I: Materials and their characteristics

(c) Secondary creep: Recovery and work hardening processes proceed at the same rate.

(d) Cracks in the grain boundaries are tertiary creep.

The test specimen's cross-sectional area is decreased via necking. Blades and other components of gas and steam turbines operating at high temperatures are designed using creep strength.

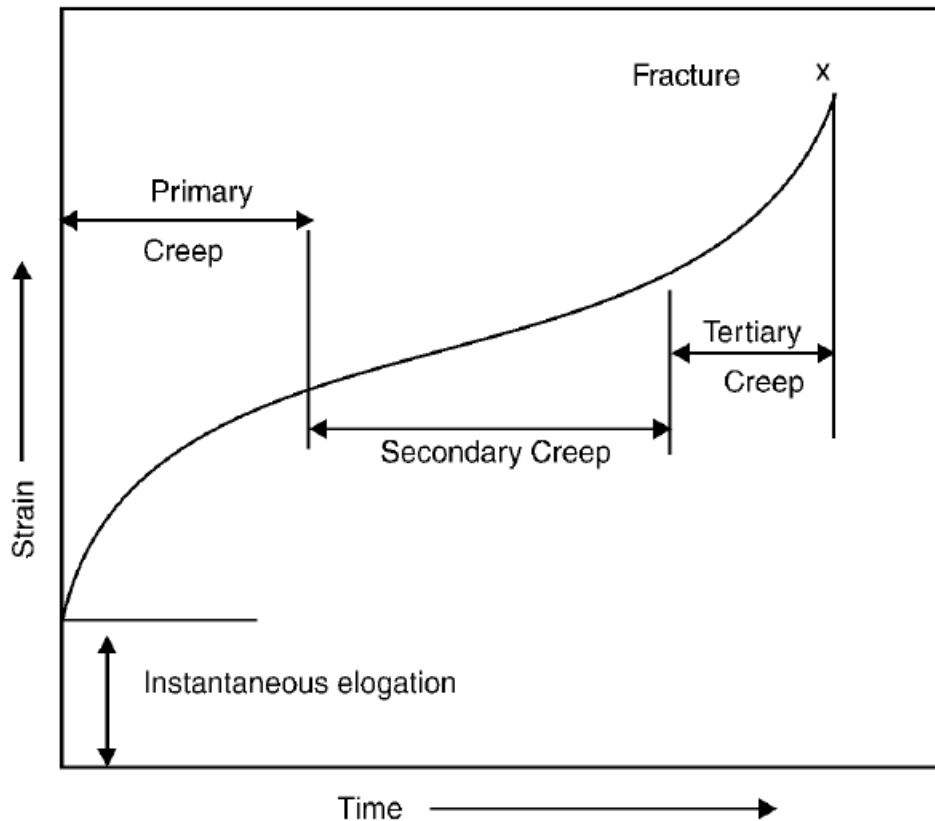


Figure I.8. Creep test curve.

I.2.2.11 Basics of Stress Analysis

We briefly go over the fundamentals of solid mechanics, which are crucial to comprehending when materials break. This is essential in manufacturing, where the majority operations, like cutting, are accomplished by essentially "breaking" the material; it is also important in the design of products, where we typically do not want the substance to break. In essence, stress is created throughout a solid by any weight that is given to it.

The figure I.10 illustrates the two kinds of stresses: shear and tensile/compressive. Suppose that a solid is subjected to one or more forces, causing it to undergo stress while maintaining a stable equilibrium. Under such conditions, we examine a minuscule constituent within the

Part I: Materials and their characteristics

solid.

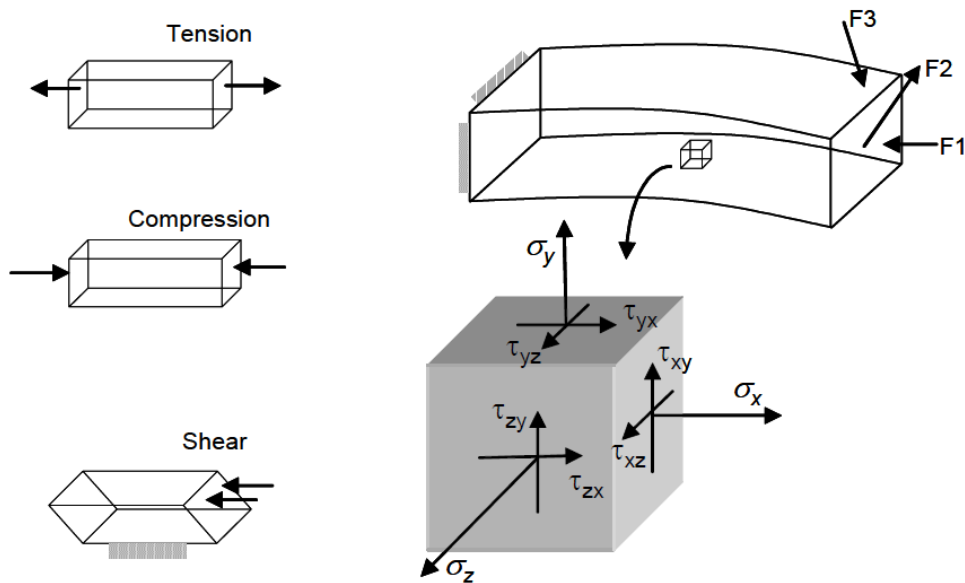


Figure I.9. Stresses in a beam's smallest component, including tensile, compressive, and shear stresses.

We must determine whether the material will fail under the specified set of pressures as indicated. To keep things simple, let's examine the 2D scenario (XY plane only).

We first determine the resulting stresses, σ and τ , along an arbitrary vector sloped at angle ϕ to the y direction in order to answer our issue (see Figure I.11). The sum of all forces must be equal since the material is in equilibrium. Furthermore, stress is described as force/area. We derive the following relationship from this:

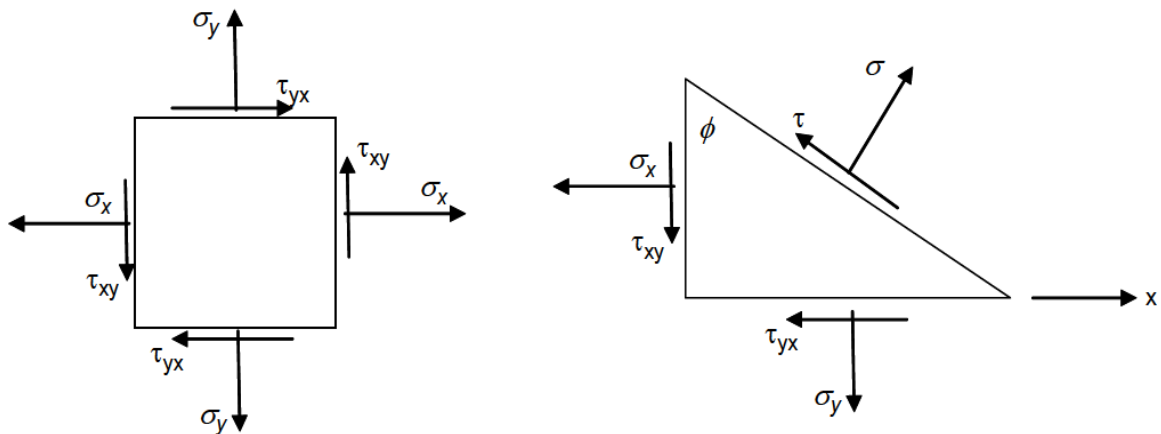


Figure I.10. Computing the principal stresses (2D case).

Part I: Materials and their characteristics

$$\sigma = \frac{\sigma_x + \sigma_y}{2} + \frac{\sigma_x - \sigma_y}{2} \cos(2\phi) + \tau_{xy} \sin(2\phi) \quad \text{I.5}$$

$$\tau = \frac{\sigma_y - \sigma_x}{2} \sin(2\phi) + \tau_{xy} \cos(2\phi) \quad \text{I.6}$$

Differentiating (I.5) and equating to zero, we get:

$$\tan(2\phi) = \frac{\tau_{xy}}{\sigma_x - \sigma_y} \quad \text{I.7}$$

Two values of the angle ϕ are provided by equation (I.7): one at which the primary stress σ is at its highest, and another at which it is at its minimum. The primary stresses are the corresponding values of σ . There is always a 90° angle between the two major stresses. The shear stress τ is 0 if you compute it along the major stress's direction (also known as the principal directions).

Similarly, we may find the angles at which we obtain the maximum and minimum shear stresses by differentiating (I.6) and equal it to zero:

$$\tan(2\phi) = \frac{\sigma_x - \sigma_y}{2\tau_{xy}} \quad \text{I.8}$$

Additionally, you will obtain the following results if you compute the tensile/compressive stress associated with these angles:

$$\sigma = \frac{\sigma_x + \sigma_y}{2} \quad \text{I.9}$$

The two normal stresses are equal (but not zero) in the direction of the primary shear stress. The general, 3D situation has comparable relationships, but this is outside the purview of this course. The fact that we can calculate the stresses in any area of the part (by taking into account a small element at that place) and then calculate the corresponding major stresses under specific loading conditions is all that interests us. The material will fail if its strength—which we will describe shortly—is less than the major stresses, whether shear or normal. It is outside the purview of this course to examine in detail how to calculate the stresses in non-uniformly formed pieces, but we will examine several straightforward but crucial examples.

I.2.3 Chemical properties

What Constitutes Matter's Chemical Properties?

Part I: Materials and their characteristics

The ability of matter to transform into new matter is described by its chemical characteristics. Reactivity is one of matter's chemical characteristics. A substance's reactivity is its capacity to transform into another substance.

Flammability is one type of reactivity. The tendency of an object to burn is known as flammability. Wood, for instance, has the chemical characteristic of being flammable. The effect of burning wood in a campfire or fireplace may be familiar to you. Wood transforms into a variety of chemicals when it burns. Among these new compounds are smoke and ash. The new materials' characteristics differ from the wood's initial characteristics. Smoke and ash don't burn. They are chemically non-flammable, in contrast to wood.

Changes in color or odor, heat production, fizzing and foaming, and the emission of sound or light are some indicators of chemical changes.

- When comparing chemical and physical properties, how can one distinguish between the two types of properties? Since a physical attribute does not alter a substance's identity, it can be observed or recognized.

When gold is melted or silver is pounded to create jewellery, a physical shift takes place. Following the alteration, the gold remains gold and the silver remains silver. A substance's chemical characteristics cannot be observed unless its identification is altered. For instance, it could be impossible to determine if a liquid is combustible unless you attempt to light it. It possesses the chemical characteristic of flammability if it burns. Burning, however, has transformed the fluid into new compounds.

Chemical characteristics are always present in a substance. Even when a piece of wood isn't burning, it might still catch fire. Iron that hasn't corroded can nevertheless develop rust.

Part II:
Solid solutions

Part II : Solid solutions

Introduction

Since prehistoric times, the significance of solid solutions has been understood. In the disciplines of physics, metallurgy, materials science, chemistry, and Earth science, including mineralogy, petrology, and geochemistry, solid solutions also known as mixed crystals are studied.

The characteristics of the end-member composition phase and solid solution phases might differ greatly. For instance, the bulk modulus of MgSiO_3 with a perovskite structure can be significantly altered by the addition of trace amounts of Al_2O_3 .

Therefore, it is a problem for all disciplines that deal with the solid-state to comprehend the behavior of solid solutions under various situations as well as their microscopic and macroscopic characteristics.

There are three types of solid solutions: interstitial, substitutional, and others. Different atoms may be dispersed across one or more common structural locations in a substitutional solid solution. The solute atoms in interstitial solid mixtures are found in the host structure's interstices, which are not regarded as typical atomic locations.

II.1 Solid solutions

In the solid state, it is a uniform mixing of two or more types of atoms (see Figure II.1). The more common atomic form is called a solvent, whereas the less common form is called a solute.

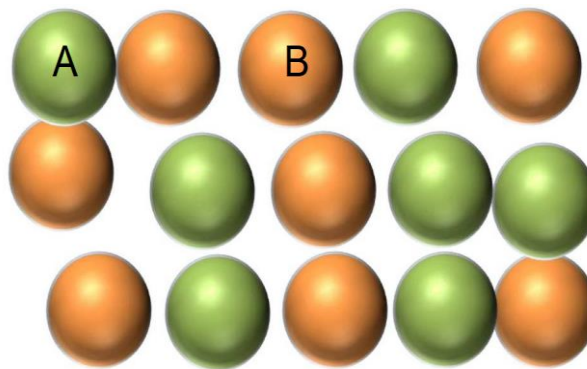


Figure II.1. Schematic illustration of a solid solution.

II.2 Types of Solid Solution

There are two different kinds of solid solutions: interstitial and substitutional solid solutions.

Part II : Solid solutions

II.2.1 Substitutional solid solution

Here, one kind of atom is directly swapped out for another, allowing solute atoms (copper) to enter the crystal and occupy spaces that would typically be filled by atoms of solvent (nickel) (see Figure II.2).

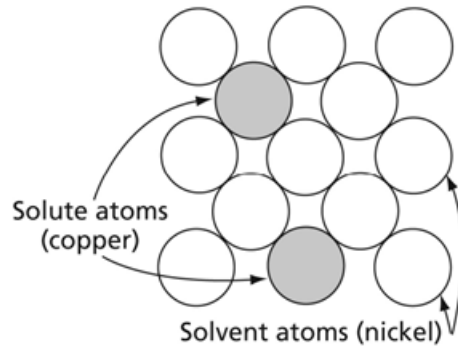


Figure II.2. Schematic illustration of substitutional solid solution type.

II.2.1.1 Ordered and disordered substitutional solid solution

There are two types of substitution in substitutional solid solutions: disordered and ordered (see Figure II.3).

On their lattice site, the solute atoms have replaced the solvent atoms in the situation of an organized substitutional solid solution.

On their lattice location, the solute atoms have haphazardly replaced the solvent atoms in a disordered substitutional solid solution.

When an AB alloy reaches a critical temperature (the order-disorder transformation temperature), its ordered structure vanishes. The degree of order at this temperature is as follows:

$$\delta = \frac{P_A - x_A}{1 - x_A} = \frac{P_B - x_B}{1 - x_B} \quad \text{II.1}$$

where, P_A and P_B are the probabilities of occupation of a specific sites by A and B atoms, respectively. x_A and x_B are the atomic ratios of A and B atoms, respectively.

For a complete disorder $P_A = x_A$, $P_B = x_B$ and $\delta = 0$; if, $P_A = P_B = 1$ and $\delta = 1$, is the case of a perfect order.

Part II : Solid solutions

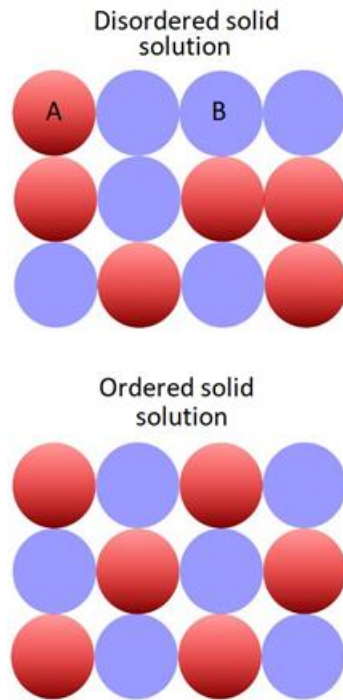


Figure II.3. Schematic illustration of an ordered and disordered substitutional solid solution.

The Figure II.4 below gives some examples of ordered structures, which are:

- L10 structure (AuCu type)
- L12 structure (AuCu₃ type)
- L2 structure (CsCl or beta brass type).

Part II : Solid solutions

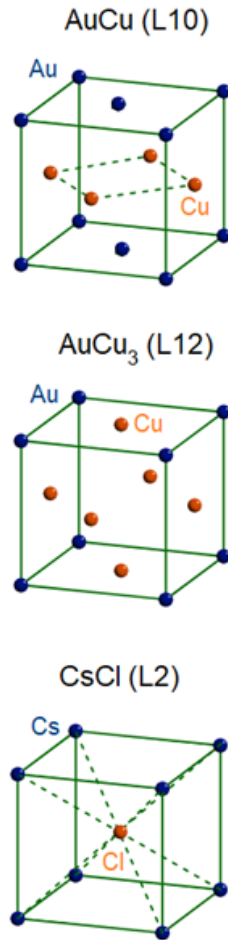


Figure II.4. Schematic illustration of some ordered structures, L10, L12 and L2.

II.2.1.2 Conditions for extensive solid solubility

The Hume-Rothery rules for the production of substitutional solid compounds are a set of guidelines that were developed by Hume Rothery through the study of several alloy systems. These are:

- **Crystal structure factor:** The two elements should have either F.C.C (Face Centred Cubic), B.C.C (Body Centred Cubic), or H.C.P (Hexagonal Close-Packed) structure when both elements (pure metals) have identical valence, resulting in total solid solubility.
- **Relative size factor:** The solubility of one substance in other is contingent upon the sizes of the substances differing by less than 15%. This is known as the relative size factor. Hume-Rothery's empirical rule for evaluating the atomic radii r (size) of compounds that produce solid solutions is as follows:

$$\text{Mismatch} = \left(\frac{r_{\text{solute}} - r_{\text{solvent}}}{r_{\text{solvent}}} \right) \times 100 \leq 15\%. \quad \text{II.2}$$

Part II : Solid solutions

- **Relative valence factor:** To attain maximal solubility, the atoms of the solute and solvent should normally have the same valence.
- **Chemical affinity factor:** When the two metals have a lower chemical affinity, solid solubility is preferred. The two metals have a higher affinity for chemicals and are more likely to form a compound rather than a solid solution if they are separated significantly in the periodic table.

II.2.2 Interstitial solid solution

As seen in Figure II.5, the carbon atom (i.e. solute atom) penetrates one of the interstices, or holes, between the solvent atoms (iron), rather than dislodging one of them.

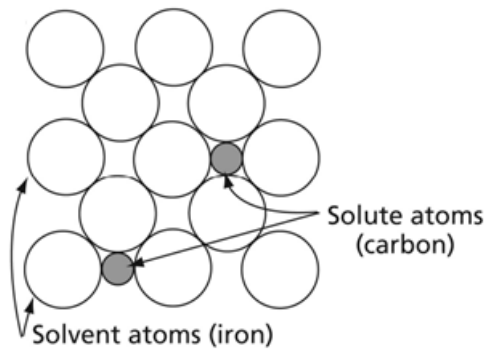


Figure II.5. Schematic illustration of interstitial solid solution type.

II.2.2.1 Octahedral and tetrahedral interstitial sites

An "interstitial defect" develops if the interstitial space is not empty. Many of the most crucial material characteristics, such the ductility of metals, are made possible by defects. Only in the case that the atoms of the additional element are much smaller than those of the parent metal can they fit into the gaps or interstices in the parent metal's crystal lattice and create interstitial solid solutions.

Based on the quantity of surrounding atoms, there are two sorts of interstitial sites that could exist:

- Octahedral site (O),
- Tetrahedral site (T).

- **Octahedral sites in FCC structure**

In F.C.C (Face Centred Cubic) structure, we can find four sites. (See Figure II.6) These are three at the middle of the edges ($\frac{1}{2}, 0, 0$) and one in the middle of the cube ($\frac{1}{2}, \frac{1}{2}, \frac{1}{2}$). Six

Part II : Solid solutions

neighbors are located at a distance of $a/2$ from each site (a represents the lattice parameter's value).

The elements are in contact along the $\langle 110 \rangle$ directions in the FCC lattice. The site's dimension (radius) is determined by the minimum dimension R_i of the space that the first neighbor atoms leave unoccupied. This gives:

$$R_s = a\sqrt{2}/4, \text{ whence, } R_i = a \cdot (1/2 - \sqrt{2}/4) = 0.147 a.$$

- **Tetrahedral sites in FCC structure**

There are eight sites. In $(1/4, 1/4, 1/4)$, these are the centres of the elementary cube's little eighth cubes. At distance R ($R = (a\sqrt{3})/4$, which is the quarter diagonal of the lattice), each site has four neighbors: Its radius is,

$$R_i = R - R_s = a/4 \cdot (\sqrt{3} - \sqrt{2}) = 0.08 a.$$

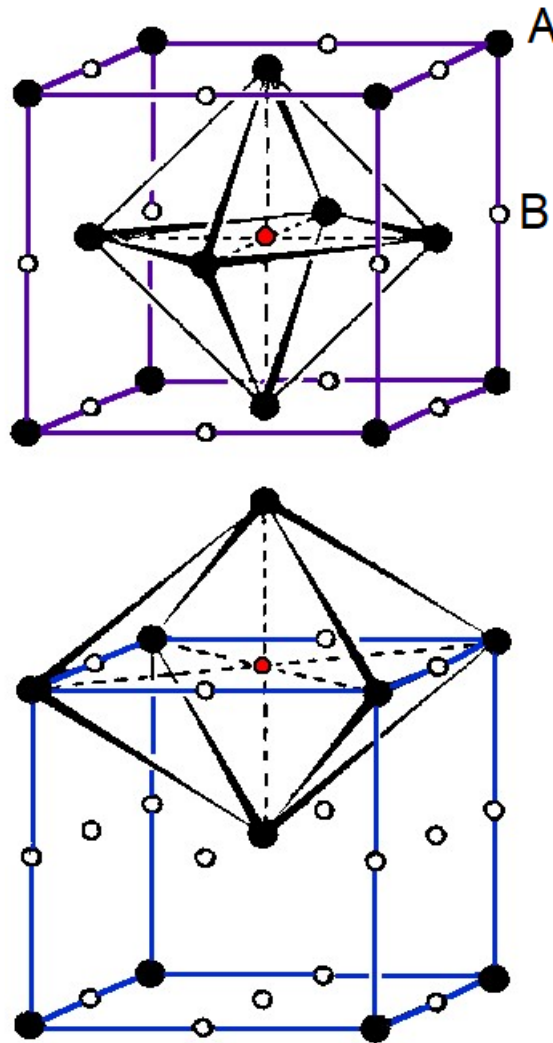


Figure II.6. Octahedral sites in FCC structure.

Part II : Solid solutions

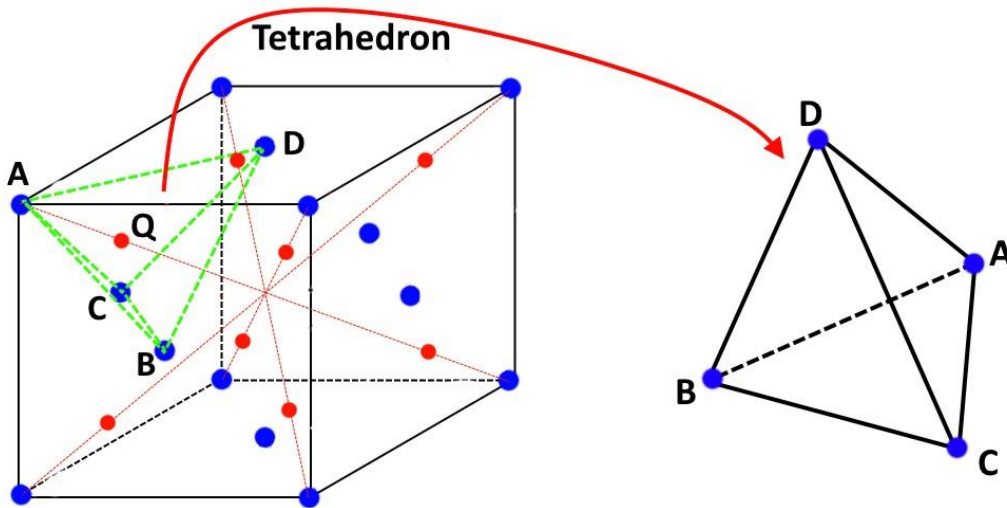


Figure II.7. Tetrahedral sites in FCC structure.

By inserting octahedral and/or tetrahedral defects in densely packed lattices, several different inorganic crystal forms are created (at least hypothetically). Figure II.8 displays a few of the most prevalent structures that originate from the fcc lattice, including fluorite, halite, and zinc-blende, as well as a somewhat uncommon one called Li_3Bi . The hexagonal relatives of zinc-blende and NaCl , respectively, the NiAs and wurzite systems, can be formed from the hcp lattice.

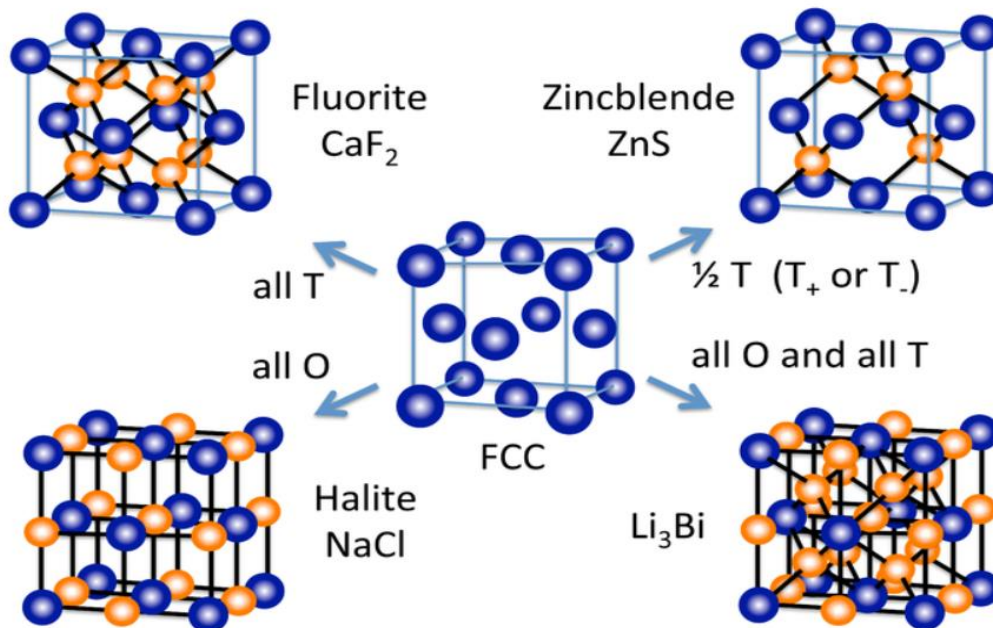


Figure II.8. Some FCC crystal structures.

- **Octahedral sites in BCC structure**

Part II : Solid solutions

For B.C.C (Body Centred Cubic) structure, we can find six sites. In $(\frac{1}{2}, \frac{1}{2}, 0)$ and $(0, 0, \frac{1}{2})$, these are the faces' centres and the midpoints of the lattices of the BCC cube. The base lattice has six atoms surrounding each side. This gives:

$$R_s = a\sqrt{3}/4, \text{ whence, } R_i = a.(1/2 - \sqrt{3}/4) = 0.067 a.$$

- **Tetrahedral sites in BCC structure**

There are twelve locations in all. These are located on the faces in $(\frac{1}{2}, \frac{1}{4}, 0)$ halfway between two octahedral sites. Four elements of the base of the lattice are spaced (equidistant) from each site:

$$R = a\sqrt{5}/4, \text{ then, the dimension of the site is: } R_i = R - R_s = (a\sqrt{5}/4 - a\sqrt{3}/4) = 0.127 a.$$

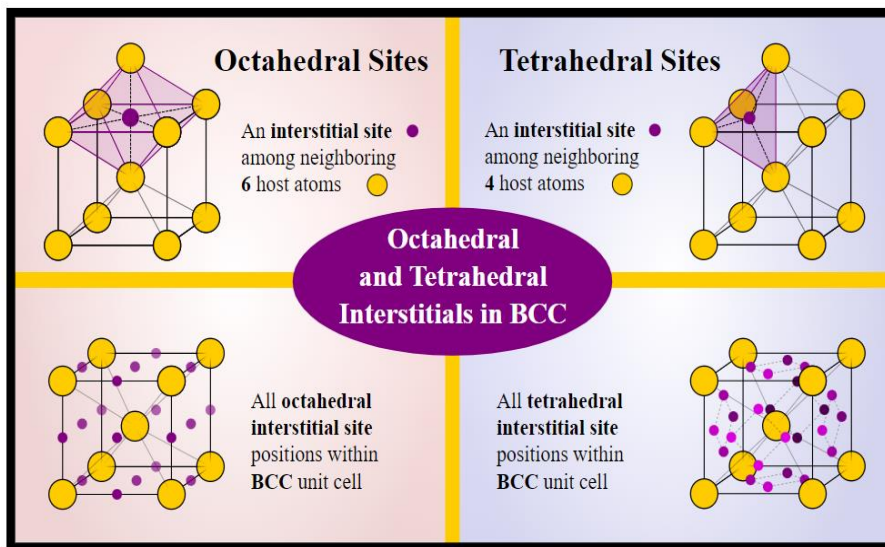


Figure II.9. Octahedral and tetrahedral sites in BCC structure.

- **Interstitial Sites in HCP**

With 6 and 12 octahedral and tetrahedral sites, respectively, the HCP (Hexagonal Close-Packed) unit cell has precisely 50% more sites than the FCC. Given that HCP is precisely fifty percent bigger than FCC and that both are densely populated, this shouldn't come as a surprise.

Part II : Solid solutions

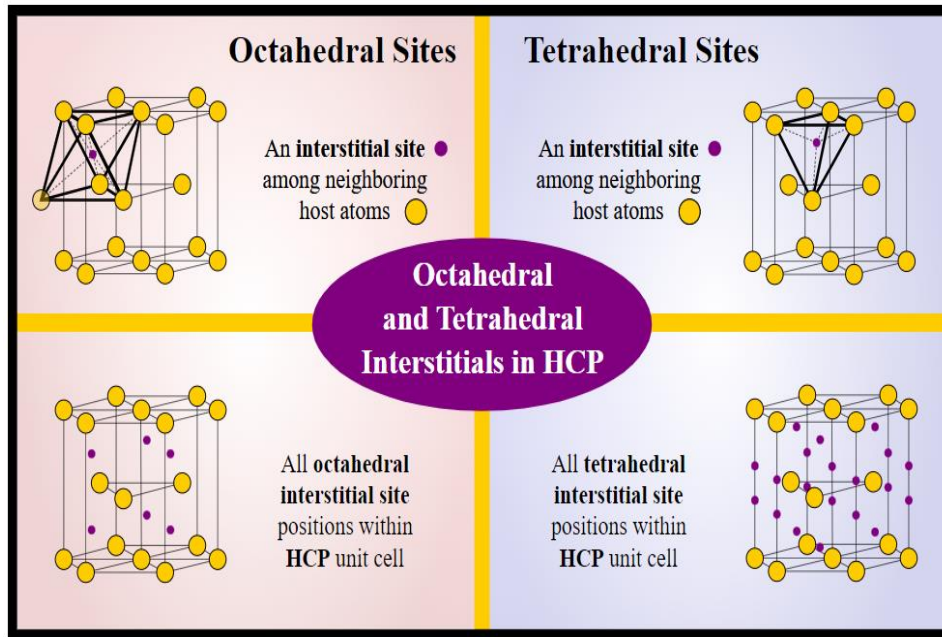


Figure II.10. Octahedral and tetrahedral sites in HCP structure.

II.3 Intermediate phases

There are several alloy systems that have phases that differ from the primary components (pure metals). As solid solutions, these formations are referred to as nonstoichiometric compounds or nonstoichiometric intermetallic compounds if they occur throughout a range of compositions. Nonetheless, the novel crystal structures are intermetallic compounds having stoichiometric contents when they arise with straightforward whole-number fixed ratios of the constituent atoms.

Examples

Example 1

The alloying of copper and zinc to create brass results in the formation of several new structures with varying compositions. This new phase's crystal structure is body-centered cubic, while zinc's is close-packed hexagonal and copper's is face-centered cubic. Since this BCC structure is the sole stable phase at ambient temperature within 47 and 50 weight percent of zinc, it can exist throughout a wide range of compositions, making it a solid solution rather than a compound. This is sometimes referred to as a non-stoichiometric intermetallic compound or nonstoichiometric compound (occasionally).

Example 2

A distinct intermetallic complex is seen when carbon is introduced to iron in quantities with a small amount at room temperature. In contrast to either iron (body-centered cubic) or carbon

Part II : Solid solutions

(graphite), this compound has a stable content (6.67 weight percent of carbon) and a complicated phase (orthorhombic, with 12 atoms of iron and 4 carbon atoms per unit cell).

Example 3

The impact of nanoscale intermediate phases on α precipitation in a high-strength titanium alloy that is close to β [3]:

- A “ β -solutionized Ti-5Al-3Mo-3V-2Cr-2Zr-1Nb-1Fe” alloy showed two types of intermediate phases, O' and ω , depending on the rate of cooling. Prior to α precipitation, the isothermal ω precipitated from β when the as-solutionized sample was heated to the ageing temperature. On the other hand, the O' was continually generated and eventually helped precipitate the α . Because the air cooling sample contained more O' domains, the aged sample had a finer microstructure and more strength [3].

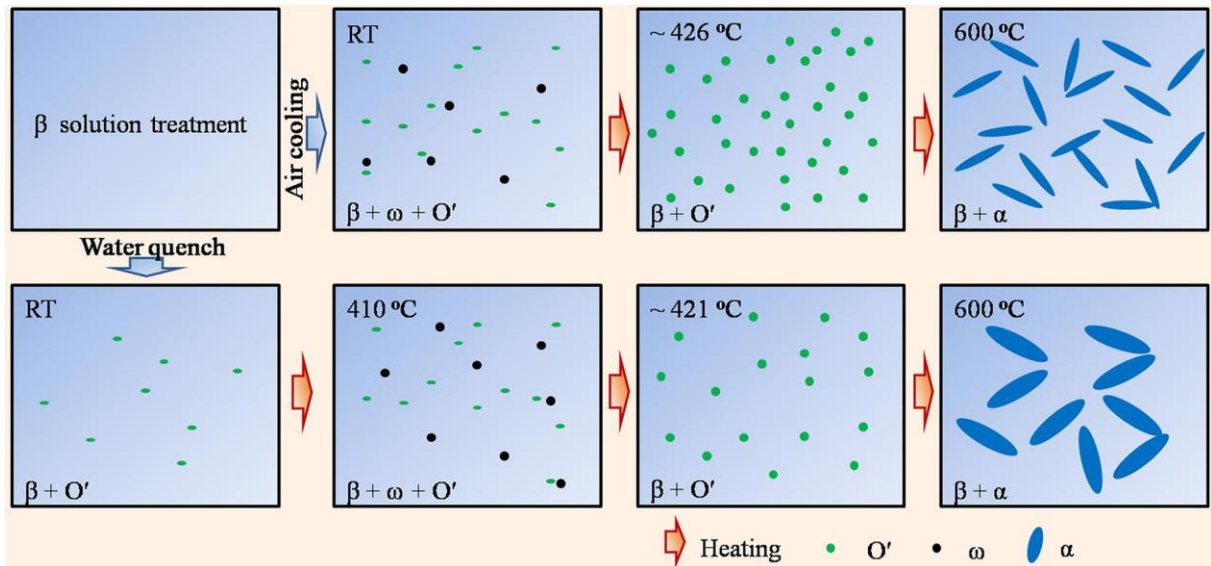


Figure II.11. Depending on the heating and cooling procedures, the Ti-5Al-3Mo-3V-2Cr-2Zr-1Nb-1Fe alloy can have intermediate phases [3].

Metal solid solutions can have interesting mechanical properties when intermetallic compounds precipitate or are finely dispersed within them.

Part III:
Binary phase diagrams

Part III: Binary phase diagrams

Introduction

To study materials science, one must have a basic understanding of phase diagrams. A system's equilibrium state under a specific set of circumstances serves as the foundation for the description of numerous processes and occurrences.

When a system's phases are in equilibrium, every one of the thermodynamic parameters are represented graphically in a phase diagram. The most common phase diagrams that materials scientists are familiar with include those that include temperature, T , and mixture as variables.

III.1 Phase diagram

A temperature-composition map that shows the phases present at a specific temperature and composition is called a phase diagram (see Figure III.1).

Three distinct stages are shown in the phase diagram:

- α a primary solid solution of A (or solid solution of B in A).
- β a primary solid solution of (or solid solution of A in B).
- L a liquid phase.

The liquidus line, which divides a liquid state from a solid + liquid phases region, is shown as a line in blue on a phase diagram. For a system to become fully liquid, it needs to be heated exceeding the liquidus temperature.

A solid phase and the solids + liquid phase area are separated by the solidus line, which is shown as a line in green on a phase diagram. The system must cool below the solidus point in order to be fully solid.

The intersection of liquidus and solidus lines for a pure component (in our case 100% A or 100%B) represents its melting temperature.

Part III: Binary phase diagrams

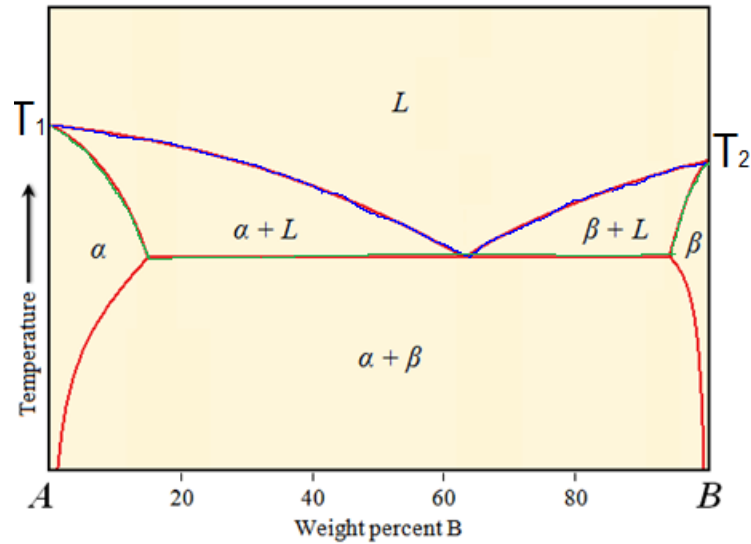


Figure III.1. Example of A-B phase diagram.

A phase is a section of the microstructure that is homogeneous in both structure and chemistry. Phase is a term used in metallurgy to describe a physically homogeneous condition of matter that has a specific chemical composition, atomic bonding, and elemental arrangement.

Microstructure: What is it? The term "microstructure" originally referred to the internal structure of a substance that could be seen under a microscope.

Phase diagrams allow us to:

- For each particular alloy composition system, determine the temperature where the freezing or melting starts or stops.
- At a given temperature, identify the number, kind, and makeup of phases that are present in any given alloy.
- Determine the proportions of each phase in a double-phase alloy.
- Forecast an alloy's microstructure at a specific temperature.
- Estimate potential heat treatments.
- To provide the optimum qualities, select the alloy composition.

III.2 Limitations of Phase Diagrams

Although phase diagrams are very helpful in interpreting the microstructures formed in alloys, they have a number of drawbacks:

Part III: Binary phase diagrams

- Alloys are usually cooled sufficiently slowly to reach equilibrium in typical industrial operations; phase diagrams only depict the state of equilibrium of alloys, or under extremely slow cooling rates.
- Fast cooling rates do not produce distinct phases, which are not shown in phase diagrams. The Fe-Fe₃C phase diagram, for instance, does not depict the production of martensite.
- The nature of the changes is not revealed by phase diagrams, even in the presence of equilibrium. They don't show how quickly the equilibrium will be reached.
- Phase diagrams don't show the distribution of the phases, shape or their size, which influences their final mechanical properties; instead, they don't provide details about the structural distribution of the phases.

III.3 Phase diagram applications

In four main fields, phase diagrams are helpful to researchers like metallurgists, materials scientists, and engineers:

- (1) Developing novel alloys for particular uses,
- (2) Using these alloys to create practical configurations,
- (3) Developing and managing heat treatment processes for particular alloys that will yield the necessary mechanical, chemical, and physical characteristics;
- (4) Resolving issues that arise with particular alloys' effectiveness in commercial applications, hence enhancing product predictability.

III.4 Intensive and extensive properties

While extensive qualities are directly related to the amount of material in the system, such as V (volume), S (entropy), H (enthalpy), U (or E, internal energy), and G (Gibbs free energy), intensive properties such as T (temperature) and P (pressure) are independent of the system's size.

III.5 Concept of Free energy

The Gibbs free energy of the system determines its relative stability for changes that take place at constant pressure and temperature:

$$G = H - TS \quad \text{III.1}$$

where H is the enthalpy. Enthalpy is a measure of the heat content of the system and is given by:

$$H = U + PV \quad \text{III.2}$$

Part III: Binary phase diagrams

The sum of the kinetic and potential energies of all the atoms in the system is the internal energy, or E . Kinetic energy is the consequence of the rotational as well as energies of atoms and translational molecules in a liquid or gas, as well as the vibration of atoms in solids or liquids. Interactions or bonding between the elements in the system provide potential energy.

When a system reaches its most stable condition and shows no signs of changing over time, it is said to be in equilibrium. A system with a set weight and composition (a closed system) and a constant pressure and temperature will be in stable equilibrium if its Gibbs free energy is as low as possible:

$$dG = 0 \qquad \text{III.3}$$

The state with the highest entropy and the lowest enthalpy will have the most stability according to this description of free energy. Solid phases are therefore the most stable at low temperatures due to their strongest atomic bonds and, consequently, their smallest enthalpy (internal energy). The $-TS$ term takes over at high temperatures, though, and the liquid and finally vapor phases become the most stable.

Figure III.2 provides a graphic representation of equilibrium as defined by Eq. III.3. Along the abscissa, the points reflect the different potential atomic configurations. The configuration with the stable equilibrium will be the one with the lowest free energy, G . Consequently, arrangement A would be the configuration of stable equilibrium. Other configurations do not have the lowest conceivable value of G , such as configuration B, but they do lie at a local minimum of free energy. To differentiate these configurations from the stable equilibrium state, they are referred to as metastable equilibrium states. The remaining configurations that fall between A and B are unstable intermediate states with $dG = 0$.

Part III: Binary phase diagrams

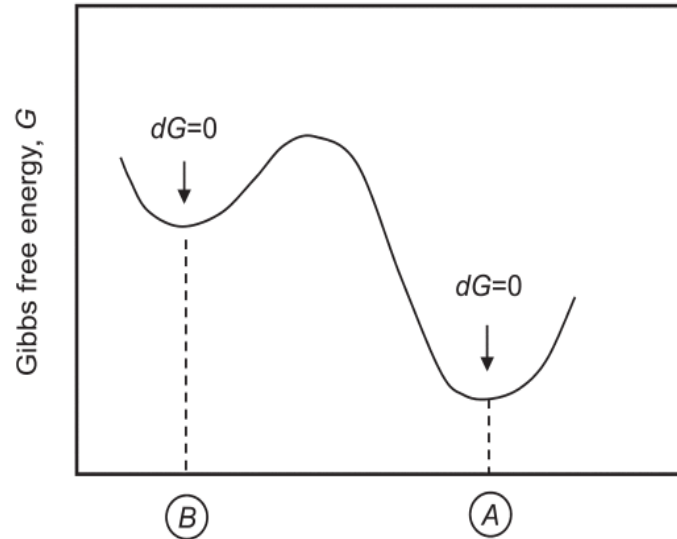


Figure III.2. Gibbs energy for various system atomic configurations. Since configuration (A) has lowest free energy, it is the stable equilibrium arrangement. The state of configuration (B) is metastable equilibrium.

III.6 Gibbs phase rule

According to Gibbs' phase rule, a closed system at equilibrium may have as many degrees of freedom (F) as there are distinct phases (P) and chemical constituents (C) in the system.

$$F = C - P + 2 \quad \text{III.4}$$

Composition, pressure, and temperature are the three variables that can be altered separately without altering the system's phases, which is known as the degree of freedom (or variance) F.

Under realistic circumstances, pressure can be regarded as a constant (1 atm.) in metallurgical and materials systems. Consequently, the Condensed Gibbs phase rule is expressed as:

$$F = C - P + 1 \quad \text{III.5}$$

III.7 Some binary phase diagrams

III.7.1 Complete solid and liquid solution diagram

Figure III.3, which shows the Cu-Ni system, is an example of a binary diagram of phases that is straightforward to read and comprehend. The three distinct phase zones in this diagram, the liquid (L), the alpha (α), and the alpha + liquid regions are characterized by certain compositions and temperatures. The full solubility of its elements in both liquid and solid media is a notable characteristic of the Cu-Ni system.

Part III: Binary phase diagrams

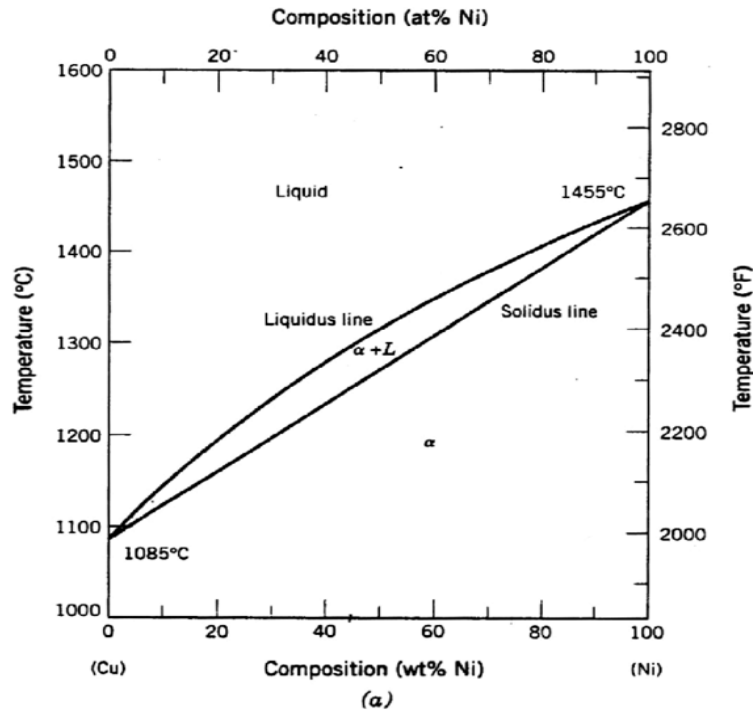


Figure III.3. Cu-Ni phase diagram [4].

III.7.2 Binary diagram corresponding to domains of partial miscibility

Many materials are frequently found to exhibit very little mutual miscibility in the solid state yet to be extremely miscible in the liquid state. Thus, a 2-phase field with two distinct solid structures—one highly enriched in component A (the phase) and one highly enriched in component B (the phase)—dominates a large portion of the phase diagram at low temperatures. These binary systems are known as eutectic systems because of their poor or nonexistent solid state miscibility and infinite liquid state miscibility.

We use the Pb-Sn system scenario shown in Figure III.4 as an example. This phase diagram shows that alloys with 0–2% Sn solidify to form a single solid solution (α , or solid solution of tin in lead), while alloys with 2–19% Sn solidify to form a single solid solution (α), but as the alloy cools, a solid state reaction takes place, allowing a second solid phase (β , or solid the mixture of lead in tin) to precipitate from the initial α phase.

Tin has a limited solubility in α solid solution. Only 2% of Sn may dissolve in α at 0°C. The solubility of tin in lead increases with temperature, reaching its maximum solubility of 19% Sn at 183°C. This is because additionally tin dissolves into the lead as the temperature rises. The phase border between α and $\alpha + \beta$ indicates the solvus curve, which provides the dissolution of tin in solid lead at any temperature.

Part III: Binary phase diagrams

This diagram shows an eutectic reaction (upon cooling or heating) at 183°C with composition of 61.9% Sn and 38.1% Pb, as follows:

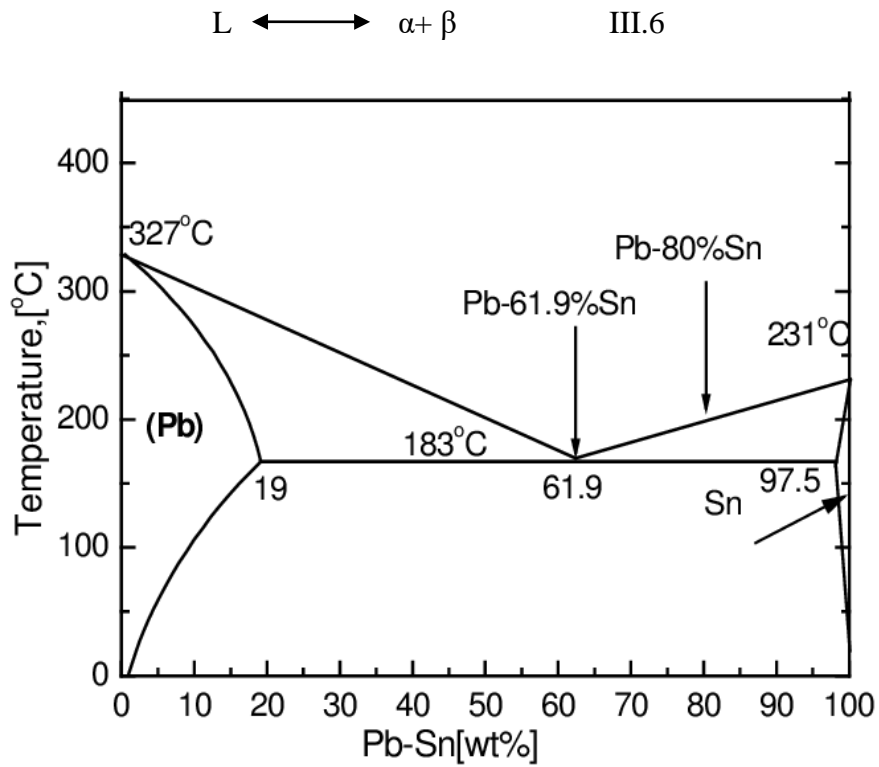


Figure III.4. Pb-Sn phase diagram [5].

Figure III.5 shows the evolution of microstructure change for lead-tin alloy of composition C₄ (Pb-40%Sn) from liquid phase to solid state under cooling.

Part III: Binary phase diagrams

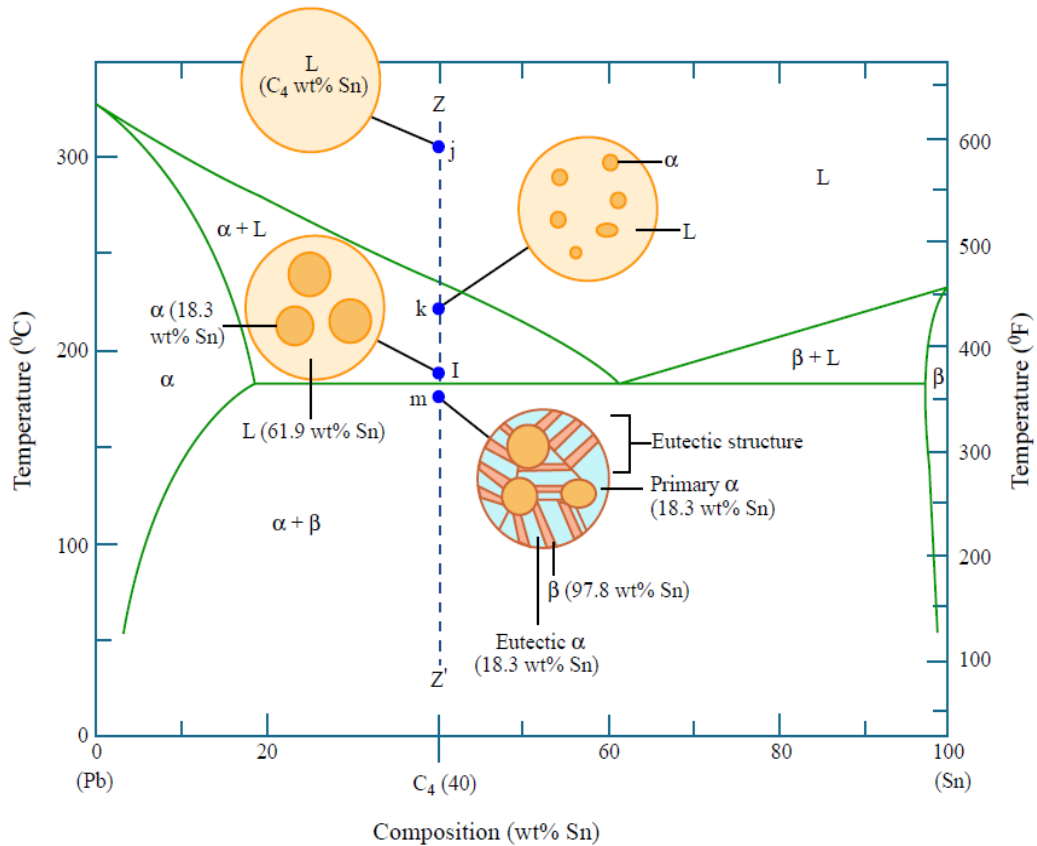


Figure III.5. Diagrammatic depictions of the a state of equilibrium microstructures formed by cooling a C₄ lead-tin alloy from the liquid-phase region.

III.7.3 Binary diagram showing intermediate phases

Figure III.6 shows the nickel-sulfur phase diagram up to 52% (wt.%) of sulfur content. This diagram shows several nonstoichiometric (or a nonstoichiometric intermetallic compounds) and stoichiometric (or stoichiometric intermetallic compounds) compounds. The nonstoichiometric intermetallic compounds are ϵ , δ , β_1 and β_2 , while intermetallic compounds are β' , γ (Ni_7S_6), ξ (Ni_3S_4) and η (NiS_2).

This diagram shows many reactions among them, we mention:

- Eutectic reaction at 637°C with 21%S: $\text{L} \longleftrightarrow (\text{Ni}) + \beta_1$.
- Eutectoid reaction at 540°C with 24%S: $\beta_1 \longleftrightarrow (\text{Ni}) + \beta'$.
- Peritectic reaction at 840°C with 29%S: $\text{L} + \delta(\text{NiS}) \longleftrightarrow \beta_2$.

Part III: Binary phase diagrams

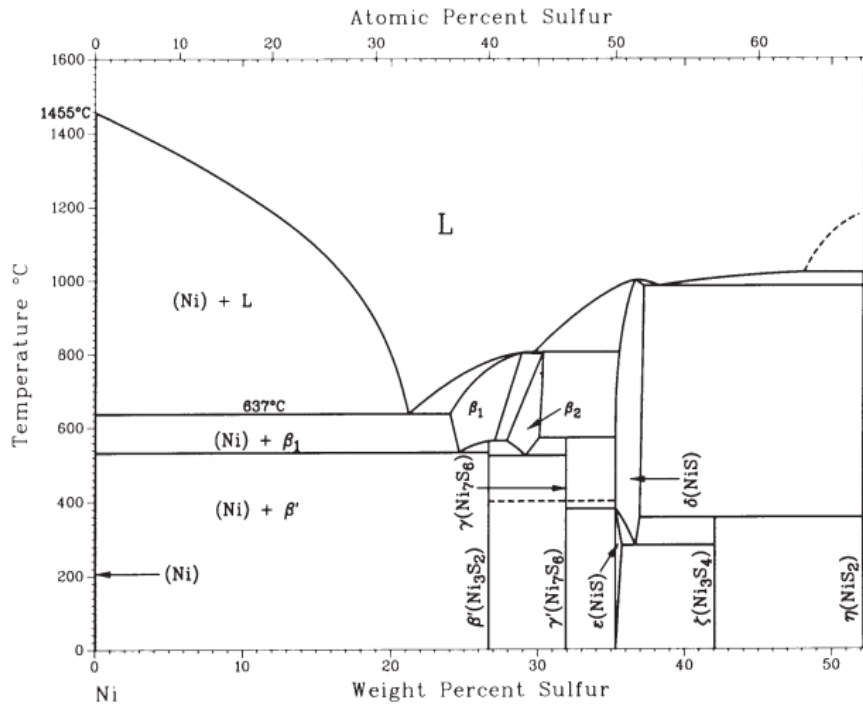


Figure III.6. The Ni-S phase diagram [6].

III.8 The Lever rule

The lever rule can be applied to the phase diagram in order to determine the quantity of every phase present in an alloy that includes many phases.

A basic balance can be used to illustrate the lever rule. The ends of a bar represent the chemical compositions of the two phases, whereas the fulcrum represents the alloy's composition. As shown in Figure III.7, the weights required to equilibrium the system dictate the ratios of the phases that are present.

$$\text{Fraction of phase 1 (L)} = (C_2 - C) / (C_2 - C_1)$$

$$\text{Fraction of phase 2 (}\beta\text{)} = (C - C_1) / (C_2 - C_1)$$

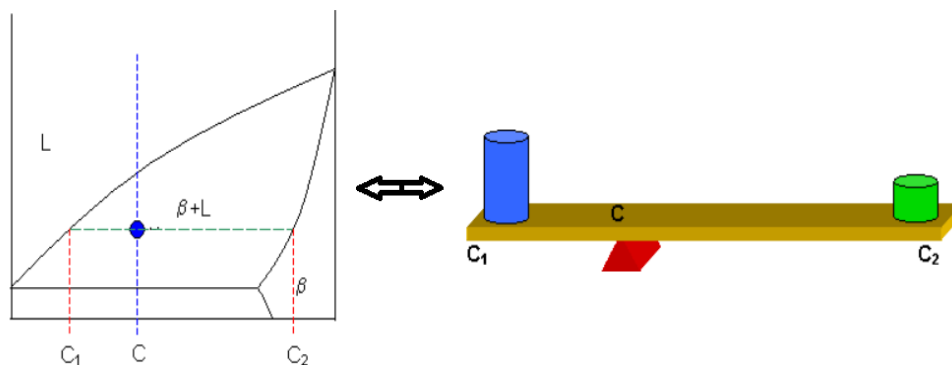


Figure III.7. Schematic illustration of Lever rule.

Part III: Binary phase diagrams

III.9 Experimental determination of phase equilibriums diagrams

After preparing the specimens, there are several techniques to build a diagram of phase by characterize the number and nature of phases present:

- Differential Thermal Analysis, (DTA),
- Thermogravimetric analysis, (TG),
- Differential Scanning Calorimetry, (DSC),
- In situ X-Ray diffraction, (XRD),
- Optical Microscopy, (OM),
- Scanning Electron Microscopy (SEM), etc.

III.10 Phase diagram determination examples

This section uses two phase diagrams as examples to demonstrate the process of determining them step-by-step. We begin with the example of the Cu–Nd binary and then move on to a basic ternary Al–Be–Si system.

- **The Cu–Nd Binary System**

The Cu–Nd system serves as the first illustration (Fig. III.8). Several groups determined the phases of the binary compounds (NdCu, NdCu₂, NdCu₄, NdCu₅, and NdCu₆). This binary phase diagram was created by combining metallography, DTA, and XRD. The initial materials were chips of 99.9% pure Nd and 99.999% pure Cu. Acetone was used to clean them, followed by water flushing and drying. The oxides on the Cu chips' surface were eliminated by additional submersion in diluted sulphuric acid. A high-frequency induction furnace with an argon shield and a pressure marginally greater than one atmosphere was used to manufacture the binary alloys. The containers were aluminum oxide crucibles with covers. The melting time was approximately 4 minutes for the Nd-rich samples (≤ 50 weight percent Cu), and 4 to 15 minutes for the other alloys, depending on their composition. For every alloy, the melting loss was less than 0.6%. After being enclosed in evacuated quartz tubes, the as-cast alloys underwent homogenization heat treatments. Samples containing 0–51 at.% Cu were annealed for 42 days at 410°C, and samples containing 51–67 at.% Cu were annealed for 50 days at 500°C. For 42 days, the remaining samples were homogenized at 720 °C. Samples that had been annealed were gradually cooled to room temperature. The homogenized alloys were subjected to chemical analysis in order to ascertain the departure from nominal compositions.

Part III: Binary phase diagrams

The annealed samples' surfaces were polished and lightly ground before being ground into powders. For residual stress alleviation treatment, the powders were sieved using 325 meshes and then placed in evacuated glass tubes. This was done for five days at 410°C for alloys with Cu < 51 at.% and for three days at 500°C for the other alloys. The annealed materials were cooled at a rate of 10°C per hour to room temperature.

Bulk samples of alloys having a composition between Nd and NdCu were sealed in evacuated quartz tubes, encapsulated with Ta foils, and annealed at extreme temperatures for 20 hours before being quenched in water to collect phase distribution data at elevated temperatures. For XRD examination, they were subsequently ground into powders and put through the same procedure as previously mentioned.

To maximize the peak to background ratio, one guideline for choosing an XRD radiation source is to have the sample's characteristic X-ray mass absorption coefficient as low as feasible. XRD was carried out using CuK α radiation at 26 kV and 22 mA for the alloys having a Cu concentration more than 50 at.%. FeK α radiation produced better XRD patterns for the other alloys. The phase disappearance approach was used to identify the phase boundaries. The peak positions of the two-phase alloys' XRD patterns match those of the nearby single phases, according to the results; no peak shift was seen. As a result, every binary compound is basically stoichiometric. The studies of the lattice parameter also showed that Cu and Nd had very little mutual solid solubility.

Using DTA and Al₂O₃ crucibles as a container, phase change temperatures were determined in an argon environment. Temperature calibration was performed using Cu, Ag, Sb, Al, and Zn. Table III.1 provides a summary of the findings together with the XRD data. A number of as-cast samples were examined microstructurally, particularly those with nominal compositions at the eutectic or peritectic point. According to the findings, there are three peritectic and three eutectic reactions. The DTA readings and the OM observations agreed with one other. XRD, DTA, and metallography experimental findings are used to build the Cu–Nd phase diagram, which is displayed in Fig. III.8 [7].

Part III: Binary phase diagrams

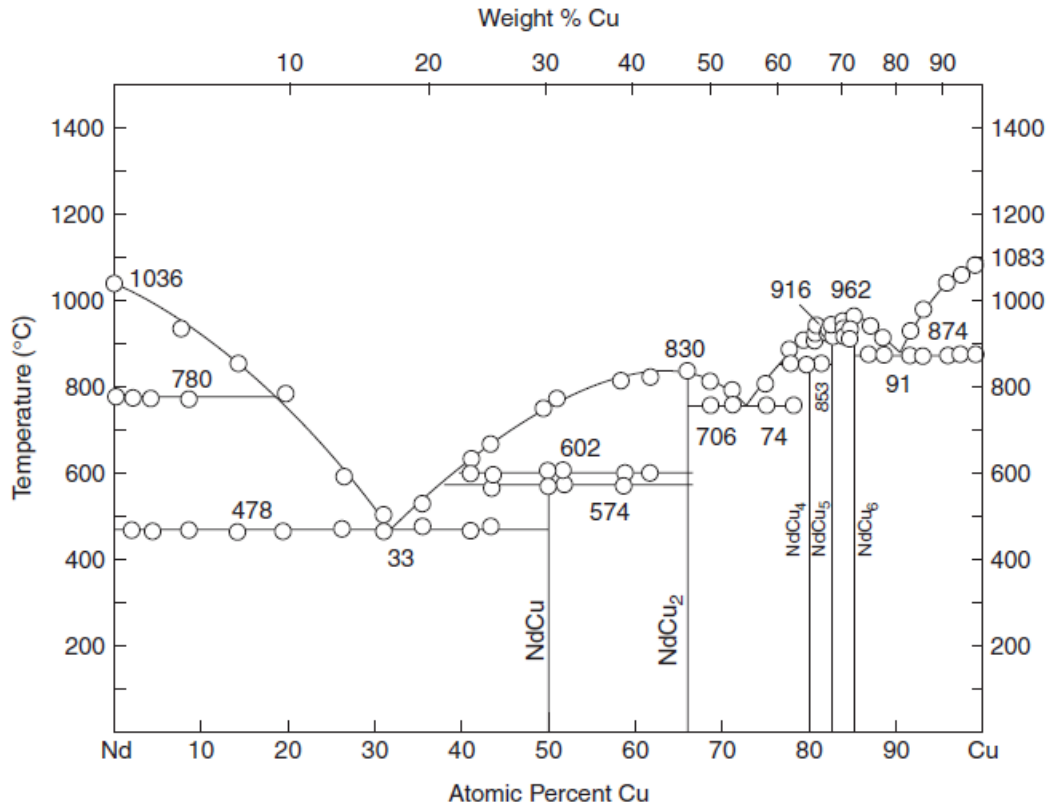


Figure III.8. Phase diagram of Cu-Nd system [7].

Part III: Binary phase diagrams

Table III.1. Some measurements data using DTA and XRD in the Cu-Nd system [7].

Composition at.% Cu	Phase at room temperature	Phase transition temperature from DTA (°C)								
		1	2	3	4	5	6	7	8	9
2.24	Nd + NdCu	470			778					
4.43		471			782					
8.64	Nd + NdCu	480			778					920
14.59		475								864
20.14	Nd + NdCu	469								790
26.98		482								600
31.73		474								510
36.20	Nd + NdCu	486								534
41.75		477		600						640
44.36	Nd + NdCu	485	568	602						670
50.00	NdCu		572	604						754
51.64	NdCu + NdCu ₂		576	614						777
59.20			574	607						813
62.17	NdCu + NdCu ₂			602						818
66.67	NdCu ₂									830
69.41	NdCu ₂ + NdCu ₄					758				813
71.90						764				800
75.81	NdCu ₂ + NdCu ₄					759				810
78.74	NdCu ₂ + NdCu ₄					762	846			890
80.00	NdCu ₄						853			900
81.50	NdCu ₄ + NdCu ₅						853	908	928	
83.33	NdCu ₅							916	936	
84.12	NdCu ₅ + NdCu ₆							920	940	
84.75	NdCu ₅ + NdCu ₆							918	953	
85.71	NdCu ₆									962

(Continued)

Part III: Binary phase diagrams

Table III.1. (Continued) [7].

Composition at.% Cu	Phase at room temperature	Phase transition temperature from DTA (°C)								
		1	2	3	4	5	6	7	8	9
87.78	NdCu ₆ + Cu							876		944
88.95	NdCu ₆ + Cu							872		918
92.26								872		932
93.82	NdCu ₆ + Cu							874		980
96.79								876		1044
98.20								874		1068
99.56	NdCu ₆ + Cu							880		1082

III.11 Thermodynamics of phase diagrams

The purpose of this part is to cover the basic principles of thermodynamics that are necessary for phase diagram interpretation and computation. The following sections will continue the development of phase diagram thermodynamics [7].

III.11.1 Thermodynamics' First and Second Law

The thermodynamic system in question is considered open if it is allowed to interchange mass and energy with its surroundings. The system is deemed closed if mass cannot be exchanged but energy may. The state of a system is determined by both extensive characteristics, like volume as well as internal energy, which change directly with the system's mass, and intensive qualities, like temperature and pressure, that are independently of the system's mass.

III.11.1.1 Nomenclature

Uppercase symbols will be used to express extensive thermodynamic properties. G = Gibbs energy in J, for instance. Lowercase symbols will be used to represent molar characteristics. For instance, where n is the total number of moles in the system, $g = G/n =$ molar Gibbs energy in J mol^{-1} .

III.11.1.2 The First Law

The entire thermal as well as chemical bond energy held in a system is its internal energy, or U (or E). It is a large piece of state land. Imagine a closed system going through a state transition in which it exchanges work (dW) and heat (dQ) with its environment. Given the need to conserve energy:

Part III: Binary phase diagrams

$$dU_n = dQ + dW \quad \text{III.7}$$

The First Law is this. It is accepted that energy entering the system from the environment is good. The system is closed (unchanged number of moles), as indicated by the subscript on dU_n . It is important to emphasize that dQ and dW do not represent modifications to state attributes. Since dU_n represents the change of a state attribute, it does not depend of the process path for a system moving from a given starting state to a particular final state; in contrast, dQ and dW are typically path-dependent.

III.11.1.3 The Second Law

The reader is directed to classic thermodynamics texts for a thorough and rigorous explanation of the Second Law. According to Boltzmann's equation, the system's entropy, S , is an extended state attribute that is as follows:

$$S = k_B \ln(t) \quad \text{III.8}$$

where k_B denotes Boltzmann's constant and t represents the system's multiplicity. Loosely defined, t represents the quantity of potential equivalent microstates within a macrostate, which corresponds to the number of quantum states accessible to the system given specific conditions such as energy and volume. For instance, in a system characterized by a collection of single-particle energy levels, t is the number of methods for allocating the particles across the energy levels while maintaining a constant total internal energy. At low temperatures, the majority of particles will occupy or be in proximity to the ground state. Consequently, t and S will be minimal. As the temperature, and consequently U , rises, a greater number of energy levels become populated. As a result, t and S rise. In solutions, an extra contribution to t results from the various potential configurations for spreading atoms or molecules over the lattice or quasilattice sites. In a rather imprecise manner, S might be seen as an indicator of a system's dysfunction.

In any spontaneous process, the overall entropy of the cosmos will rise, as disorder is inherently more probable than order. Specifically, for every spontaneous process:

$$dS_{total} = (dS + dS_{surr}) \geq 0 \quad \text{III.9}$$

dS and dS_{surr} represent changes in the entropy of the system and the surroundings, respectively. The presence of a state property S that fulfils Eq. (III.9) is fundamental to the Second Law.

Part III: Binary phase diagrams

Equation (III.9) constitutes a requisite condition for the occurrence of a process. Nonetheless, even if Equation (III.9) is fulfilled, the process may remain unobserved due to kinetic obstacles impeding its occurrence. The Second Law does not address the rate of a process, which may range from exceedingly rapid to infinitely slow.

The entropy change of the system, dS , may be negative for a spontaneous process provided that the sum ($dS + dS_{\text{surr}}$) is positive. For instance, during the process of solidification of a liquid, the change in the entropy of the system is negative when it transitions from the liquid to the more structured solid state. Nonetheless, a liquid under its melting point will undergo spontaneous freezing due to a sufficiently positive entropy change in the surroundings resulting from heat transfer from the system.

It is important to emphasise that the change in the entropy of the system dS , when transitioning from a specific starting state to a certain final state, is path-independent as it pertains to a state property change. Nonetheless, dS_{surr} is contingent upon its historical trajectory.

III.11.1.4 The Fundamental Equation of Thermodynamics

Examine an open system that is in equilibrium with its environment and maintains internal equilibrium. No spontaneous irreversible processes are occurring. Assume a state shift happens in which S , V (volume), and n_i (number of moles of component i in the system) vary by dS , dV , and dn_i , respectively. A change of state at equilibrium is termed a reversible process, with the associated heat and work represented as dQ_{rev} and dW_{rev} , respectively. We can thereafter express:

$$dU = (\partial U / \partial S)_{V,n} dS + (\partial U / \partial V)_{S,n} dV + \sum_i \mu_i dn_i \quad \text{III.10}$$

where

$$\mu_i = (\partial U / \partial n_i)_{S,V,n_{j \neq i}} \quad \text{III.11}$$

μ_i is the chemical potential of component i .

The absolute temperature is given as:

$$T = (\partial U / \partial S)_{V,n} \quad \text{III.12}$$

We anticipate that temperature should be delineated in a manner that facilitates the spontaneous transfer of heat from regions of high temperature to those of low temperature. To demonstrate that T , as defined by Eq. (III.12), is a thermal potential, examine two closed systems that are insulated from their environment yet in thermal contact, exchanging solely heat at constant volume. Designate the temperatures of the systems as T_1 and T_2 , with T_1

Part III: Binary phase diagrams

being greater than T_2 . Assume that thermal energy transfers from system 1 to system 2. Then $dU_2 = -dU_1 > 0$. Therefore, from Eq. (III.12):

$$dS = dS_1 + dS_2 = \frac{dU_1}{T_1} + \frac{dU_2}{T_2} > 0 \quad \text{III.13}$$

The transfer of heat from a higher to a lower temperature leads to an increase in total entropy and, according to the Second Law, occurs spontaneously. The second term in Eq. (III.10) is evidently $(-PdV)$, representing the labour of reversible expansion.

According to Eq. (III.12), the initial term in Eq. (III.10) is equivalent to TdS , which represents the reversible heat.

$$TdS = dQ_{rev} \quad \text{III.14}$$

In the specific instance of a reversible process, (dQ_{rev}/T) is path-independent since it corresponds to the change in a state function dS . Equation (III.14) constitutes the definition of entropy in the standard formulation of the Second Law. Equation (III.10) can now be expressed as:

$$dU = T dS + P dV + \sum_i \mu_i dn_i \quad \text{III.15}$$

Equation (III.15), derived from the integration of the First and Second Laws, is referred to as the fundamental equation of thermodynamics. We have posited that the sole work term is the reversible work of expansion, sometimes referred to as "PV work." This will generally be the case in this chapter. If additional forms of work are performed, then non-PV terms, $dW_{rev}(\text{non-PV})$, must be incorporated into Eq. (III.15). For instance, in a galvanic cell, $dW_{rev}(\text{non-PV})$ represents the reversible electrical work in the external circuit. Equation (III.15) can therefore be expressed more generally as:

$$dU = T dS + P dV + \sum_i \mu_i dn_i + dQ_{rev(\text{non-PV})} \quad \text{III.16}$$

III.11.2 Enthalpy

Eq. (III.2) defines enthalpy, H , as an extended state property. Examine a closed system going through a state transition that can entail irreversible procedures (like chemical reactions). We will assume that any work of expansion is roughly reversible (that is, that the exterior and internal pressures are equivalent) and that there is no work other than work of expansion, even though the process as a whole may be irreversible. Then, from Eq. (III.7):

Part III: Binary phase diagrams

$$dU_n = dQ - PdV \quad \text{III.17}$$

From Eqs (III.2) and (III.17) it follows that:

$$dH_n = dQ - VdP \quad \text{III.18}$$

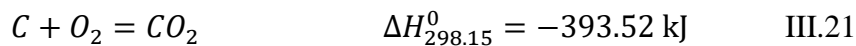
Furthermore, if the pressure remains constant throughout the process, then:

$$dH_P = dQ_P \quad \text{III.19}$$

Integrating both sides of Eq. (III.19) gives:

$$\Delta H_P = Q_P \quad \text{III.20}$$

That is, when a closed system transitions from an initial state to a final state at constant pressure, its enthalpy change is equal to the heat that is transferred to the environment. Because it is equivalent to the change of a state property, the heat for a process that takes place at constant pressure is hence path-independent. This outcome is significant. As an illustration, let's say that a system starts out with 1.0 mol of C and 1.0 mol of O₂ at 298.15 K and 1.0 bar of pressure, and ends up with one mole of CO₂ at the same pressure and temperature. This reaction has the following enthalpy change:



where the superscript on o indicates the standard state reaction involving $\Delta H_{298.15}^0$ pure solid graphite, O₂ and CO₂ at 1.0 bar. Therefore, regardless of the reaction path, an exothermic heat of -393.52 kJ will be recorded as long as the pressure is constant. For example, the reactants and products may reach high, unknown temperatures during the combustion reaction. Regardless of the intermediate temperatures, the total heat that has been transferred to the environment will be -393.52 kJ once the CO₂ product has cooled back to 298.15 K. The standard molar enthalpy of iron as a function of temperature is displayed in Figure III.9.

The y-axis, $(h_T^0 - h_{298.15}^0)$, is the amount of heat needed to raise one mole of iron from 298.15 K to temperature T while maintaining constant pressure. At constant pressure, the curve's slope represents the molar heat capacity:

$$C_P = (dh/dT)_P \quad \text{III.22}$$

Part III: Binary phase diagrams

The following formula, assuming no phase changes throughout the period, is derived from Eq. (III.22) and represents the amount of heat needed to heat one mole of an element at constant P from a temperature T_1 to a temperature T_2 :

$$(h_{T_2} - h_{T_1}) = \int_{T_1}^{T_2} C_P dT \quad \text{III.23}$$

Adiabatic calorimetry can be used to measure the heat capacity directly, or drop calorimetry can be used to measure the enthalpy curve. According to Figure III.9 [8], the typical equilibrium temperature of fusion (melting) for iron is 1811 K. Because the fusion process takes place at a constant temperature, it is a first-order phase transition. According to Δh_f in Fig. III.9, the typical molar enthalpy of fusion is $13.807 \text{ kJ mol}^{-1}$. It can also be seen on Fig. III.9 that Fe undergoes two other first-order phase changes, the first from α (bcc) to γ (fcc) Fe at $T_{\alpha \rightarrow \gamma} = 1184.8 \text{ K}$ and the second from γ to δ (bcc) at 1667.5 K . The enthalpy changes are 1.013 and $0.826 \text{ kJ mol}^{-1}$, respectively. $T_{\text{curie}} = 1045 \text{ K}$, the Curie temperature, is likewise displayed on Fig. III.9.

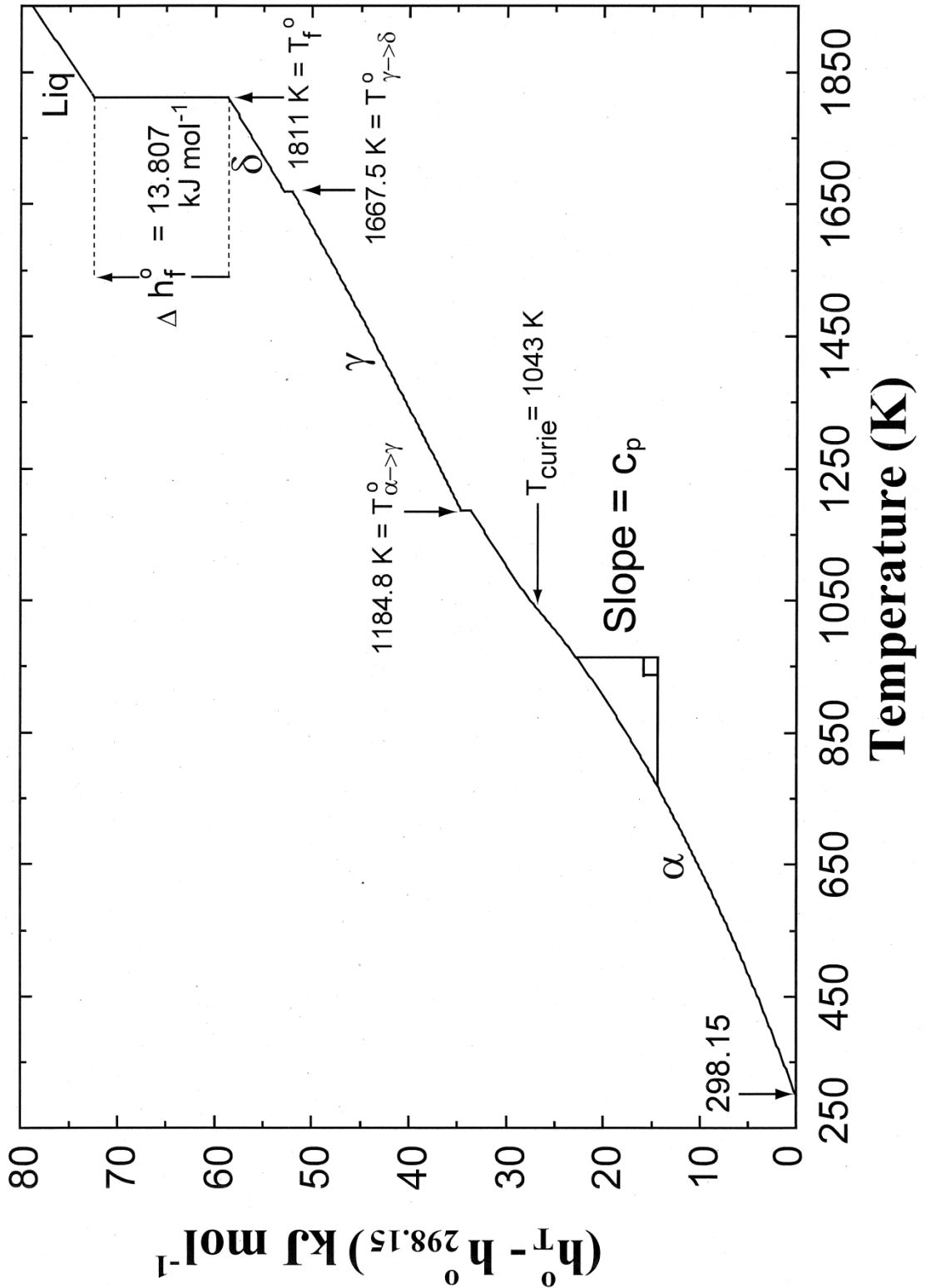


Figure III.9. Standard molar enthalpy of Fe [8].

III.11.3 Gibbs Energy

The Gibbs energy (or Gibbs free energy), G , is defined following the expression III.1.

Part III: Binary phase diagrams

Similar to the Section on Enthalpy, we assume that the work of expansion is the only work term in a closed system and that this is reversible. Based on Equations III.1 and III.18:

$$dG_n = dQ + V dP - T dS - S dT \quad \text{III.24}$$

As a result, given a process taking place in a closed system at constant P and T:

$$dG_{T,P,n} = dQ_P - T dS = dH_P - T dS \quad \text{III.25}$$

Imagine that the "surroundings" are just a heat reservoir that is the same temperature as the system's T. In other words, the environment only receives a reversible transfer of heat (-dQ) at a constant temperature, and no irreversible reactions take place. Thus, based on Eq. (III.14):

$$dS_{surr} = -dQ/T \quad \text{III.26}$$

Substituting into Eq. (III.25) and using Eq. (III.9) yields:

$$dG_{T,P,n} = -T dS_{surr} - T dS = -T dS_{total} \leq 0 \quad \text{III.27}$$

For a process taking place in a closed system at constant T and P, Eq. (III.27) can be seen as a specific version of the Second Law. According to Eq. (III.27), if dG is negative, such a process will occur spontaneously.

The most practical version of the Second Law for our needs in this chapter is Equation (III.27). One could argue that Eq. (III.27) only works when the environment and the system are at the same temperature T. If, on the other hand, the ambient temperature differs, we merely assume a hypothetical heat reservoir that is between the system and the surroundings, at the same temperature, and we treat the irreversible heat transfer between the reservoir and the actual surroundings as a second distinct process.

When Eqs. III.14 and III.26 are substituted into Eq. (III.27), the result is:

$$dG_{T,P,n} = (dQ - dS_{rev}) \leq 0 \quad \text{III.28}$$

dQ is the heat of the actual process in Eq. (III.28), whereas dQ_{rev} is the heat that would be seen if the process were reversible. When the system is at equilibrium, or when the actual process is reversible, $dQ = dQ_{rev}$ and $dG = 0$.

Part III: Binary phase diagrams

Take the fusion of Fe in Fig. III.9 as an example. Solid and T_f liquid are in balance at $T_f^0 = 1181$ K. In other words, melting is reversible at this temperature. Consequently, at 1811 K:

$$dg_f^0 = dh_f^0 - TdS_f^0 = 0 \quad \text{III.29}$$

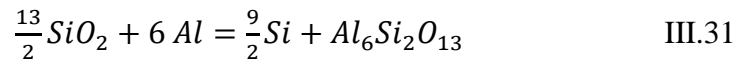
Therefore the molar entropy of fusion at 1811 K is given by:

$$\Delta S_f^0 = (\Delta h_f^0/T) \quad \text{when } T = T_f^0 \quad \text{III.30}$$

Only at the state of equilibrium melting point does Eq. (III.30) apply. The liquid and solid are not in balance at temperatures lower and higher than this one. Melting is a spontaneous process (liquid more stable than solid) above the melting point, where $\Delta g_f^0 < 0$. Below the melting point, solidification occurs spontaneously and $\Delta g_f^0 > 0$. The amount of Δg_f^0 , or the driving force, increases as the temperature moves farther away from the equilibrium melting point.

III.11.4 Chemical Equilibrium

First, consider whether silica fibers in an aluminum matrix will react to generate $Al_6Si_2O_{13}$, or mullite, at 500°C.



The stoichiometry of the reaction indicates that $dn_{Al} = -6 d\xi$, $dn_{Si} = (9/2) d\xi$, and $dn_{SiO_2} = -13/2 d\xi$ if the reaction proceeds with the creation of $d\xi$ moles of mullite. The Gibbs energies of the four substances are identical to their standard molar Gibbs energies, g_i^0 (also called the standard chemical μ_i^0 potentials), because they are practically immiscible at 500°C. The pure compound at $P = 1.0$ bar is the standard state of a solid or liquid compound. The system's Gibbs energy then fluctuates as follows:

$$\frac{dG}{d\xi} = g_{Al_6Si_2O_{13}}^0 + \left(\frac{9}{2}\right) g_{Si}^0 - \left(\frac{13}{2}\right) g_{SiO_2}^0 - 6 g_{Al}^0 = \Delta G^0 = -830 \text{ kJ} \quad \text{III.32}$$

where ΔG^0 is called the Gibbs energy change of reaction (III.31) at 500°C.

A reduction in G is necessary for the production of mullite because $\Delta G^0 < 0$. In order to minimize G , the reaction will therefore continue spontaneously. There will never be equilibrium, and reaction will continue until it is finished.

Part III: Binary phase diagrams

III.11.4.1 Gaseous Phase Equilibrium

A mixture that complies with the ideal state gas equation is called an ideal gas mixture.

$$PV = n R T \quad \text{III.33}$$

where n represents all of the moles. Additionally, each gaseous species' partial pressure in the combination can be found using:

$$P_i V = n_i R T \quad \text{III.34}$$

where $n = \sum n_i$ and $P = \sum p_i$ (Dalton's Law for ideal gases). R is the ideal gas constant.

The pure state of a gaseous chemical at 1.0 bar of pressure is its standard condition. It is simply demonstrated that a species's standard molar Gibbs energy, g_i^0 (also known as the standard chemical potential μ_i^0), may be used to calculate its partial molar Gibbs energy, g_i (also known as the chemical potential μ_i), in an ideal gas mixture.

$$g_i = g_i^0 + RT \ln P_i \quad \text{III.35}$$

Entropy is the last term in Eq. (III.5). A gas's entropy rises as it expands while maintaining a constant temperature.

A gaseous combination of S_2 , H_2 , and H_2S with partial pressures of p_{H_2} , p_{S_2} and p_{H_2S} is considered. The gases may react in the following ways:



The system's Gibbs energy fluctuates as follows if reaction (III.36) progresses to the right and produces $2d\xi$ moles of H_2S :

$$\begin{aligned} \frac{dG}{d\xi} &= 2g_{H_2S} - 2g_{H_2} - g_{S_2} = 2g_{H_2S}^0 - 2g_{H_2}^0 - g_{S_2}^0 + RT[2 \ln(p_{H_2S}) - 2 \ln(p_{H_2}) - \ln(p_{S_2})] \\ &= \Delta G^0 + RT \ln(p_{H_2S}^2 p_{H_2}^{-2} p_{S_2}^{-1}) = \Delta G \end{aligned} \quad \text{III.37}$$

Partial pressures are therefore a function of ΔG , the Gibbs free energy change of reaction (III.36). The response will move to the right in order to minimize G if ΔG is less than 0. In a closed system, p_{H_2S} will rise while p_{H_2} and p_{S_2} will fall as the reaction proceeds and H_2S is produced. Consequently, ΔG will gradually become less negative.

When $dG/d\xi = \Delta G = 0$, an equilibrium state will eventually be reached.

Part III: Binary phase diagrams

For the equilibrium state, therefore:

$$\Delta G^0 = -RT \ln K = -RT \ln (p_{H_2S}^2 p_{H_2}^{-2} p_{S_2}^{-1})_{equilibrium} \quad \text{III.38}$$

where the system will be in equilibrium at temperature T for the single value of the ratio $(p_{H_2S}^2 p_{H_2}^{-2} p_{S_2}^{-1})$, which is K, the "equilibrium constant" of the reaction. In order to minimize G until the equilibrium condition of Eq. (III.38) is reached, reaction (III.36) will move to the left if the initial partial pressures are such that $\Delta G > 0$. Consider the potential precipitation of graphite from a gaseous mixture of CO and CO₂ as an additional example. This is the response:

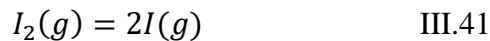
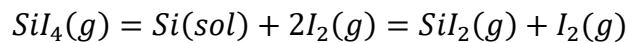


Proceeding as above, we can write:

$$\begin{aligned} \frac{dG}{d\xi} &= g_{CO_2} + g_C - 2g_{CO} = g_{CO_2}^0 + g_C^0 - 2g_{CO}^0 + RT \ln [p_{CO_2} p_{CO}^{-2}] \\ &= \Delta G^0 + RT \ln (p_{CO_2} p_{CO}^{-2}) = \Delta G = -RT \ln K + RT \ln (p_{CO_2} p_{CO}^{-2}) \end{aligned} \quad \text{III.40}$$

In order to reduce G, graphite will precipitate if $(p_{CO_2} p_{CO}^{-2})$ is smaller than the equilibrium value K.

Of course, real life is always more complicated. Three separate reaction equations must be created in order to handle the formation of solid Si from a vapor of SiI₄, for instance, since we must take into account the creation of gaseous I₂, I and SiI₂.



Nonetheless, the state that minimizes the system's overall Gibbs energy remains the equilibrium state. This is equal to concurrently meeting the reactions' equilibrium constants in (III.41).

III.11.4.2 Predominance Diagrams

One of the most straightforward kinds of phase diagrams, prevalence diagrams are used extensively in hot corrosion, chemical vapor deposition, and other fields. Additionally, the principles of Gibbs energy minimization are well demonstrated by their construction. Figure III.10 displays the Cu-SO₂-O₂ system's predominant diagram at 700 °C [4]. The

Part III: Binary phase diagrams

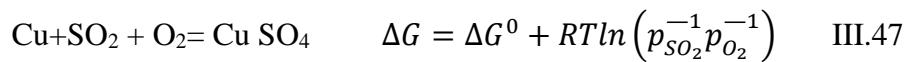
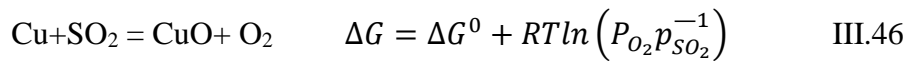
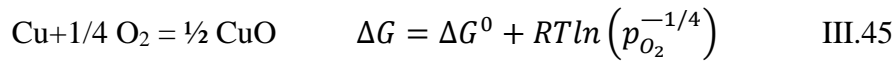
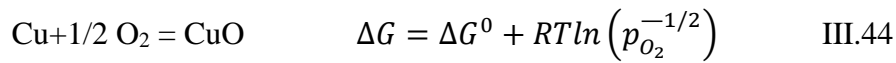
logarithms of the gas phase partial pressures of SO₂ and O₂ serve as the axes. Areas or domains of stability for the different solid compounds of Cu, S, and O are separated out in the diagram. The stable phase, for instance, is Cu₂O at point Z, where $p_{CO_2}=10^{-2}$ and $p_{O_2}=10^{-7}$ bar. The lines and triple points on the diagram represent the requirements for two and three solid phases to coexist, respectively. For instance, the following reaction's equilibrium constant, $K=p_{SO_2}^{-2}p_{O_2}^{-3/2}$ is satisfied along the line that divides the Cu₂O and CuSO₄ domains:



Hence, along this line:

$$\log K = \frac{\Delta G^0}{RT} = -2 \log P_{SO_2} - \left(\frac{3}{2}\right) \log P_{SO_2} = \text{constant} \quad \text{III.43}$$

With a slope of $(-3/2)/2 = -3/4$, this line is therefore straight. By using the process described by Bale et al. (1986), we may generate Fig. III.10. Using the gaseous substances whose pressures serve as the axes (in this case, SO₂ and O₂), we devise a process for the production of every solid phase, always starting with one mole of Cu:



as well as the production of Cu₂S, Cu₂SO₄, and Cu₂SO₅. ΔG^0 values are derived from thermodynamic property tables. It is then possible to determine ΔG for each formation reaction for every given value of p_{SO_2} and p_{O_2} . The chemical with the largest negative ΔG is simply the stable one. The stable compound is pure Cu if all of the ΔG values are positive. To construct a preponderance diagram using $\log p_{S_2}$ and $\log p_{O_2}$ as axes, Eqs. (III.44) to (III.47) can be reformulated in terms of, say, S₂ and O₂ instead of SO₂ and O₂. It is also possible to use logarithms of ratios or products of partial pressures as axes. The total pressure on Fig. III.10 is 1.0 bar along the curve that the crosses represent. This means that in addition to SO₂ and O₂, the gas also contains additional species, including S₂, whose equilibrium partial pressures can be determined. The sum of the partial pressures of SO₂ and O₂ may be

Part III: Binary phase diagrams

less than 1.0 bar, but above this line, the total pressure is larger than 1.0 bar. A comparable $RT \ln p_{O_2}$ vs T phase diagram for the Cu-O₂ system can be found in Fig. III.11. For the reaction of formation:



we can write:

$$\Delta G^0 = -RT \ln K = RT \ln (p_{O_2})_{equilibrium} = \Delta H^0 - T \Delta S^0 \quad \text{III.49}$$

Plotting the conventional Gibbs energy of production of Cu₂O against T is what the line between the Cu and Cu₂O domains in Fig. III.11 represents. The melting points of Cu and Cu₂O are represented by the temperatures denoted by the symbols M and M inside a square. For the creation of oxides, this line is therefore just a line drawn from the well-known Ellingham diagram, often known as the G_0 vs. T diagram. But, as illustrated in Figure III.11 [8], we can change the Ellingham diagram into a phase diagram by drawing vertical lines at the melting points of Cu and Cu₂O.

As functions of T and the imposed equilibrium p_{O_2} , the stability regions for Cu_(sol), Cu_(liq), Cu₂O_(sol), Cu₂O_(liq), and CuO_(sol) are displayed. Two- and three-phase equilibrium conditions are indicated by the lines and triple points.

Part III: Binary phase diagrams

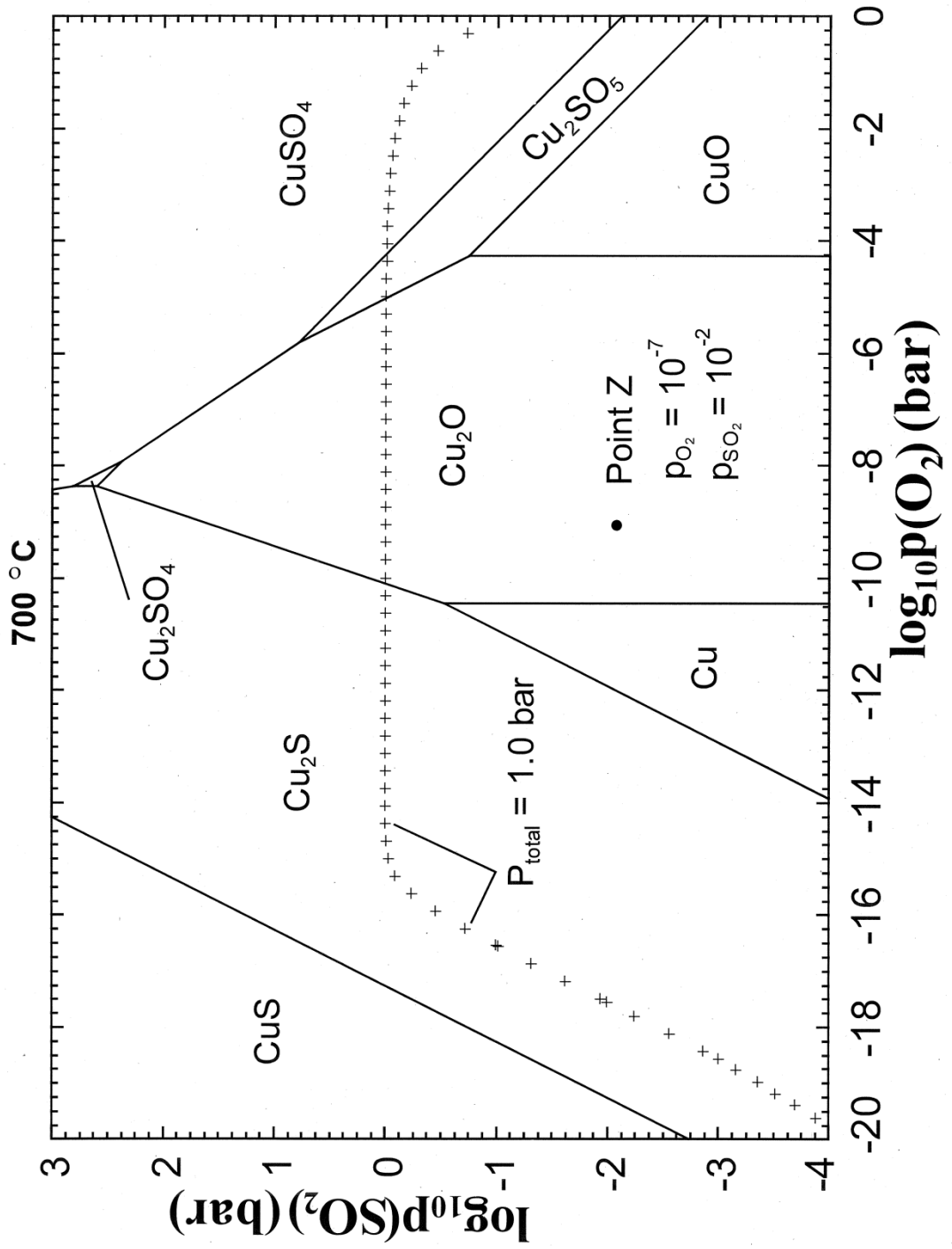


Figure III.10. Cu-SO₂-O₂ phase diagram at 700 °C [8].

Part III: Binary phase diagrams

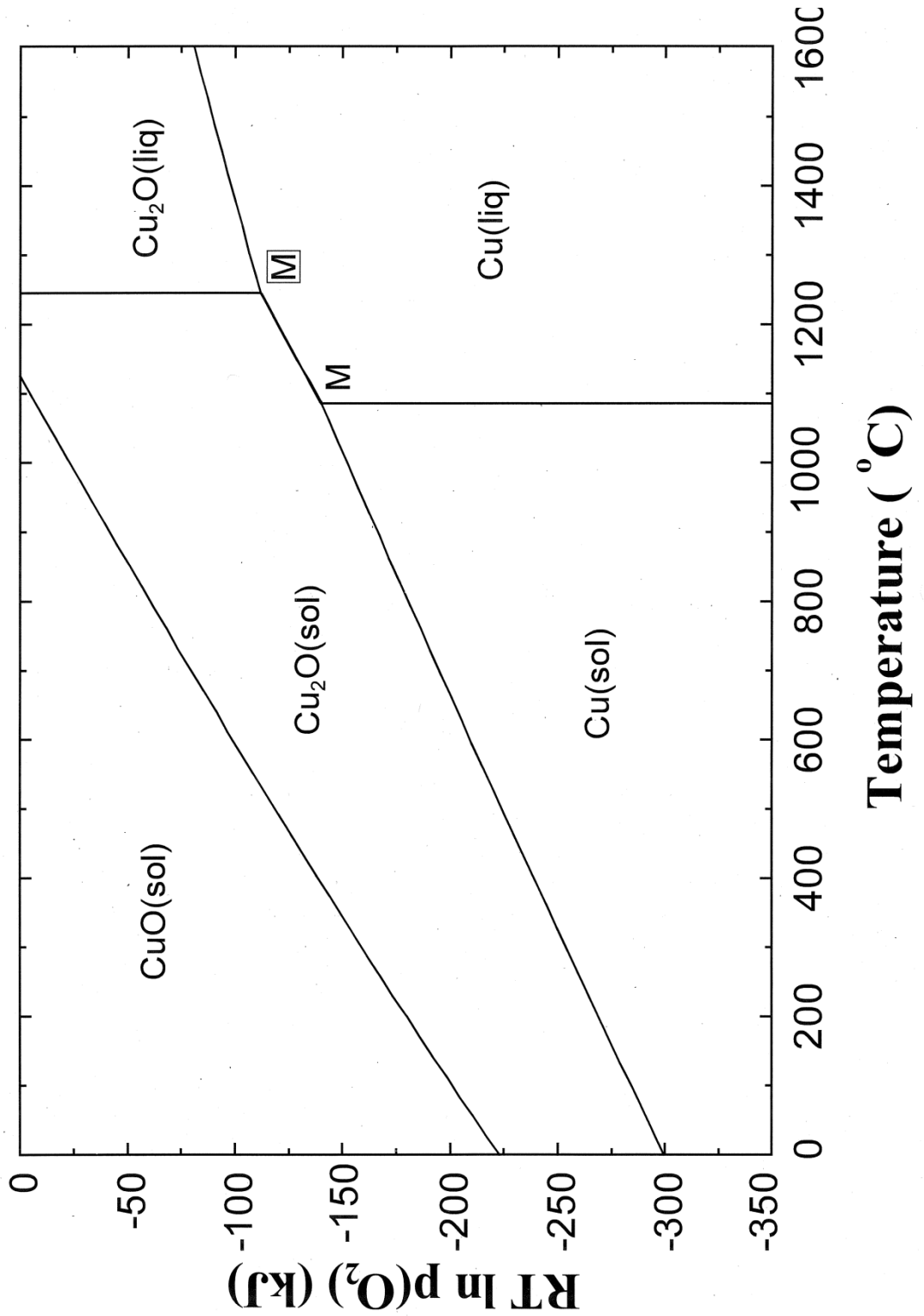


Figure III.11. The melting temperatures of Cu and Cu₂O are represented by M and M dedans le care in the Cu-O₂ system's predominant phase diagram [8].

Part III: Binary phase diagrams

III.11.5 Gibbs, Entropy, and Enthalpy energies measurements

III.11.5.1 Gibbs Energy Change

Generally speaking, data under equilibrium conditions can be used to calculate a process's Gibbs energy change.

Take, for instance, the reaction ($2\text{Co} \longleftrightarrow \text{C} + \text{CO}_2$). By monitoring the partial pressures of CO and CO₂, the equilibrium constant is determined once the equilibrium between solid C and the gas phase has been achieved experimentally. After that, ΔG° is computed using Equation III.40.

Using an electrochemical cell is another popular method of reaching equilibrium. A galvanic cell is made in such a way that an electric current flowing through an external circuit is the only way for a reaction (the cell reaction) to take place. To ensure that no current flows, an external voltage is applied that is equal to the cell potential, E (volts), but opposite in sign. At that point, the system is in balance. Edz joules of work are produced when dz coulombs move through the external circuit. Since the process is in equilibrium, $dW_{rev(non-PV)}$ is the reversible non-PV work. After differentiating and substituting Eq. (III.16) and Eq. (III.2) into Eq. (III.1), the following results are obtained:

$$dG = V dP - S dT + \sum_i \mu_i dn_i + dQ_{rev(non-PV)} \quad \text{III.50}$$

For a system that is closed at points T and P:

$$dG_{T,P,n} = dW_{rev(non-PV)} \quad \text{III.51}$$

If the cell reaction is designed so that the passage of dz coulombs through the external circuit is linked to the reaction's advancement by $d\xi$ moles, then from Eq. (51):

$$\Delta G \cdot d\xi = -Edz \quad \text{III.52}$$

Hence,
$$\Delta G = -F \cdot E \quad \text{III.53}$$

where the Faraday constant, or the amount of coulombs in a mole of electrons, is $F = dz/d\xi = 96500$ coulombs mol⁻¹, the negative sign adheres to the standard electrochemical sign convention, and ΔG represents the Gibbs energy change of the cell reaction. Therefore, one may calculate the ΔG of the cell reaction by measuring the open-circuit voltage E .

Part III: Binary phase diagrams

III.11.5.2 Enthalpy Change

Calorimetry can be used to measure a process's enthalpy change, or ΔH , directly. As an alternative, ΔH can be ascertained from the recorded temperature dependence of ΔG if ΔG is obtained using an equilibration approach, as was covered in the previous section. According to Eq. (III.50), for a process operating at constant pressure in a closed system without non-PV work:

$$(dG/dT)_{P,n} = -S \quad \text{III.54}$$

Substitution of Eq. (III.16) into Eq. (III.54) gives:

$$(d(G/T)/d(1/T))_{P,n} = H \quad \text{III.55}$$

Eqs. (III.54) and (III.55) apply to both the initial and final states of a process. Hence:

$$d(\Delta G/dT)_{P,n} = -\Delta S \quad \text{III.56}$$

$$(d(\Delta G/T)d(1/T))_{P,n} = \Delta H \quad \text{III.57}$$

Eqs. (III.54) to (III.57) are various forms of the Gibbs-Helmholtz equation.

III.11.5.3 Entropy

Similar to enthalpy, ΔS of a process can be calculated using Eq. (III.56) from the measured temperature dependence of ΔG . This approach to measuring entropy is referred to as the "second law method."

Entropy can also be measured using the Third Law of thermodynamics, which states that at 0 K, the entropy of a perfect crystal of a pure substance in internal equilibrium is zero. Eq. (III.8) and the idea of entropy as disorder lead to this conclusion. At absolute zero, $S = 0$ and $t = 1$ for a properly ordered system.

Let's start by obtaining an expression for the entropy shift that occurs when a substance is heated. The result of combining Eqs. III.54 and III.55 is:

$$(dH/dT)_{P,n} = T(dS/dT)_{P,n} \quad \text{III.58}$$

After integrating and substituting Eq. (III.15) into Eq. (III.58), the entropy change as one mole of a substance is heated from T_1 to T_2 at constant P can be expressed as follows:

$$(S_{T_2} - S_{T_1}) = \int_{T_1}^{T_2} (C_P/T) dT \quad \text{III.59}$$

Part III: Binary phase diagrams

Setting $T_1 = 0$ in Eq. (III.59) and using the Third Law gives:

$$S_{T_2} = \int_0^{T_2} (C_P/T) dT \quad \text{III.60}$$

Therefore, Eq. (III.60) can be used to determine the absolute entropy if CP has been measured below to temperatures that are close enough to 0 K. This approach to measuring entropy is referred to as the "third law method."

III.11.5.4 Zero Enthalpy and Entropy

A substance's absolute entropy can be measured using the third law approach, but entropy changes, or ΔS , can only be measured using the second law method. A convention is not what the Third Law is. For entropy, it offers a natural zero. Conversely, as there is no simple natural zero for internal energy, there is no corresponding natural zero for enthalpy. However, it is customary to assign the absolute enthalpy of a pure element in its stable state at $T = 298.15$ K and $P = 1.0$ bar to zero.

A compound's standard enthalpy of formation from the pure elements in their stable standard states at 298.15 K is therefore, by convention, equal to its absolute enthalpy.

III.11.6 The Chemical Potential

Equation (III.11) provided the definition of the chemical potential. This equation isn't very helpful, though, because it's hard to see how S can be kept constant. Differentiating and inserting Eq. (III.15) and Eq. (III.2) into Eq. (III.16), respectively, yields:

$$dG = V dP - S dT + \sum_i \mu_i dn_i \quad \text{III.61}$$

which indicates that μ_i is also provided by:

$$\mu_i = (\partial G / \partial n_i)_{T,P,n_{j \neq i}} \quad \text{III.62}$$

Using Eq. (III.15) in place of Eq. (III.2) to differentiate Eq. (III.2) yields:

$$dH = T dS + V dP + \sum_i \mu_i dn_i \quad \text{III.63}$$

where,

$$\mu_i = (\partial H / \partial n_i)_{T,V,n_{j \neq i}} \quad \text{III.64}$$

Similarly it can be shown that:

$$\mu_i = (\partial A / \partial n_i)_{T,V,n_{j \neq i}} \quad \text{III.65}$$

Part III: Binary phase diagrams

The most practical of these equations for μ_i is Eq. (III.62). The increase in Gibbs energy as a component is added to a system at constant T and P while maintaining the same number of moles of all other components is the chemical potential of that component, μ_i .

A system's intense characteristics are its component chemical potentials, which are independent of the system's mass for a particular system at a given T, P, and composition. In other words, using Eq. (III.62), if dn_i moles of component i are added to a solution with a given composition, the Gibbs energy dG will change regardless of the solution's total mass.

The following thought experiment demonstrates why this attribute is known as a chemical potential. Consider two systems, I and II, that are separated by a membrane that allows just one component, let's call component 1, to pass through, and that are at the same temperature and pressure. In systems I and II, component 1's chemical potentials are $\mu_1^I = \partial G^I / \partial n_1^I$ and $\mu_1^{II} = \partial G^{II} / \partial n_1^{II}$. Component 1 is transferred across the membrane with $dn_1^I = -dn_1^{II}$. The total Gibbs energy shift that results from this transfer is then:

$$dG = d(G^I + dG^{II}) = -(\mu_1^I - \mu_1^{II})dn_1^{II}$$

When dn_1^{II} is positive, $d(G^I + dG^{II})$ is negative if $\mu_1^I > \mu_1^{II}$. That is, the transfer of component 1 from system I to system II lowers the total Gibbs energy. As a result, component 1 moves spontaneously from a higher μ_1 system to a lower μ_1 system. Because of this, μ_1 is referred to as component 1's chemical potential.

Similarly, it can be demonstrated that μ_i is the potential for component i to be transferred at constant T and V, at constant S and V, etc., by employing the proper auxiliary functions. It is now possible to state a crucial phase equilibrium principle. Any component's chemical potential is the same in every phase when two or more crystal structures are in equilibrium. Thus, this phase equilibrium criterion is the same as the G minimization requirement.

Part IV:

Diffusion

Part IV : Diffusion

Introduction

Diffusion in solids is a key topic in physical chemistry, solid-state physics, materials science, and physical metallurgy since it is essential to the art and science of materials. The dynamics of several microstructural alterations that take place during material preparation, processing, and heat treatment are influenced by diffusion processes. For instance, new phase nucleation, diffusive phase transitions, second phase precipitation and dissolution, alloy homogenization, recrystallization, and thermal oxidation are typical instances. In ionic conductors, diffusion and electrical conduction are closely connected processes. Diffusion's direct technological applications include surfaces hardening steel through carburization or nitridation, diffusion bonding, sintering, solid electrolytic solutions for batteries and fuel cells, and doping during the manufacturing of microelectronic devices.

Therefore, understanding diffusion is especially crucial for engineers who construct various pieces of equipment and for scientists who create materials for high temperatures. Information about the location and motion of atoms within solids is necessary to gain a greater understanding of diffusion. Defects are intimately related to the atomic mechanics of diffusion in crystalline materials. The most basic flaws are point defects, like vacancies or interstitials, which frequently mediate diffusion in crystals.

IV.1 Diffusion

Diffusion is the process by which atoms or molecules move thermally from one location to another.

Diffusion occurs very slowly in solids, slowly in liquids, and moderately quickly in gases. Many metallurgical processes, including phase changes, solidification, precipitation, and others, are governed by diffusion phenomena.

IV.2 Diffusion Mechanisms

Atoms gradually migrate across the crystal from one lattice position to another, causing diffusion. Although it can form in vacancies, interstices, and alternative sites, it happens more frequently in areas where the crystal exhibits flaws. The following mechanisms can be used to accomplish atomic diffusion:

IV.2.1 Interstitial Mechanism

Figure IV.1 illustrates how impurity atoms in interstices migrate from one location to another without taking up a lattice position.

Part IV : Diffusion

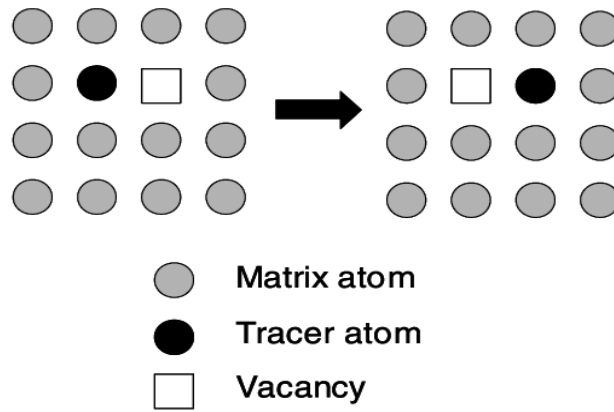


Figure IV.3. Vacancy diffusion mechanism.

IV.2.5 Interstitial-substitutional exchange mechanism

It is possible for certain solute atoms (B) to dissolve on both substitutional (B_s) and interstitial (B_i) sites.

Two types of interstitial-substitutional exchange mechanisms can be distinguished, as shown in Figure IV.4 :

- **Dissociative mechanism** : When vacancies (V) are present during the transition, as per, $B_i + V \rightleftharpoons B_s$
- **Kick-out mechanism** : When self-interstitials (A_i) are involved in the transition, as per, $B_i \rightleftharpoons B_s + A_i$

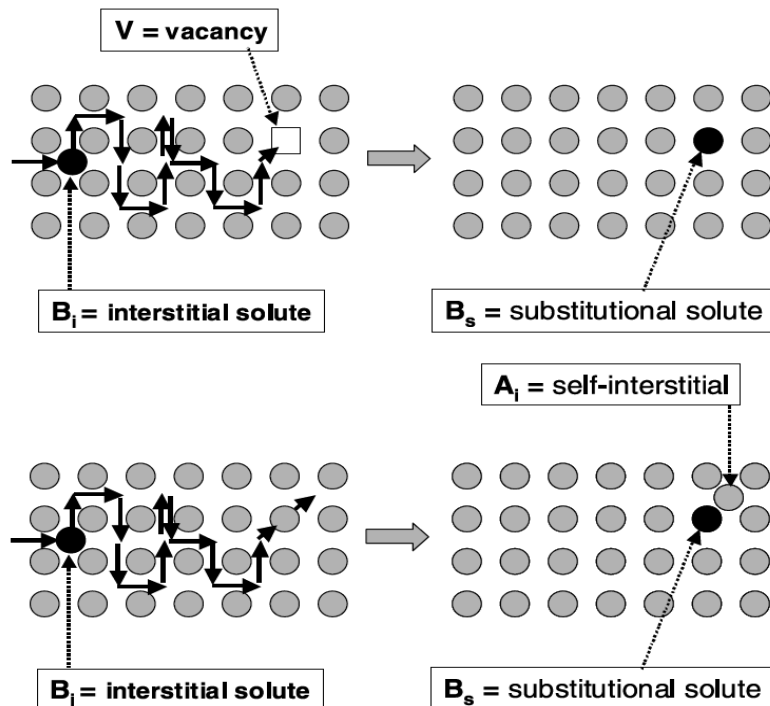


Figure IV.4. Interstitial-substitutional exchange mechanisms; Dissociative mechanism at the top. Kick-out mechanism at the bottom.

Part IV : Diffusion

IV.3 Laws of Fick

IV.3.1 First law of Fick

The flux of diffusing particles (i.e. atoms, molecules, or ions) can occur in one dimension, as illustrated in Figure IV.5. The first law of Fick for an isotropic medium can be expressed as:

$$J_x = -D \frac{\partial C}{\partial x} \quad \text{IV.1}$$

In this case, C represents the particle's number density (concentration), and J_x is the particle flux (diffusion flux). D represents the species under consideration's diffusivity or diffusion coefficient, with:

$$D = D_0 \cdot \exp\left(-\frac{\Delta H_t + \Delta H_f}{kT}\right) \quad \text{IV.2}$$

with ΔH_t is the vacancy migration activation enthalpy and ΔH_f corresponds to the vacancy formation enthalpy .

J_x is expressed in $\text{mol} \cdot \text{m}^{-2} \cdot \text{s}^{-1}$ (or $\text{g} \cdot \text{m}^{-2} \cdot \text{s}^{-1}$) and D is expressed in $\text{m}^2 \cdot \text{s}^{-1}$

The first law of Fick is generalized to three dimensions using a vector notation:

$$\mathbf{J} = -D \nabla C \quad \text{IV.3}$$

In diffusion processes, the quantity of diffusing particles is typically maintained. The following equation of continuity can be created for a diffusing species that complies with conservation law:

$$\frac{\partial C}{\partial t} = -\nabla \cdot \mathbf{J} \quad \text{IV.4}$$

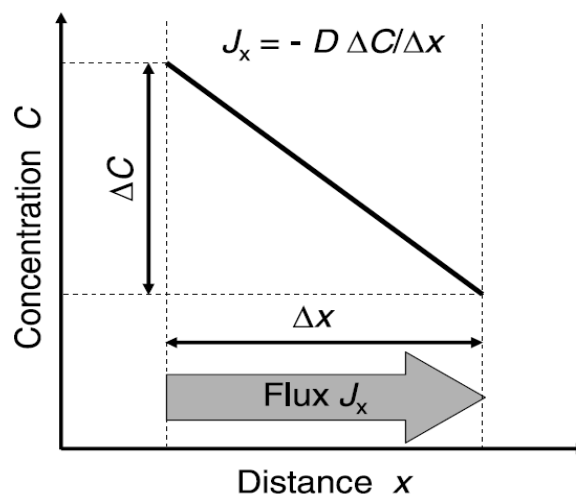


Figure IV.5. Schematic illustration of first Fick law.

The first law of Fick is formally equivalent to *Fourier's law* of heat flow, as follows:

Part IV : Diffusion

$$J_q = -\kappa \nabla T \quad \text{IV.5}$$

where T is the temperature field, κ is the thermal conductivity, and J_q is the heat flux. It is comparable to Ohm's law as well:

$$J_e = -\sigma \nabla V \quad \text{IV.6}$$

where σ is electrical conductivity, V is electrostatic potential, and J_e is electric current density. Ohm's law depicts the movement of electric charge, Fourier's law represents the movement of heat, and Fick's law defines the movement of particles.

IV.3.2 Second law of Fick

Fick's second law, often known as the diffusion equation, is the result of combining Fick's first law (Eq. IV.3) with the equation of continuity (Eq. IV.4):

$$\frac{\partial C}{\partial t} = \nabla \cdot (D \nabla C) = D \cdot \left(\frac{\partial^2 C}{\partial x^2} + \frac{\partial^2 C}{\partial y^2} + \frac{\partial^2 C}{\partial z^2} \right) \quad \text{IV.7}$$

IV.4 Kirkendall Effect

Think about the diffusion couple between A and B in Figure IV.6, where the two species' diffusion rates diverge ($|J_A| > |J_B| \Leftrightarrow D_A > D_B$). The couple will shift bodily in relation to the markers because of the net flow of matter past the inert markers caused by the differing diffusion fluxes (during thermal heating). Only if diffusion is caused by a vacancy mechanism can this occur.

Consequently, the distinction in intrinsic diffusivities of the chemical elements of replacement solid solutions leads to the well-known Kirkendall effect.

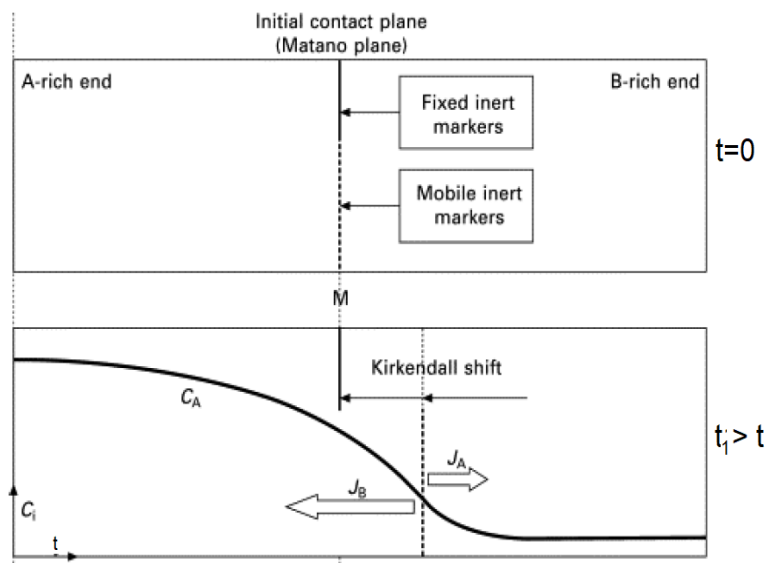


Figure IV.6. Schematic illustration of Kirkendall experience.

Part IV : Diffusion

IV.5 Darken Equations

Darken sought to provide the first theoretical explanation of inter-diffusion and the Kirkendall phenomenon in 1948. He employed the two intrinsic diffusivities to characterize the inter-diffusion process for a binary substitutional alloy (A-B alloy). It is necessary for the net flux of atoms, $J_B - J_A$, to equal the net flux of vacancies, J_V .

$$J_V = (D_A - D_B) \frac{\partial C_A}{\partial x} \quad \text{IV.8}$$

The velocity of Kirkendall v_K can be obtained by, $J_V = v_K \cdot C_0$, (C_0 is the total concentration, $C_0 = C_A + C_B$)

then, the first equation of Darken is as following:

$$v_K = \left(\frac{1}{C_0}\right) (D_A - D_B) \frac{\partial C_A}{\partial x} = (D_A - D_B) \frac{\partial X_A}{\partial x} \quad \text{IV.9}$$

Using Darken's method, the laboratory-fixed inter-diffusion flux J (at the Kirkendall plane) can be expressed as the sum of a Kirkendall drift term $v_K \mp C_i$ plus (or minus) an intrinsic diffusion flux of one of the components i :

$$J = -D_i \left(\frac{\partial C_i}{\partial x}\right) \mp v_K \cdot C_i \quad (i = A \text{ or } B) \quad \text{IV.10}$$

The inter-diffusion coefficient (\tilde{D}) can be expressed generally by substituting the expression of Kirkendall velocity in the final equation:

$$\tilde{D} = D_A X_B + D_B X_A \quad \text{IV.11}$$

This formula is referred to as the second Darken's equation.

Part V:

Phase transformations

Part V : Phase transformations

Introduction

A metal or alloy can undergo solidification or melting, which are changes from crystallographic to non-crystallographic phases. The technological applications of ingot casting, foundry casting, continuous casting, semiconductor single-crystal growth, directionally solidified composite alloys, and, more recently, rapidly solidified alloys and glasses all depend on these transitions. Fusion welding is a significant and intricate melting and solidification process that is sometimes overlooked in solidification literature. Controlling the mechanical properties of cast metals and fusion welds requires an awareness of the solidification mechanism and how it is influenced by variables including alloying, cooling rate, and temperature distribution.

It can be any change that causes the energy of Gibbs, G , to decrease. Any reaction that causes G to rise is not possible and will not take place. Consequently, the following need must be met for any phase transformation:

$$\Delta G = G_2 - G_1 < 0 \quad \text{V.1}$$

where the initial and final states' free energies are denoted by G_1 and G_2 , respectively. The transformation does not have to reach the stable equilibrium state right away. It could experience a wide range of unstable intermediate states.

V.1 Nucleation in pure metals

The process by which a substance or mixture self-organizes to generate a new thermodynamic phase or structure is known as nucleation in thermodynamics. The process that establishes the duration of time an observer must wait for the new phase or self-organized structure to emerge via homogeneous or heterogeneous type is commonly referred to as nucleation.

While heterogeneous nucleation takes place at the system's surface, homogeneous nucleation takes place farther away. This is the main distinction between the two types of nucleation.

V.1.1 Homogeneous nucleation

Examine a given volume of liquid with a free energy G_1 ($G_1 = (V_s + V_L) G_V^L$) at a temperature ΔT below the melting temperature T_m (Figure V.1a). The system's free energy will change to G_2 if some of the liquid's atoms group together to create a tiny solid sphere (Figure V.1b), as shown by:

$$G_2 = V_s G_V^S + V_L G_V^L + A_{SL} \cdot \gamma_{SL} \quad \text{V.2}$$

Part V : Phase transformations

where A_{SL} is the solid/liquid interface area, V_S is the solid sphere's volume, V_L is the liquid's volume, G_v^S and G_v^L are the solid/liquid free energies per unit volume, respectively, and γ_{SL} is the solid/liquid contact free energy.

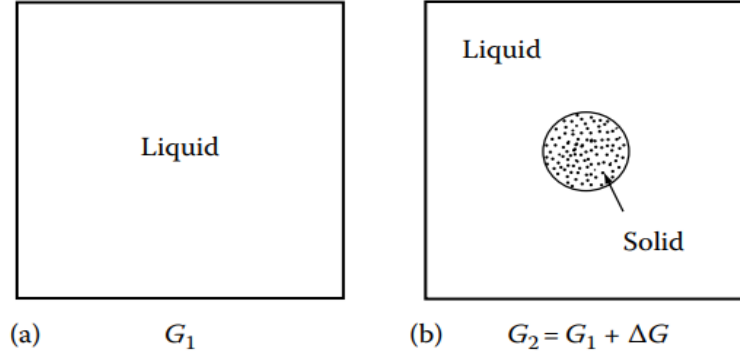


Figure V.1. Homogeneous nucleation.

The formation of solid therefore results in a free energy change $\Delta G = G_2 - G_1$ where:

$$\Delta G = -V_s \cdot \Delta G_v + A_{SL} \cdot \gamma_{SL} \quad \text{V.3}$$

where $\Delta G_v = G_v^S - G_v^L = \Delta H_v \cdot (\Delta T / T_m)$. ΔH_v is the enthalpy of formation of the new phase per unit volume, T_m is the melting temperature and $\Delta T = T_m - T$.

Assuming a germ with spherical shape and has a radius r , hence, $V_s = \frac{4}{3}\pi r^3$ and $A_{SL} = 4\pi r^2$, then:

$$\Delta G = \frac{4}{3}\pi r^3 \cdot \Delta H_v \cdot (\Delta T / T_m) + 4\pi r^2 \cdot \gamma_{SL} \quad \text{V.4}$$

The critical nucleus is practically in equilibrium with the neighboring liquid since $dG = 0$ for $r = r^*$. It can to determine the r^* expression by differentiation of Equation V.4 and equaling it to zero:

$$\frac{d}{dr} (\Delta G) = \frac{d}{dr} \left[\frac{4}{3}\pi r^3 \cdot \Delta H_v \cdot \left(\frac{\Delta T}{T_m} \right) \right] + \frac{d}{dr} [4\pi r^2 \cdot \gamma] = 0 \quad \text{V.5}$$

so,

$$r^* = -\frac{2\gamma T_m}{\Delta H_v \Delta T} \text{ and } \Delta G^* = \frac{16\pi\gamma^3}{3(\Delta H_v)^2} = \frac{16\pi\gamma^3 T_m^2}{3(\Delta H_v)^2 \Delta T^2} \quad \text{V.6}$$

Part V : Phase transformations

Figure V.2 shows how the free energy of nuclei varies with their radius, r . This graphic shows that a maximum excess free energy is linked to a specific radius, r^* (critical nucleus size), for a particular under cooling.

- If $r < r^*$: Clusters or embryos of unstable solid particles can be seen, where the system can reduce its free energy by dissolving the solid (nuclei decrease).
- When $r > r^*$: Steady particles are called nuclei, and the solid develops (nuclei grow) as the system's free energy falls.
- The crucial nucleus and the surrounding liquid are essentially in equilibrium when $r = r^*$.

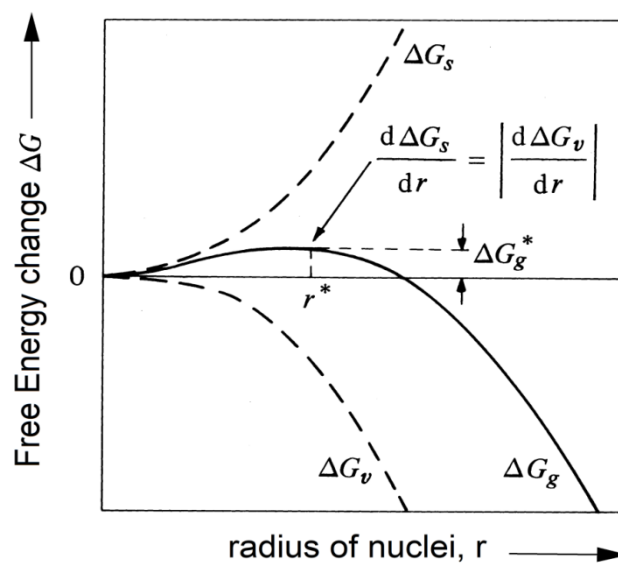


Figure V.2. The shift in free energy that occurs when a sphere of radius r is homogeneously nucleated.

We can therefore say that at each temperature there exist in equilibrium a determined number n_r of germs of radius r per unit volume:

$$n_r = n_0 \cdot \exp\left(-\frac{\Delta G_r}{k_B T}\right) \quad \text{V.7}$$

where the entire number of atoms in the system is denoted by n_0 .

V.1.2 Heterogeneous nucleation

As shown in Figure V.3, imagine a solid embryo developing in contact with a completely flat mould wall. The following describes how the interfacial tensions γ_{ML} , γ_{SM} , and γ_{SL} balance in the mould wall plane:

Part V : Phase transformations

$$\gamma_{ML} = \gamma_{SM} + \gamma_{SL} \cos\theta \quad \text{V.8}$$

$$\cos\theta = (\gamma_{ML} - \gamma_{SM})/\gamma_{SL} \quad \text{V.9}$$

where, γ_{ML} , γ_{SM} and γ_{SL} are the Gibbs free energies for mould/liquid, solid/mould and solid/liquid interfaces, respectively.

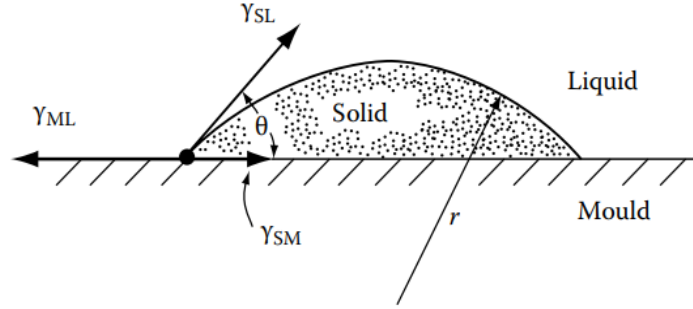


Figure V.3. Spherical cap nucleation that is heterogeneous on a flat mould wall.

The formation of such an embryo will be associated with an excess free energy given by:

$$\Delta G_{het} = -V_S \Delta G_v + A_{SL} \cdot \gamma_{SL} + A_{SM} \cdot \gamma_{SM} - A_{SM} \cdot \gamma_{ML} \quad \text{V.10}$$

where A_{SL} and A_{SM} are the regions of the solid/liquid and solid/mold interfaces, respectively, and V_S is the volume of the spherical cap.

The wetting angle (θ) and cap radius (r) can be used to express the above equation as follows:

$$\Delta G_{het} = \left\{ -\frac{4}{3} \pi r^3 \cdot \Delta G_v + 4 \pi r^2 \cdot \gamma_{SL} \right\} \cdot S(\theta) \quad \text{V.11}$$

Where, $S(\theta)$ is referred to as a shape factor ≤ 1 (with, $S(\theta) = (2 + \cos\theta)(1 - \cos\theta)^2/4$).

It should be noted that this expression is identical to the one derived for homogeneous nucleation, with the exception of factor $S(\theta)$.

Equation V.11 can be differentiated to demonstrate that:

$$r^* = -\frac{2\gamma_{SL}}{\Delta G_v} \text{ and } \Delta G_{het}^* = \frac{16\pi\gamma_{SL}^3}{3(\Delta G_v^2)} \cdot S(\theta) \quad \text{V.12}$$

Combining the expressions of free energies for homogeneous and heterogeneous nucleation, gives:

$$\Delta G_{het}^* = \Delta G_{hom}^* \cdot S(\theta) \quad \text{V.13}$$

As a result, ΔG_{het}^* has a lower activation energy barrier than ΔG_{hom}^* against heterogeneous nucleation.

Part V : Phase transformations

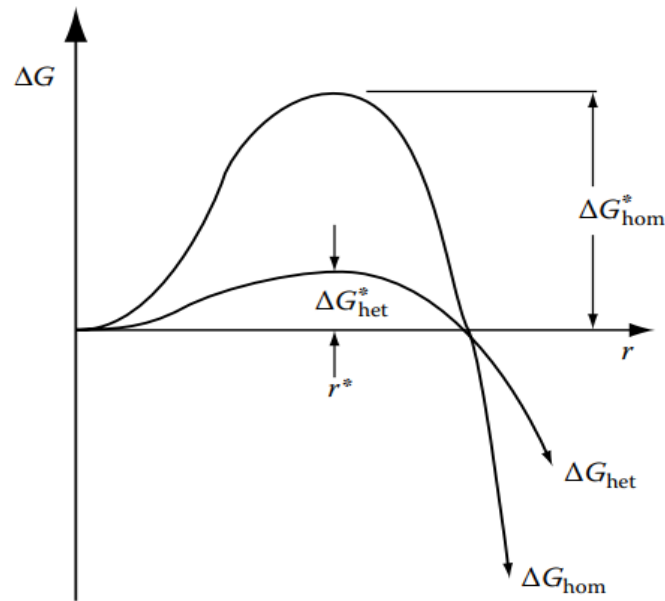


Figure V.4. Solid clusters' excess free energy for both heterogeneous and homogeneous nucleation.

The number of nuclei if n_1 atoms are in touch with the mould wall can be determined using:

$$n^* = n_1 \cdot \exp\left(-\frac{\Delta G_{\text{het}}^*}{k_B T}\right) \quad \text{V.14}$$

V.2 Gibbs free energy of binary solutions

The free energies of pure A and pure B can be used to compute the energy of Gibbs for a binary solution of A and B atoms. In their pure states, A and B are thought to have identical crystal structures, and they can be combined in any ratio to create a solid solution with a crystal structure that is the same. Examine the scenario where X_A mol of A and X_B mol of B are combined to create 1 mol of homogenous solid solution. Since there is one mol of solution in total, $X_A + X_B = 1$.

There are two ways to mix an alloy in order to determine its free energy (Figure V.5):

1. Combine the X_A and X_B mol of pure A and B, respectively.
2. To create a uniform solid solution, let the A and B atoms combine.

Part V : Phase transformations

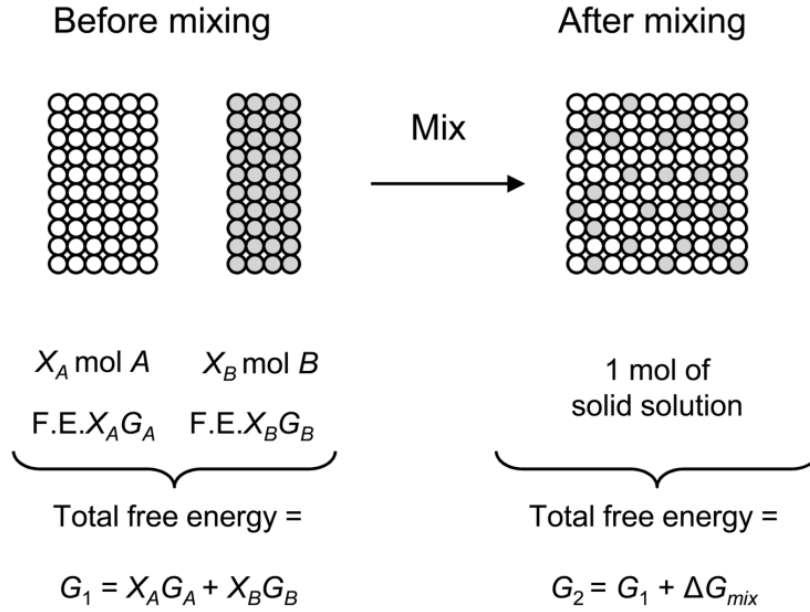


Figure V.5. Mixing's Free energy.

The free energies of the system before (G_1) and after mixing (G_2) are respectively:

$$G_1 = X_A G_A + X_B G_B \quad \text{V.15}$$

$$G_2 = G_1 + \Delta G_{\text{mix}} \quad \text{V.16}$$

where G_A and G_B represent the temperature and pressure-dependent molar free energies of pure A and pure B, respectively.

Because:

$$G_1 = H_1 - TS_1 \text{ and } G_2 = H_2 - TS_2 \quad \text{V.17}$$

Putting:

$$\Delta G_{\text{mix}} = G_2 - G_1 = (H_2 - H_1) - T(S_2 - S_1) \quad \text{V.18}$$

$$\Delta G_{\text{mix}} = \Delta H_{\text{mix}} - T\Delta S_{\text{mix}} \quad \text{V.19}$$

where ΔS_{mix} is the entropy difference between the mixed and unmixed states, and ΔH_{mix} is the heat that is absorbed or produced during mixing.

V.2.1 Ideal Solutions

The most straightforward kind of mixing takes place in the ideal solution, where $\Delta H_{\text{mix}} = 0$.

As a result, the free-energy change upon mixing is $\Delta G_{\text{mix}} = -T\Delta S_{\text{mix}}$.

Part V : Phase transformations

The Boltzmann equation in statistical thermodynamics, where k is Boltzmann's constant and ω is a measure of randomness, statistically connects entropy and unpredictability: $S = -k \ln \omega$. The A and B atoms are kept apart in the system prior to mixing, and there is only one distinct manner for the atoms to be ordered. Consequently, $\Delta S_{\text{mix}} = S_2$ since $S_1 = k \ln 1 = 0$.

The number of distinct ways to arrange the atoms on the atom sites is as follows, assuming that A and B combine to produce a substitutional solid solution and that all possible configurations of A and B atoms are equally likely:

$$\omega = (N_A + N_B)! / N_A! N_B! \quad \text{V.20}$$

Since 1 mol of solution that is, Avogadro's number of N_a atoms is involved, where, $N_A = X_A N_a$, $N_B = X_B N_a$, $X_A + X_B = 1$ and $N_A + N_B = N_a$ (N_a is the Avogadro number).

Using the Stirling's approximation ($\ln N! \approx N \ln N - N$), we have:

$$\ln \omega = \ln[(N_A + N_B)! / N_A! N_B!] = \ln (N_A + N_B)! - \ln N_A! - \ln N_B!$$

$$\ln \omega = (N_A + N_B) \ln (N_A + N_B) - (N_A + N_B) - N_A \ln N_A + N_A - N_B \ln N_B + N_B$$

$$\ln \omega = N_a \ln N_a - X_A N_a \ln X_A N_a - X_B N_a \ln X_B N_a$$

$$\ln \omega = N_a \ln N_a - X_A N_a (\ln X_A + \ln N_a) - X_B N_a (\ln X_B + \ln N_a)$$

$$\ln \omega = N_a \ln N_a - N_a (X_A \ln X_A + X_B \ln X_B) - N_a (X_A + X_B) \ln N_a$$

$$\ln \omega = N_a \ln N_a - N_a (X_A \ln X_A + X_B \ln X_B) - N_a \ln N_a$$

here,

$$\ln \omega = -N_a (X_A \ln X_A + X_B \ln X_B) \quad \text{V.21}$$

Then,

$$\Delta S_{\text{mix}} = S_2 = -k \ln \omega = -k N_a (X_A \ln X_A + X_B \ln X_B) = -R (X_A \ln X_A + X_B \ln X_B) \quad \text{V.22}$$

where $R = N_a k$ is the universal gas constant.

The free energy of mixing is given by:

$$\Delta G_{\text{mix}} = -T \Delta S_{\text{mix}} = TR (X_A \ln X_A + X_B \ln X_B) \quad \text{V.23}$$

V.3 Time-Temperature-Transformation (TTT) Diagram

An isobaric representation of the phases' characteristics as a function of transformation temperature and time is provided by the T (Time), T (Temperature), and T (Transformation) diagram. For a specific temperature, it is employed to forecast the diffusion phase transformation kinetics. The later phase is nucleated and grows as a result of diffusion

Part V : Phase transformations

changes from a parent phase to a product phase, such as in the cases of solidification or precipitation. Temperature affects the pace at which a new phase is formed from a parent phase and, consequently, the transformation time.

V.4 Austenite to Pearlite isothermal transformation

At 0.76 weight percent C, the TTT diagram for the Fe-Fe₃C system is displayed in Figure V.6. It is possible to obtain the austenite stable phase above the eutectoid temperature ($T_E = 727^\circ\text{C}$). The new pearlite phase would emerge and the austenite parent phase would eventually vanish if this material had been quickly cooled and maintained at 625°C .

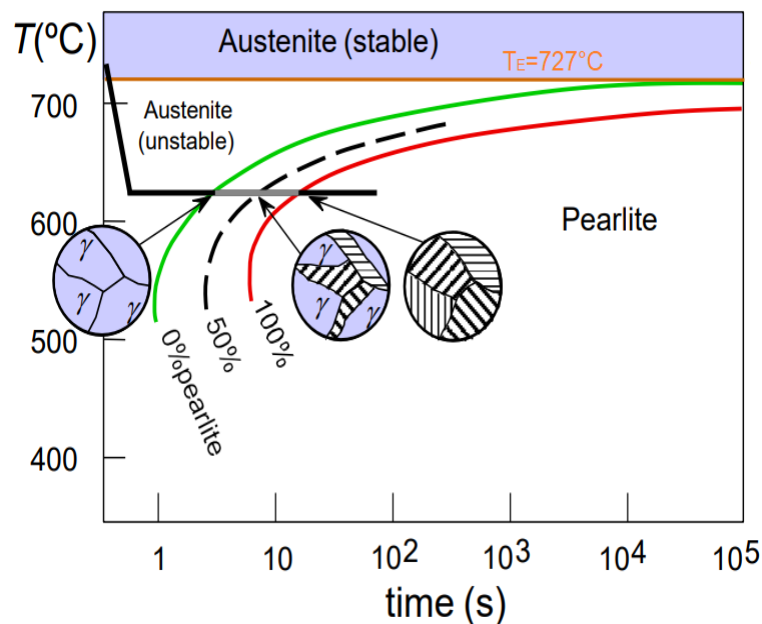


Figure V.6. TTT diagram illustrates Austenite to Pearlite isothermal transformation.

For the eutectoid steel, Davenport and Bain created the first TTT diagram. While they identified the sections of pearlite and bainite, Cohen subsequently changed and added the temperatures for martensite's MS (Martensite start temperature) and MF (Martensite completion temperature).

The TTT diagram is obtained by plotting temperature vs time on a logarithmic scale in Figure V.7, which illustrates the transition of austenite (eutectoid carbon steel). The diagram appears to be either S-shaped or C-shaped.

One way to visualise the progression of an isothermal phase transformation is to plot the fraction transformation (X or % of phase) against time. The following is how the Jonson-Mehl-Avrami (JMA) equation displays the X expression vs. time:

Part V : Phase transformations

$$X = 1 - \exp(-kt^n) \quad \text{V.24}$$

where t is the isothermal time, k is the reaction rate constant, and n is the Avrami exponent. The diagram in Figure V.7 is described as follows:

Coarse pearlite occurs at temperatures near Ae_1 , while very fine pearlite forms above the TTT diagram's nose.

It is reconstructive to undergo pearlitic metamorphosis. Following an incubation period (t_2 , at T_1), the transformation begins at a specific temperature (let's say T_1). The transformation start line is the locus of t_2 .

- The 50% transformation line is the period (t_3 at T_1) after the 50% transformation locus for various temperatures.
- The transformation finish temperature is the time at which the transformation is complete (t_4 at T_1), and the transformation finish line is the location of that.
- As a result, the TTT diagram is made up of many isopercentage lines, of which the transformation lines for 1%, 50%, and 99% are displayed. At high temperature while under cooling is low form coarse pearlite. At the nose temperature fine pearlite and upper bainite form simultaneously. The nose is the result of superimposition of two transformation one for pearlitic reaction other for bainitic reaction. Upper bainite forms at high temperature close to the nose of TTT diagram while the lower bainite forms at lower temperature but above M_s temperature.
- The temperature at which 99% martensite forms is called martensite finish temperature or M_F .
- Below M_F only martensite phase can be found.

Part V : Phase transformations

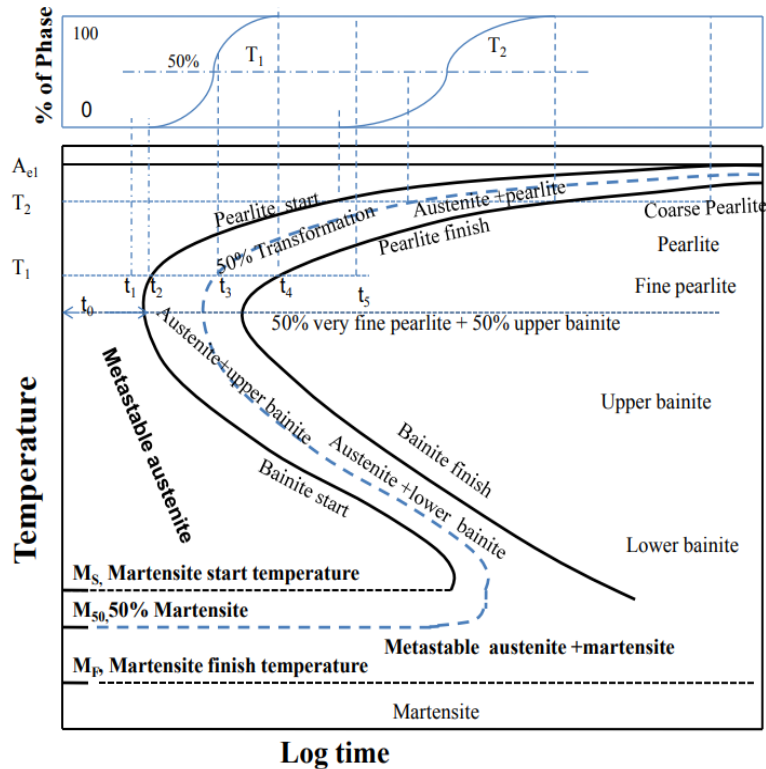


Figure V.7. TTT diagram for eutectoid carbon steel.

V.5 Illustration of the binary phase diagram with several reactions

The phase compositions and temperature are unchanged if there are three phases in equilibrium ($P = 3$). These three-phase invariant reactions can exist in a number of ways, as shown by the four temperature-composition diagrams in Figs. V.8 (a–d). Eutectic, peritectic, monotectic, eutectoid, peritectoid, monotectoid, metatectic, and syntectic reactions are the names given to the eight types of these processes. Table V.1 describes the types of reactions and provides a schematic illustration of them. In Fig. V.8, the majority of these responses are demonstrated.

The Fe–Pd system shown in Fig. V.8 (a) [7] includes a peritectic reaction ($\gamma + L$) at about 1500°C , a monotectoid reaction ($\gamma\text{Fe}_1 \longleftrightarrow \gamma\text{Fe}_2 + \alpha\text{Fe}$) at 815°C with a critical point at 900°C), two eutectoid reactions ($\gamma\text{Fe} \longleftrightarrow \alpha\text{Fe} + \text{FePd}$ at 605°C and $\text{Fe} \longleftrightarrow \text{FePd} + \text{FePd}_2$ near 740°C), and three congruent transitions.

The Fe–Sc system shown in Fig. V.8 (b) [7] includes a metatectic reaction ($\delta\text{Fe} \longleftrightarrow \gamma\text{Fe} + L$) at 1360°C), two eutectic reactions ($L \longleftrightarrow \alpha\text{Fe} + \beta\text{Fe}_2\text{Sc}$ at 1200°C and $L \longleftrightarrow \alpha\text{Fe}_2\text{Sc} + \beta\text{Sc}$ at 910°C), two peritectoid reactions ($\gamma\text{Fe} + \alpha\text{Fe}_2\text{Sc} \longleftrightarrow \alpha\text{Fe}$ at 925°C and $\beta\text{Sc} + \alpha\text{Fe}_2\text{Sc} \longleftrightarrow \text{FeSc}_3$ at 800°C), and a eutectoid reaction ($\beta\text{Sc} \longleftrightarrow \text{FeSc}_3 + \alpha\text{Sc}$ at 705°C). The Ga–I system shows three eutectic reactions and a syntectic reaction in Fig.

Part V : Phase transformations

V.8(c). GaI is the syntactic reaction of $L_1 + L_2 \longleftrightarrow$ GaI. Seven of the eight types of invariant reactions are thus represented by the three systems in Figs. V.8(a)–(c).

Diagram of phase for the Co–V system is shown in Figure V.8(d). This system is used to demonstrate how a diagram with odd borders can be produced by a second-order transition. Second order magnetic transitions predominate. The Gibbs energy and its first derivative with respect to the system variable are smooth and do not have a slope discontinuity in this instance due to an inflection in the Gibbs energy as a function of a system variable; however, the second derivative is zero, which is an inflection point. There are four prerequisites that permit a second-order transition in solids:

1. A second-order transition involves two structures, and the high-symmetry structure needs to contain all of the low-symmetry structure's symmetry elements.
2. The locations of the particles (atoms or dipoles) in the two structures must be clearly connected at constant composition.
3. The Gibbs energy difference between the two symmetries' structures cannot be defined by any odd-order terms, including third-order ones.
4. A continuous path between the two structures must be feasible for the transformation to take place.

These requirements must be met for a second-order transition to take place, but fulfilling them does not guarantee that a transformation will be second order. An example of a second-order transition turning into a first-order transition will be provided. Second-order transitions can be classified as displacive, order–disorder, or a combination of the first two.

Magnetic interactions can alter the geometry of an equilibrium diagram, even though a transition from an ordered magnetic state to a disordered one is typically a second-order transition. The shape of phase barriers is most frequently impacted by magnetic interactions. In the Co–V system, an odd transition takes place. Fig. V.8(d) shows a ferromagnetic to paramagnetic transition, $\alpha_f\text{Co} \longleftrightarrow \alpha_p\text{Co}$, in the Co-rich region of the Co–V system. At a Curie temperature of 1121°C, this transition takes place in pure αCo . The phase change is second order to a mole fraction of $X_V \approx 0.03$ and is first lowered by V additions to Co in accordance to the amount of V added. With a two-phase area of $\alpha_f\text{Co} + \alpha_p\text{Co}$ separating the ferromagnetic solvus from the paramagnetic solvus, the transition from second order to first order occurs at that composition.

Part V : Phase transformations

If just first-order transitions and solvus boundaries are plotted, this phenomena results in a strange geometry in the system's phase diagram, where the $\alpha_f\text{Co}$ solvus and the $\alpha_p\text{Co}$ solvus would converge at a single point. As a result, lines for second-order transitions are typically depicted differently from those for first-order transitions. Due to uncertainty in the boundaries' placements in the Co-rich region, this was not done in Fig. V.8(d); nevertheless, the existence of a two-phase $\alpha_f\text{Co} + \alpha_p\text{Co}$ appears to be well established.

Since the magnetic ordering of magnetic dipoles can be ascertained by neutron diffraction and a displacive effect is demonstrated by magneto-striction, a structural distortion that coincides with magnetic ordering, the second-order magnetic transition is categorised as a combination of order–disorder and displacive reactions. In contrast to Fe, which has a very small magnetostrictive effect, Ni has a significant enough magnetostrictive effect to be employed as a transducer in ultrasonic cleaning tanks, like those used to clean surgical tools after surgery.

Ferroelectric transitions should be described by a similar kind of second order transition. For example, it has been demonstrated that when barium titanate, or BaTiO_3 , arranges ferro-electrically, there is a very tiny atomic displacement; yet, there is a distinct electrostriction that is adequate to enable the use of BaTiO_3 as an ultrasonic transducer in tests that are not destructive.

Part V : Phase transformations

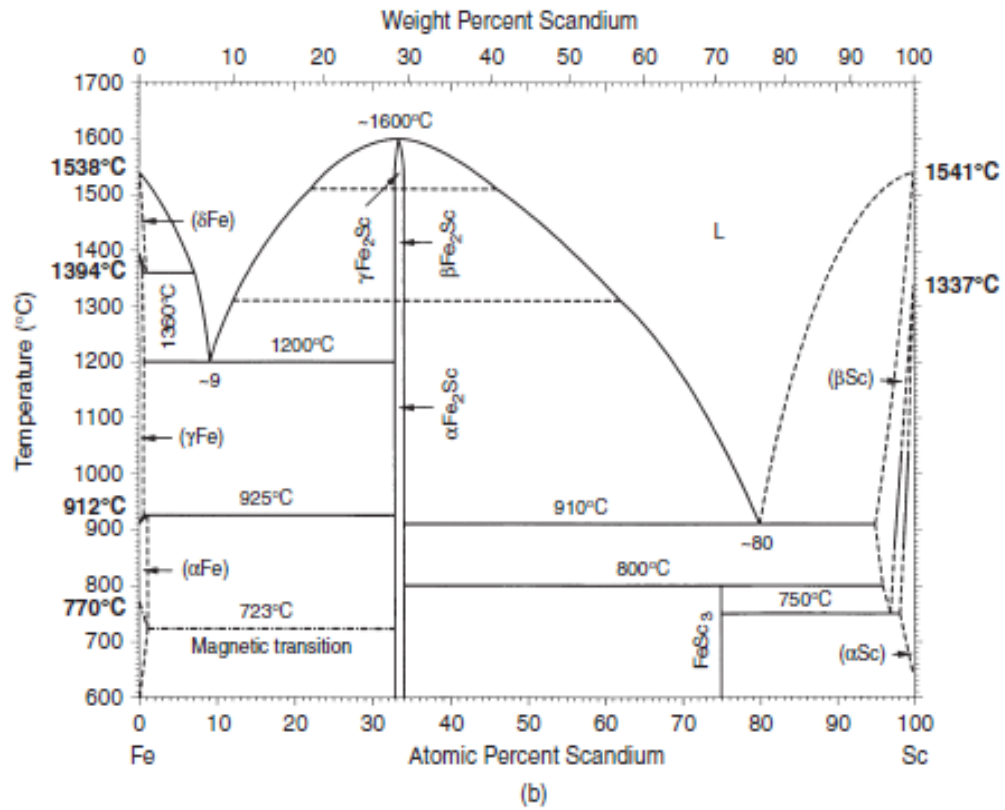
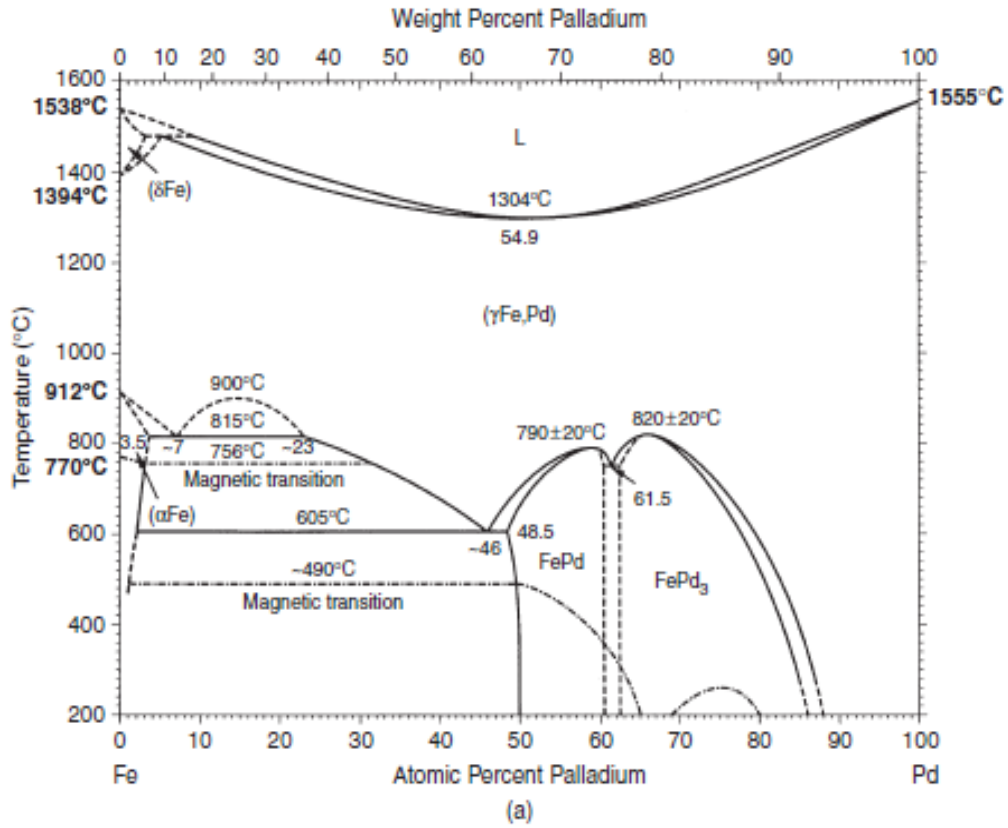


Figure V.8. Representation of different phase diagrams: (a) Fe-Pd, (b) Fe-Sc [7].

Part V : Phase transformations

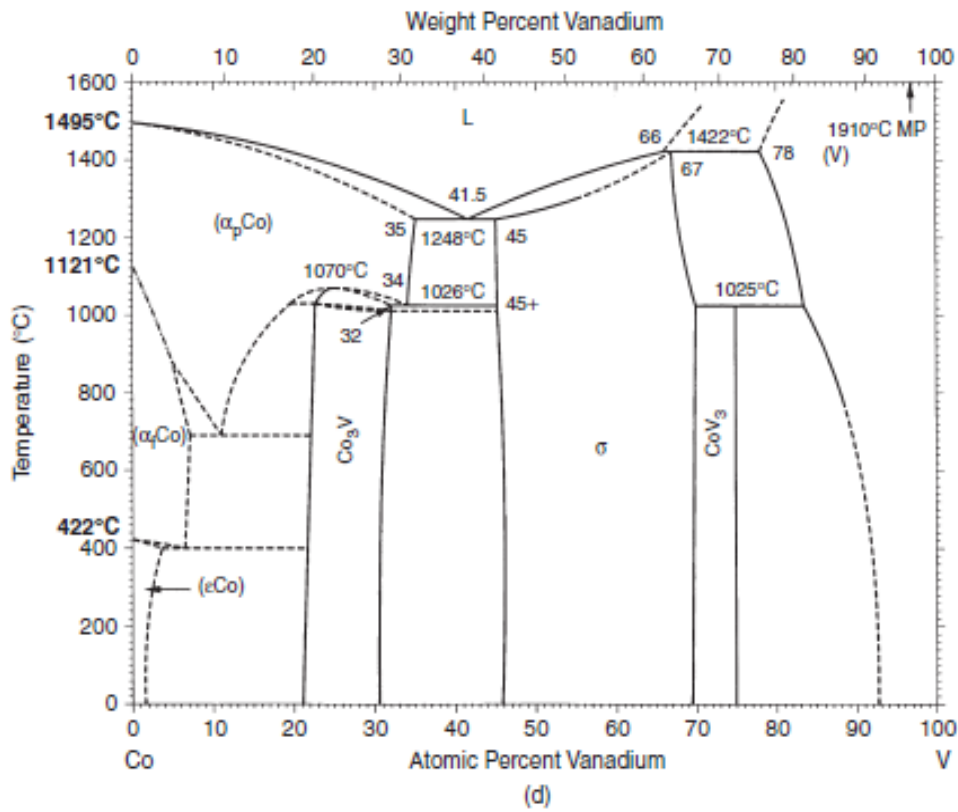
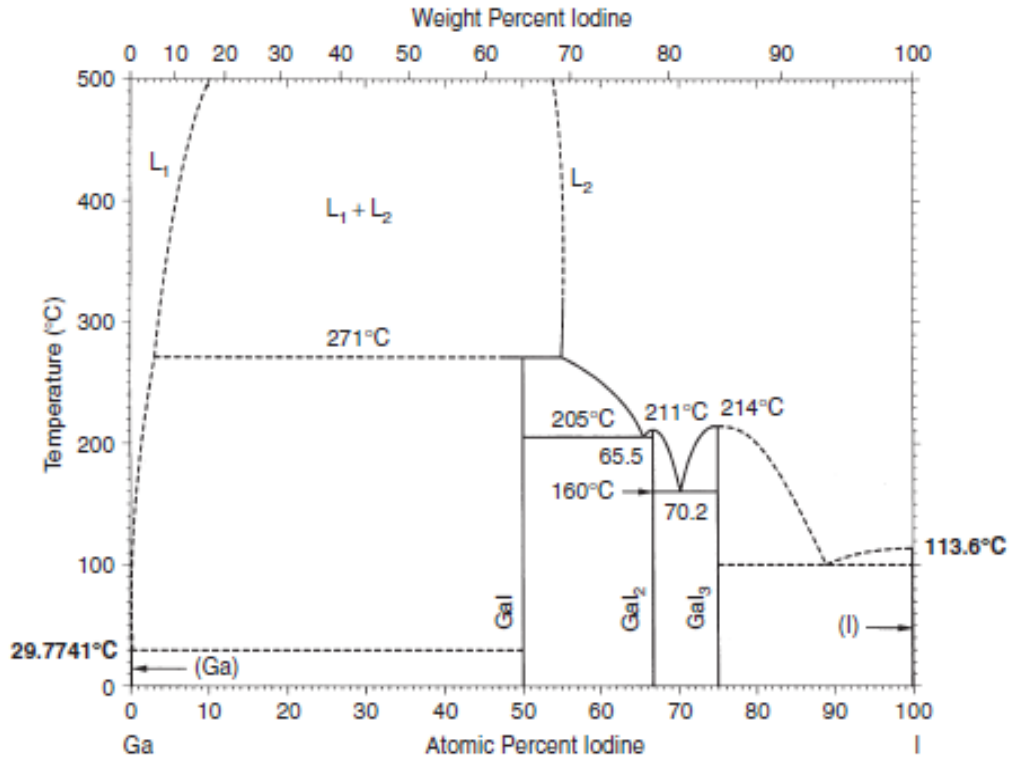


Figure V.8 (Continued). Representation of different phase diagrams: (c) Ga-I system, (b) Co-V system [7].

Part V : Phase transformations

Table V.1. Various kinds of invariant reactions at constant pressure in a dual equilibrium phase diagram [7].

Name of reaction	Phase equilibrium	Schematic representation
Eutectic	$L \leftrightarrow s_1 + s_2$	$s_1 > \frac{s_1 + L \quad \underset{s_1 + s_2}{\downarrow} \quad L + s_2}{s_1 + s_2} < s_2$
Peritectic	$s_1 + L \leftrightarrow s_2$	$s_1 > \frac{s_1 + L}{s_1 + s_2 \quad \underset{s_2}{\wedge} \quad s_2 + L} < L$
Monotectic	$L_1 \leftrightarrow s_1 + L_2$	$s_1 > \frac{s_1 + L \quad \underset{L + s_2}{\downarrow} \quad L_1 + L_2}{L + s_2} < L_2$
Eutectoid	$s_1 \leftrightarrow s_2 + s_3$	$s_2 > \frac{s_2 + s_1 \quad \underset{s_2 + s_3}{\downarrow} \quad s_1 + s_3}{s_2 + s_3} < s_3$
Peritectoid	$s_1 + s_2 \leftrightarrow s_3$	$s_1 > \frac{s_1 + s_2}{s_1 + s_3 \quad \underset{s_3}{\wedge} \quad s_3 + s_2} < s_2$
Monotectoid	$s_{1a} \leftrightarrow s_{1b} + s_2$	$s_{1b} > \frac{s_{1b} + s_{1a} \quad \underset{s_{1b} + s_2}{\downarrow} \quad s_{1a} + s_2}{s_{1b} + s_2} < s_2$
Metatectic	$s_1 \leftrightarrow s_2 + L$	$s_2 > \frac{s_2 + s_1 \quad \underset{s_2 + L}{\downarrow} \quad s_1 + L}{s_2 + L} < L$
Syntectic	$L_1 + L_2 \leftrightarrow s$	$L_1 > \frac{L_1 + L_2}{L_1 + s \quad \underset{s}{\wedge} \quad s + L_2} < L_2$

V.6 Diffusion pairs or Multiples and Phase Formation and kinetics

The use of diffusion multiples and diffusion couples as techniques for determining phase diagrams is growing in importance. Their primary benefits include:

- (1) The production of all phases at the desired annealing or interest temperature without the need for melting and solidification, hence avoiding the issue of a high temperature phase's slow disintegration.
- (2) The creation of several phases in a single sample, which makes it possible to extract several tie-lines from the local equilibrium at the phase interfaces.

Part V : Phase transformations

The biggest disadvantages are:

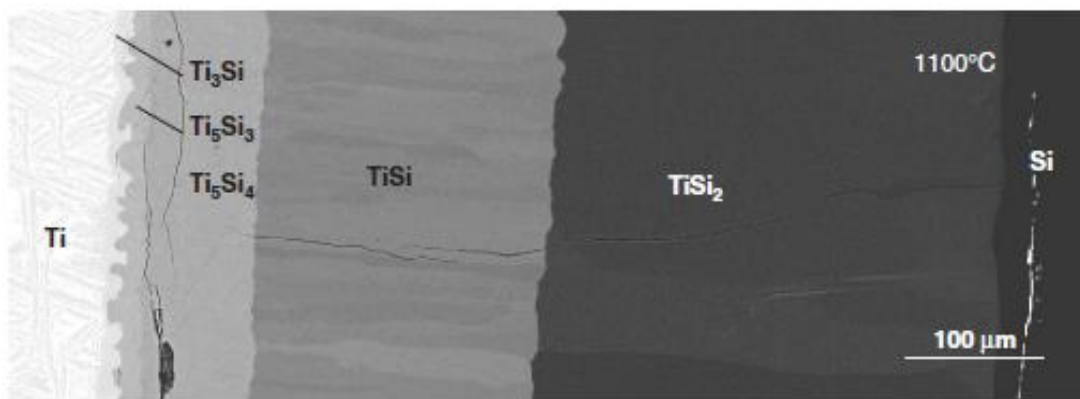
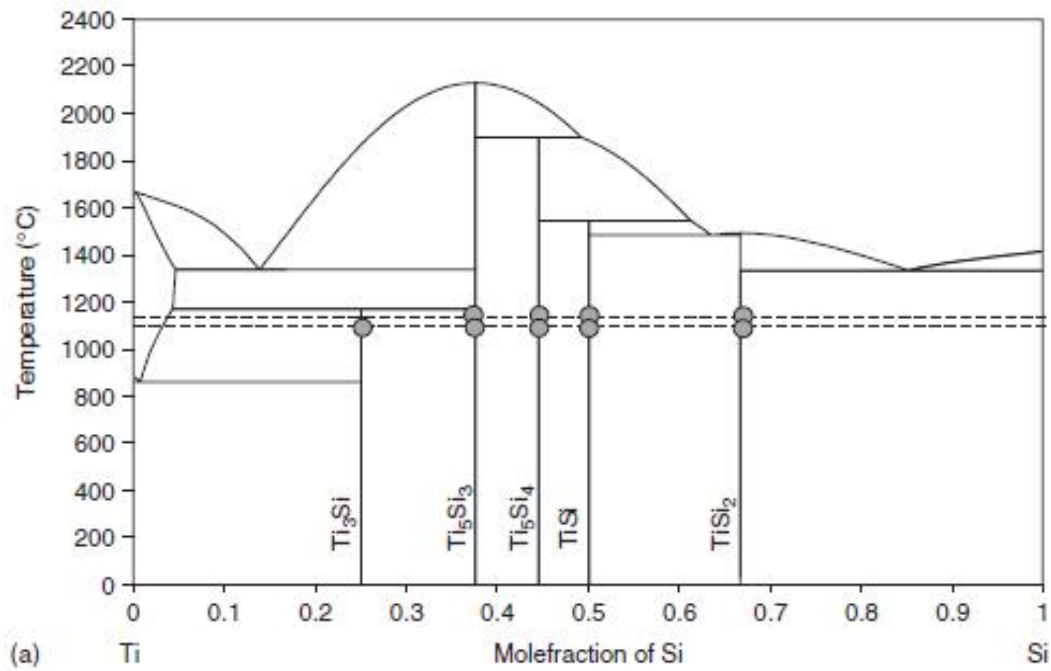
(1) In order to identify the crystal structure and do quantitative composition analysis, the phases had to grow thick enough through long-term annealing.

(2) Very infrequently, diffusion couples or multiples may occasionally have missing phases, raising questions regarding whether real equilibrium has been reached at the phase boundaries. It is practically advised to use diffusion couples and multiples only at temperatures greater than half of the system's homologous temperatures.

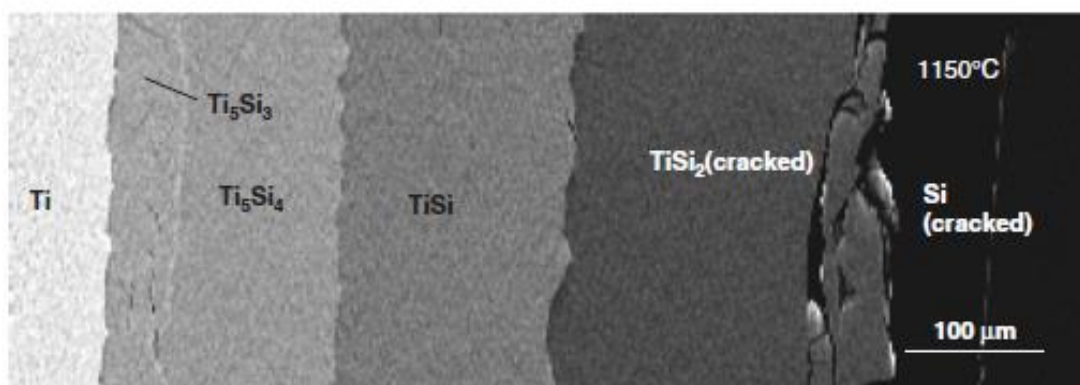
The likelihood of missing phases, the difficulty of achieving real equilibrium, and the need for an extremely long annealing period all rise at lower temperatures. There has been a lot of interest in the few, uncommon instances of missing phases. The fact is that they are quite uncommon and nearly all of them happened at temperatures lower than half of the homologous temperature, most likely as a result of the nucleation issue. The diffusion couples and multiples can be used to determine equilibrium phase diagrams with high reliability, especially for temperatures greater than half of the homologous temperature, provided that one pays close attention and carefully examines both the reported multi-component intermetallic phases and the corresponding binary phase diagrams. If one has the financial means, it would be ideal to utilise the increased efficiency of diffusion couples and diffusion multiples, followed by the usage of a few chosen alloys to examine regions in a phase diagram where there may be a suspicion of missing phases.

Some researchers question whether diffusion couples or multiples can create stoichiometric phases. This question may be dispelled by the example shown in Figure V.9 [7]. The diffusion couples/multiples have produced all of the intermetallic compounds, the majority of which are essentially stoichiometric. The $\text{bcc} + \text{Ti}_5\text{Si}_3 \longleftrightarrow \text{Ti}_3\text{Si}$ invariant reaction should be $1125 \pm 25^\circ\text{C}$, which is much lower than the prior experimental observation ($\sim 1170^\circ\text{C}$) based on chilling and heating tests. This is because all five intermetallic compounds form at 1100°C , whereas only four do so at 1150°C . Based on the changing of cooling and heating temperatures covered in this section, the results of the isothermal diffusion couple trials need to be far more trustworthy.

Part V : Phase transformations



(b)



(c)

Figure V.9. Formation of intermetallic compounds in the Ti-Si system: (a) Ti-Si phase diagram; (b) Ti-Si diffusion couple SEM picture after 4000 hours of annealing at 1100 °C; and (c) Ti-Si diffusion couple SEM image after 2000 hours of annealing at 1150 °C [7].

References

1. D. C. C. Magalhães, J. B. Rubert, O. M. Cintho, A. M. Kliauga, The Effect of Asymmetry on Strain Distribution, Microstructure and Texture of Multilayer Aluminum Composites Formed by Roll-Bonding. *Frontiers in Materials* 7:600162. DOI:10.3389/fmats.2020.600162.
2. K. Herrmann, In book: *Hardness Testing: The Fundamentals of Hardness Testing*. DOI: 10.31399/asm.tb.htpa.t53310001.
3. Bo Song, Wenlong Xiao, Yu Fu, Chaoli Ma, Lian Zhou, Role of nanosized intermediate phases on α precipitation in a high-strength near β titanium alloy, *Materials Letters*, 275, 2020, 128147, <https://doi.org/10.1016/j.matlet.2020.128147>.
4. Y. Zhang, microstructures and properties of high entropy alloys, *Progress in Materials Science*, 61(2014) 1-93. <http://dx.doi.org/10.1016/j.pmatsci.2013.10.001>.
5. D. Roy, T. Pal, Nanostage Alloying of Metals in Liquid Phase. *Advances in Chemical Engineering and Science* 11(01) (2021) 105-140, DOI: 10.4236/aces.2021.111008.
6. Okamoto, H. Ni-S (Nickel-Sulfur). *J. Phase Equilib. Diffus.* 30, 123 (2009). <https://doi.org/10.1007/s11669-008-9430-9>.
7. J. C. Zhao, In Book: *Methods for phase diagram determination*, Copyright © 2007 Elsevier Ltd. All rights reserved, ISBN 978-0-08-044629-5, <https://doi.org/10.1016/B978-0-08-044629-5.X5000-9>.
8. D. Pelton, In Book : *Thermodynamics and Phase Diagrams*, Montréal QC Canada H3C 3A7, (2011).

Additional references

1. C.A. Geiger, In book: *Solid Solutions in Silicate and Oxide Systems* Edition: v. 3 Chapter: Solid solutions: Background, history and scientific perspective Publisher: EMU Notes in Mineralogy, Eötvös University Press (2001). DOI: 10.1180/EMU-notes.3.1.
2. H. B. Huntington, F. Seitz, *Phys. Rev.* 61, 315 (1942).
3. H. B. Huntington, *Phys. Rev.* 61, 325 (1942).
4. Z. Jeffries, *Trans. AIME* 70, 303 (1924).
5. C. Zener, *Acta. Cryst.* 3, 346 (1950).
6. F. C. Frank, D. Turnbull, *Phys. Rev.* 104, 617 (1956).
7. U. Gösele, W. Frank, A. Seeger, *Appl. Phys.* 23, 361 (1980).
8. T. Y. Tan, U. Gosele, *Diffusion in Semiconductors*, Ch. 4 in: *Diffusion in Condensed Matter – Methods, Materials, Models*, P. Heitjans, J. Karger (Eds.), Springer-Verlag, 2005.

9. H. Mehrer, Diffusion in solids, Springer series in solid state science 155, Springer -Verlag, 2007.
10. H. Boyer (Ed.) Atlas of Isothermal Transformation and Cooling Transformation Diagrams, American Society for Metals, 1997, p. 28.
11. F.C. Campbell, In book: Phase Diagrams—Understanding the Basics: Chapter 14: Phase diagram applications, p. 289-301. Copyright © ASM International, (2012).
12. <https://mstudent.com/interstitial-sites-size-types-applications-and-calculations/>.
13. 15. W.D. Callister, Jr., “Fundamentals of Materials Science and Engineering,” Ch. 10S Phase Diagrams, pp. S67-S84, (2005).

Exercises

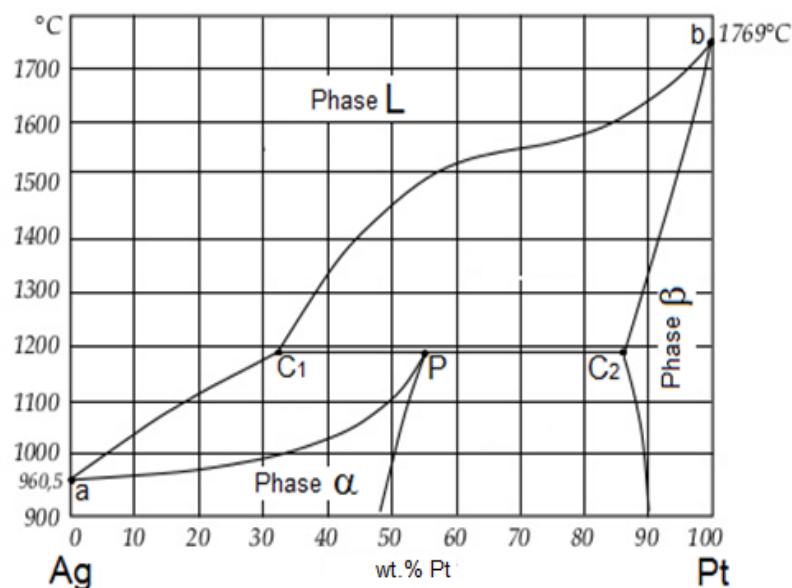
Exercise 1

- Based on the various properties of materials, they can be classified into several categories.
 - List the different families of materials. Give an example for each type.
 - List the different insertion sites in solid solution where solute atoms can occupy them.
 - List the different types of substitutional solid solution.
- Write the first law of Fick for one dimension for an isotropic medium.

Exercise 2

The Ag-Pt phase diagram is shown below (in mass fraction of Pt).

- What do the temperatures represent at points a and b?
- On the equilibrium phase diagram:
 - Indicate with red and green colors the solidus and liquidus lines, respectively.
 - Complete the phase names for each diagram domain.
- Indicate the name, the temperature, the Pt concentration and the reaction of the transformation in the point named P.
- What does the C_1C_2 line represent?
- Deduce the maximum solubility of:
 - Pt in the Ag.
 - Ag in the Pt.
- In the alloy containing 70% Pt, what are the phases exist at $T=1400^\circ\text{C}$ and at $T=1000^\circ\text{C}$?



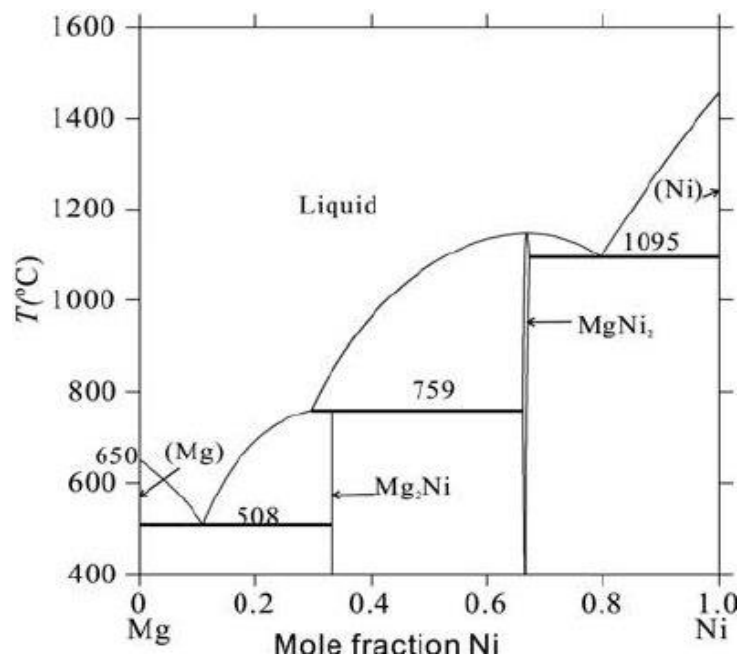
Exercise 3

1. Define the following terms and give two examples for each:
 - Metallic material, - Polymer Material, - Ceramic material.
2. The use of materials is based on several criteria, list 2 criteria that you know.
3. What are the different types of solid solution?
4. Identify the different interstitial sites that solutes can occupy in a solid solution.
5. What are the Hume-Rothery rules (Solubility rules)?
6. Write the first law of Fick for three dimensions.

Exercise 4

Consider the phase diagram of Mg-Ni as follows:

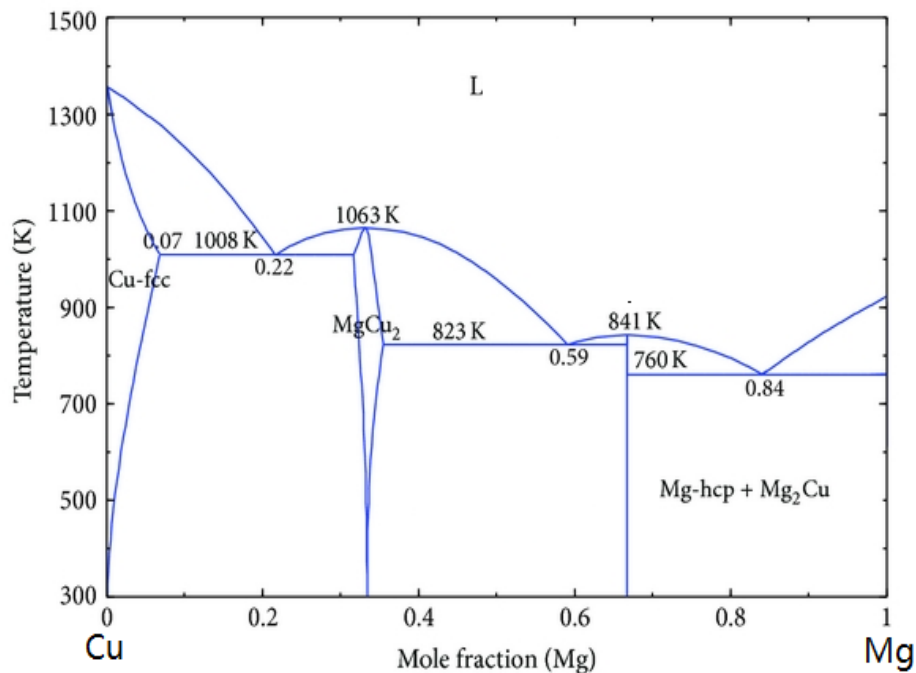
1. Fill in the empty domains in phases on the diagram.
2. Indicate on the diagram with different colors the liquidus and solidus lines.
3. What are the melting temperatures for the Mg and Ni elements?
4. Give the different reactions (phase transformations) that exist. Specify the coordinates (molar fraction in Ni, T) of each reaction.
5. At 759°C, what is the name of straight line?
6. Determine the amount of phases for the alloy 0.2 in Ni (or 20% Ni) at T= 450°C.



Exercise 5

Consider the phase diagram of Cu-Mg as follows:

1. Fill in the empty domains in phases on the diagram.
2. What is the name of the Cu-fcc phase?
3. What is the primary solid solution name of the element Mg?
4. What are the melting temperatures for the Cu and Mg elements?
5. What is the name of the MgCu_2 phase? Is its crystal structure the same or different from that of Cu and Mg?
6. Give the chemical formula of the phase located at ~ 67% in Mg? Give its melting point.



Exercise 6

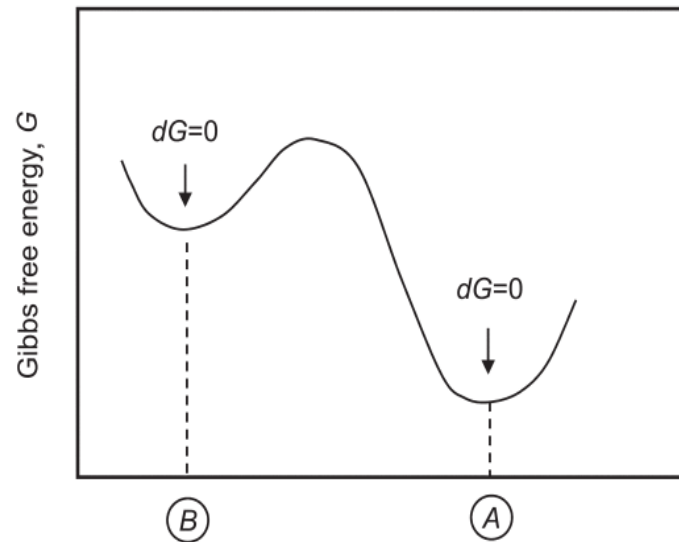
For transformations that occur at constant temperature and pressure:

1. Write the expression of Gibbs free energy that corresponds the relative stability of the system, as function of Enthalpy H and Entropy S.
2. What does Enthalpy represent?
3. Write the expression of H energy as function of internal energy, E (or U).
4. What does internal energy, E (or U) represent?

Exercise 7

Figure above presents the graphical representation of various possible atomic configurations that represented by the points along the abscissa.

1. Discuss this figure in more detail, indicating the configuration the more stable than its counterpart.
2. What is the behavior between the enthalpy and entropy for the state with the highest stability ?



Exercise 8

1. Define the term, Diffusion.
2. Give the different mechanism of diffusion.

Exercises solutions

Exercise 1

1.a

- Metallic materials: Ex: Iron, Cu,
- Ceramic materials: Ex: Constriction bricks, cement, clays,
- Polymer materials: Ex: Plastic, car dashboard,
- Composite materials: Ex: Dental prosthesis, Al/Mg/Al matrix alloys (compound),

2.a. Insertion sites in solid solution are Octahedral and Tetrahedral sites.

2.b. Types of substitutional solid solution are Ordered and disordered substitutional solid solution.

3. Fick's first law for an isotropic medium can be written as: $J_x = -D \frac{\partial C}{\partial x}$

Exercise 2

1. - T_a represents the melting (solidification) temperature of Ag.

- T_b represents the melting (solidification) temperature of Pt.

2. On the phase diagram (See figure below):

a. Solidus and liquidus lines.

b. Phase names in different domains.

3. Peritectic reaction at :

- $T \sim 1200^\circ\text{C}$,

- with Pt concentration :55%

- Reaction is : $L + \beta \rightleftharpoons \alpha$

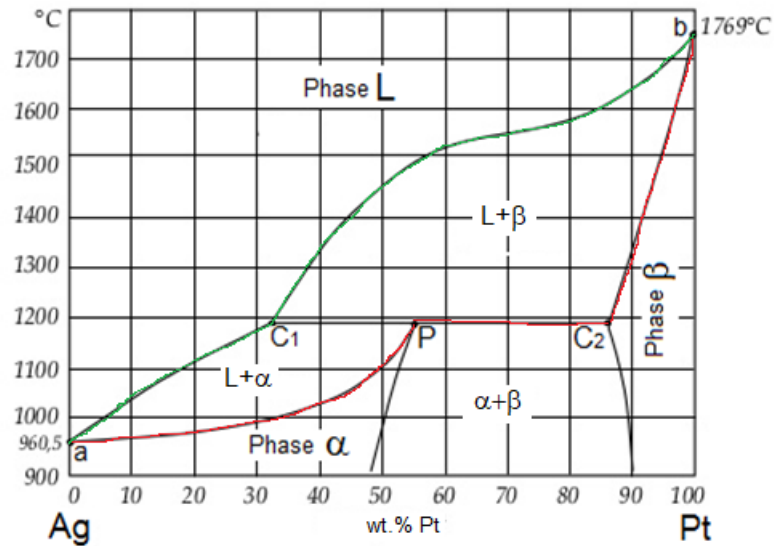
4. C_1C_2 line represents the peritectic landing.

5. The maximum solubility of:

c. Pt in the Ag is 55%

d. Ag in the Pt is 86%

6. In the alloy containing 70% Pt, the phases exist at $T=1400^\circ\text{C}$ are $L + \beta$ and at $T=1000^\circ\text{C}$ are $\alpha + \beta$.



Exercise 3

1.
 - Metallic material: It is composed of one or more metallic elements, such as copper, aluminum, iron, titanium, nickel, and gold, and often also with non-metallic elements (for example, carbon, oxygen and nitrogen). Ex: Metal of copper, Al-2%Cu alloy.
 - Polymer Materials: Polymer is typically organic material which is chemically based on carbon, hydrogen, and other nonmetallic elements (O,N, and Si). Ex: Plastics, Elastomers (car tires).
 - Ceramic materials: Ceramic is compound between metallic and nonmetallic elements; which is prepared from powdered materials, and fabricated into products through the application of heat. Ex: alumina- Al_2O_3 , Bricks.
2. The use of materials is based on several criteria: Compatibility with the environment and availability.
3. The different types of solid solution are: substitutional and interstitial solid solutions.
4. The different interstitial sites that solutes can occupy in a solid solution are octahedral and tetrahedral sites.
5. The Hume-Rothery rules (Solubility rules) are: crystal structure factor, relative size factor, relative valence factor and chemical affinity factor.
6. Fick's first law for three dimensions: $J = -D \nabla C$

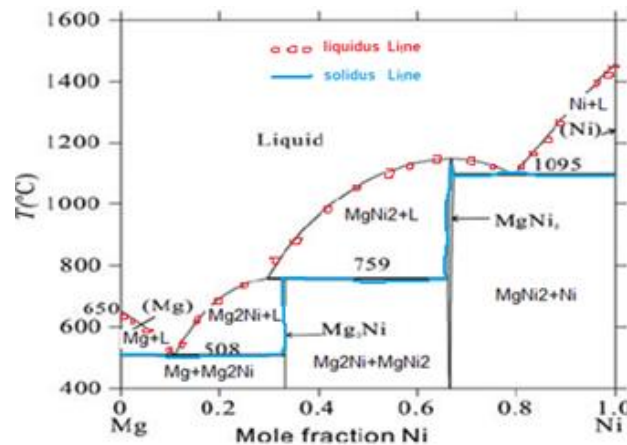
Exercise 4

1. See phase diagram.

2. See on phase diagram the liquidus and solidus lines.
3. The melting temperatures for the Mg and Ni elements are 650 and 1455°C, respectively.
4. The different reactions (phase transformations) that exist are:
 - Eutectic transformation, $L \longrightarrow \text{Mg} + \text{Mg}_2\text{Ni}$, (0.1Ni, 508°C)
 - Peritectic transformation, $L + \text{MgNi}_2 \longrightarrow \text{Mg}_2\text{Ni}$, (0.35Ni, 759°C)
 - Eutectic transformation, $L \longrightarrow \text{Ni} + \text{MgNi}_2$, (0.8Ni, 1095°C)
5. The name of the plateau is peritectic plateau.
6. The amount of phases for the alloy 0.2 in Ni (or 20% Ni) at $T = 450^\circ\text{C}$:

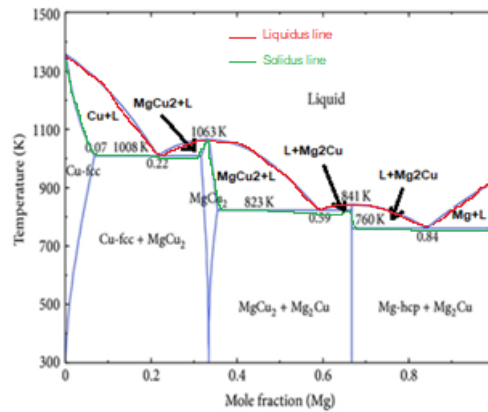
$$\text{Mg}\% = (0.35 - 0.2) / (0.35 - 0) = 0.42 = 42\%$$

$$\text{Mg}_2\text{Ni}\% = (0.2 - 0) / (0.35 - 0) = 0.58 = 58\%$$



Exercise 5

1. See the phase diagram.
2. The name of the Cu-fcc phase is a primary solid solution of Cu (or solid solution of Mg in Cu).
3. The primary solid solution name of the element Mg is Mg-hcp.
4. The melting temperatures for the Cu and Mg elements are 1350 and 923 K, respectively.
5. The name of the MgCu_2 phase is nonstoichiometric intermetallic compound. Its crystal structure is different from that of Cu and Mg.
6. The chemical formula of the phase located at ~ 67% in Mg is Mg_2Cu . Its melting temperature is 841 K.



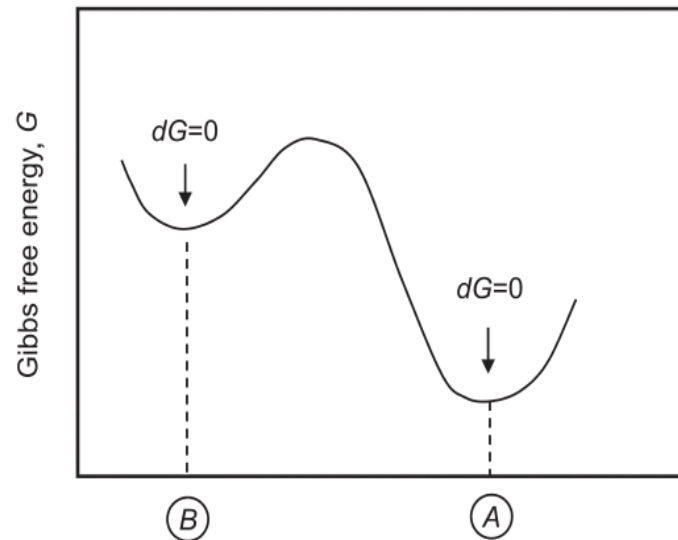
Exercise 6

1. For transformations that occur at constant temperature and pressure, the relative stability of the system is determined by its Gibbs free energy: $G = H - TS$
2. Enthalpy is a measure of the heat content of the system.
3. The expression of H energy as function of internal energy, E (or U) is : $H = U + PV$.
4. The internal energy, E, is equal to the sum of the total kinetic and potential energy of the atoms in the system. Kinetic energy results from the vibration of the atoms in solids or liquids, and the translational and rotational energies of the atoms and molecules within a liquid or gas. Potential energy results from the interactions or bonds between the atoms in the system.

Exercise 7

1. In this Figure, the various possible atomic configurations are represented by the points along the abscissa. The configuration with the lowest free energy, G, will be the stable equilibrium configuration. Therefore, configuration A would be the stable equilibrium configuration. There are other configurations, such as configuration B, which lie at a local minimum of free energy but do not have the lowest possible value of G. Such configurations are called metastable equilibrium states to distinguish them from the stable equilibrium state. The other configurations that lie between A and B are intermediate states for which $dG \neq 0$ and are unstable.
2. The state with the highest stability will be the one with the lowest enthalpy and the highest entropy. Therefore, at low temperatures, solid phases are the most stable because they have the strongest atomic bonding and therefore the lowest enthalpy (internal energy). However,

at high temperatures, the $-TS$ term dominates and the liquid and eventually the vapor phases becomes the most stable.



Exercise 8

1. Diffusion is the transport of matter from one point to another by thermal motion of atoms or molecules.
2. Different mechanism of diffusion are:
 - * Interstitial Mechanism, * Direct exchange mechanism, * Ring mechanism, * Vacancy mechanism, * Interstitial-substitutional exchange mechanism, *

Exercises without solutions

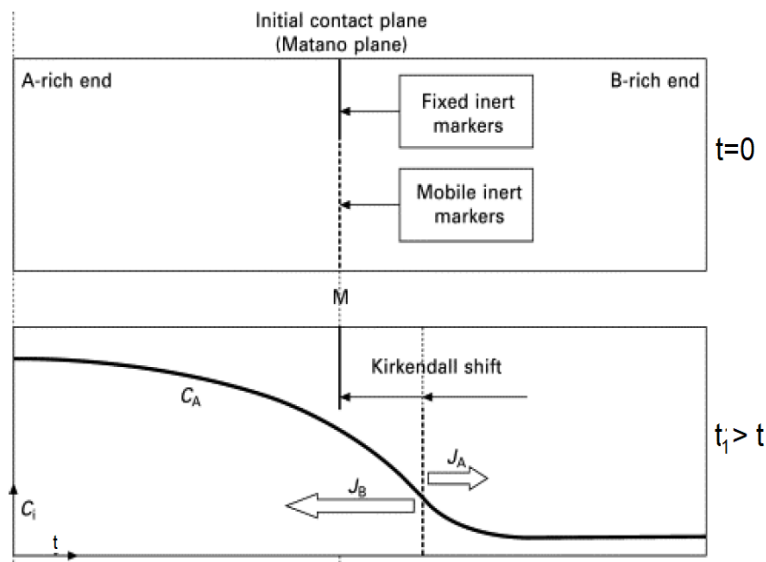
Exercise 01

1. Write the Fick's first law where the flux of diffusing particles (i.e. atoms, molecules, or ions) can occur in one dimension.
2. Write the Fick's first law for three dimensions.
3. Write the Fick's second law.

Exercise 02

Schematic illustration of Kirkendall experience is presented below.

1. Discuss this figure when the diffusion rates of the two species are different ($|J_A| > |J_B| \Leftrightarrow D_A > D_B$).



Exercise 03

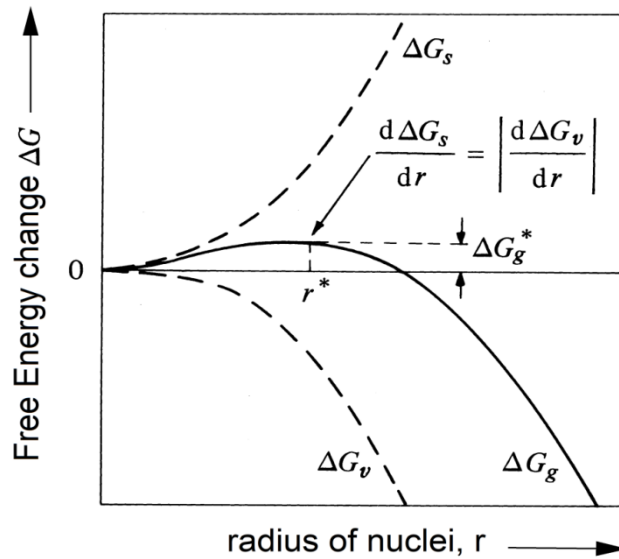
Any transformation that results in a decrease in Gibbs free energy, G , is possible and any reaction that results in an increase in G is impossible and will not occur.

1. If G_1 and G_2 are the free energies of the initial and final states, respectively, What is the necessary criterion for any phase transformation?

Exercise 04

The variation the free energy versus radius r of nuclei is presented in Figure below. It can be seen from this figure that for a given undercooling there is a certain radius, r^* (critical nucleus size), which is associated with a maximum excess free energy.

1. Discuss the different cases between r and r^* .



Exercise 05

1. What is meant by mechanical properties of materials? State their importance in the design of a machine or structural element.
2. Explain the difference between malleability and ductility. Toughness, stiffness and strength.
3. Explain the term 'fatigue'. Also explain the term fatigue strength and fatigue limit related to fatigue.
4. Explain the difference between hardness and brittleness, strength and stiffness, elasticity and creep, malleability and ductility.
5. What do you understand from the term "Mechanical Properties of Materials"? On which factors does these properties mainly depend?
6. Explain the following in brief:
 - (i) Impact strength
 - (ii) Plasticity
 - (iii) Fatigue
 - (iv) Elasticity
7. Draw a typical "creep test" curve, showing different stages of elongation for a long time, high temperature creep test. State how the information is useful to the design engineers.
8. Differentiate between:
 - (a) Hardness and impact resistance
 - (b) Hardness and toughness

9. Explain: Brittleness, Stiffness and Ductility.
10. What property is dependent on time and temperature?
11. On what factors does the hardness of steel depend?
12. Briefly explain what do you understand by: Toughness, Fatigue, Creep, Hardness
13. Differentiate among strength, stiffness and toughness.
14. Explain (i) Elasticity (ii) Plasticity (iii) Toughness. (iv) Malleability